Order Number 9304733

Applications of time-resolved surface-enhanced Raman spectroscopy in electrochemical processes

Shi, Chongtie, Ph.D.

City University of New York, 1992

U·M·I
300 N. Zeeb Rd.
Ann Arbor, MI 48106

APPLICATIONS OF TIME-RESOLVED SURFACE ENHANCED RAMAN SPECTROSCOPY IN ELECTROCHEMICAL PROCESSES

by

CHONGTIE SHI

A dissertation submitted to the Graduate Faculty in Chemistry in partial fulfillment of the requirements for the degree of Doctor of Philosophy, The City University of New York.

1992

This manuscript has been read and accepted for the Graduate Faculty in Chemistry in satisfaction of the dissertation requirement for the degree of Doctor of Philosophy.

10/1/92
Date

Chair of Examining Committee

9/24/92
Date

Executive Officer

Supervisory Committee

The City University of New York

Abstract

APPLICATIONS OF TIME-RESOLVED SURFACE ENHANCED RAMAN SPECTROSCOPY IN ELECTROCHEMICAL PROCESSES

by
Chongtie Shi

Advisor: Professor Ronald L. Birke

Professor John R. Lombardi

The protonation, adsorption and electroreduction of several compounds containing aromatic rings, 4-nitrobenzoic acid (PNBA), 4-cyanopyridine(4-CNPY), 4-pyridinecarboxaldehyde (ALPY) and 4-(hydroxymethyl)-pyridine (HMPY), were investigated systematically by surface-enhanced Raman spectroscopy (SERS), cyclic voltammetry (CV) and digital simulation. The time-resolved SERS spectra during electrochemical reactions were measured in the time scale from seconds to microseconds. Electrochemical reactions were initiated by potential sweep and potential step waveforms. Transient spectra corresponding to the short-lived species are obtained for the first time by time-resolved SERS. Products of the reactions are identified by comparison of authentic compounds with the SERS spectrum. Possible intermediates are discussed according to the proposed possible mechanisms for each reaction. The electrochemical reductions of all of the four compounds studied, give rise to chemical coupling products under our experimental conditions. However, the pathways for the product formation are different. In the reduction of p-nitrobenzoic acid, an azoxy compound is formed by the coupling of two different

intermediate products, nitroso and hydroxylamine compounds. An azo compound is produced in the electroreduction of 4-cyanopyridine through a coupling step of the reactant with a one-electron reduction intermediate. The formation of 1,2-bis(4-pyridyl)ethane is due to the direct coupling between two identical one-electron reduced radicals in pyridinecarboxaldehyde and 4(hydroxymethyl)pyridine electro-reductions. In conclusion, this thesis has demonstrated: (1) that the dramatic enhancement of Raman signal from the pretreated electrode surfaces, coupled with multichannel detection technique makes it possible to detect time-resolved SERS in milliseconds, even microseconds, without influence of fluorescence which is quenched by the SERS active surface. This quenching is very attractive since fluorescence is a major interference in resonance Raman measurements. (2) As an in-situ surface probe, SERS, especially time-resolved SERS, is ideal for studying adsorption, orientation, and electrochemical reactions. The power of time-resolved SERS is convincingly shown in the detection of short-lived surface intermediate species which are generated during electrode reactions. The information obtained from time-resolved SERS investigations provides direct evidence for the identification of products and intermediates, which are useful in the study of kinetics and mechanisms of the reactions.

ACKNOWLEDGMENT

This work has been primarily supported by the National Science Foundation (CHE-8711638) with supplementary support from the PSC-BHE award program of the City University of New York (666367, 667261, and 66875) and the National Institutes of Health MBRS program (RR-08168).

CONTENTS

List of Tables

List of Figures

Chapter I

Basic Concepts of Surface-Enhanced Raman and Time-Resolved Surface-Enhanced Raman Spectroscopy

Section 1.1 Introduction

Raman spectroscopy, along with infrared spectroscopy, plays a very important role in chemistry, especially in analytical chemistry. Raman spectroscopy, which produces structural information of chemical compounds especially organic compounds, is ideal for qualitative analysis, such as identification of molecules and following the course of reactions.[1,2,3] With careful management it can also be used for quantitative analysis. As a complimentary and competitive technique of Infrared spectroscopy, Raman spectroscopy has its own advantages. For example, it can be used in both aqueous and non-aqueous solvents. This is especially useful in biological chemistry for those compounds that can not easily dissolve in non-aqueous solvents. Another advantage is that Raman spectroscopy can be used to obtain information which can not be obtained from IR, since some transitions are IR forbidden but Raman active. The observation of an IR transition requires a change in dipole moment with vibration, while the presence of a Raman band demands a change in polarizability. Thus, if a vibration causes a change only in the molecule's dipole moment, it is IR active. If it causes a change only in the molecule's polarizability, i.e., the size of the molecule, it is Raman active. If the vibration causes changes in both dipole moment and polarizability, it is both IR and Raman active. The third advantage is that Raman spectroscopy can be used with a microprobe, which is especially useful for microanalysis. The disadvantages are (1) a Raman instrument is more expensive than an IR instrument since a laser is employed; (2) Raman spectroscopy requires more skillful operations; (3) normal Raman spectroscopy is not so sensitive and difficult for quantitative analysis. However, resonance Raman can be more sensitive than IR absorption.

Surface-Enhanced Raman Spectroscopy (SERS) is a method based on the enhancement effect of some metal surfaces on the Raman signal of adsorbed molecules.[4] When molecules are adsorbed on some metal surfaces, such as silver, gold and copper, which had been specially pretreated or activated before adsorption, the surface Raman signal per molecule is dramatically enhanced up to a million fold.[4] The metal surface could be provided either by small particles such as colloids or sols or by bulk metals, such as an electrode, which is activated before use.

SERS is a very useful tool for in-situ investigation of electrochemical reactions. The development of SERS methods for studying species on electrode surfaces has enabled detection of molecules heretofore inaccessible through normal high resolution means.[4,5] The pretreated electrode surface which enhances the Raman signal can also serve as a reaction field. Most of the electrochemical reactions of SERS active compounds, which include most organic compounds with π-ring system and their complexes, can be studied by SERS. Even those photo-sensitive compounds can also be studied with specially designed experiments. Thus the technique allows one to obtain information about the species on the electrode and furthermore to understand what is going on during the electrochemical reaction.

Since SERS is a combination of electrochemistry and Raman spectroscopy, it possesses the advantages of both techniques. For example, it has the advantage of electrochemistry in that the direction, kinetics and product formation of an electrochemical reaction can be easily controlled by controlling the potential and time of electrolysis. Most electrochemical techniques can be

employed with SERS, such as steady-state measurements, cyclic voltammetry, potential step or double potential steps and coulommetry. Like IR, SERS measures the vibrational spectrum of a molecule, which gives information about the molecular structure and helps us to identify the known species and to determine the structures of new compounds. SERS is much more sensitive than IR and normal Raman. Its detection limit can go as low as 10^{-6} mole/l.[4]

The vast majority of SERS measurements have been applied to stable species although the technique should be capable of investigating transient phenomena at very short times. Early studies of fast time resolved SERS, in the ms region, involved measuring the scattering intensity at fixed frequency vs. time.[6,7] However, coupling the surface enhancement with optical multichannel devices capable of scanning entire spectral regions in milliseconds allows the possibility of examining the structure of relatively short-lived species during the process of electrochemical oxidation or reduction. An optical multichannel analyzer (OMA) has previously been used to record a time resolved resonance Raman scattering (TR^3S) signal on a ms time scale for a species generated electrochemically,[8] however, it was shown that transient measurements using a RR process at an electrode is not straight-forward because of the distortion of the signal by self absorption.[9] With SERS this distortion is eliminated because the scattering, in most cases, comes from a layer of molecular dimensions at the surface. Although TR^3S studies from ms to ns have been accomplished in solution,[10,11] there has been a marked lack of such measurements using time-resolved SERS.[12]

Time-resolved SERS is a real-time in-situ methodology which combines SERS with time-resolve technique where multichannel detecting techniques

are commonly used. The time-resolved technique allows one to detect the rapid changes of the surface Raman spectra and the surface-enhanced effect makes the time-resolved measurement possible. When combined with fast electrochemical techniques, time-resolved SERS allows us to detect short-lived transient species generated on the electrode during the electrochemical reaction. The information about the structure of the transients and the kinetics of the reactions can be obtained. This information is very important for elucidation of the mechanism of the electrochemical process and can not be obtained from steady-state SERS measurements. In addition, time-resolved SERS can also be used to study photo reactions and photoelectrochemical reactions where a light pulse is used to initiate the process. Three other advantages over TR[3] are (1) fluorescence, which is usually encountered in TR[3], is quenched by the SERS active surface; (2) the resonance effect in TR[3] is achieved by changing the laser frequency and thus a dye laser is generally required, but the maximum surface-enhanced effect can be reached by simply adjusting the electrode potential; (3) time-resolved SERS is able to follow the electrochemical processes occurring on the electrode surface in order to obtain kinetic information.

Section 1.2 The Principle of Raman and SERS Effects

(a) Raman Effect

The oscillating electric field, ε, of an incident light interacts with a molecule and induces a dipole moment, μ_i, through its polarizability α.

$$\mu_i = \alpha\varepsilon \tag{1.1}$$

with

$$\varepsilon = \varepsilon^{()}\cos 2\pi t\nu_{()} \tag{1.2}$$

This induced dipole moment oscillates and radiates light with the same frequency as the incident light. This scattered radiation is called Rayleigh scattering. However, the molecule itself also vibrates at its own characteristic frequencies ν_V which depends the structure of the molecule,

$$Q_v = Q_0\cos 2\pi\nu_v t \tag{1.3}$$

where Q is the normal coordinate. The changes of the polarizability due to the vibration is given by

$$\alpha = \alpha^0 + (d\alpha/dQ)_0 Q_v \tag{1.4}$$

Then the induced dipole moment μ_i can be expressed as

$$\mu_i = \alpha\varepsilon = \alpha^0\varepsilon^0\cos 2\pi\nu_0 t + (d\alpha/dQ)_0 Q_0\varepsilon^0\cos 2\pi\nu_v t\cos 2\pi\nu_0 t \tag{1.5}$$

which can be rewritten as

$$\mu_i = \alpha^0 A^0\cos 2\pi\nu_0 t + (d\alpha/dQ)_0(Q_0\varepsilon^0/2)[\cos 2\pi(\nu_0-\nu_v)t + \cos 2\pi(\nu_0+\nu_v)t] \tag{1.6}$$

The first term in equation (1.6) corresponds to the elastic Rayleigh scattering and the other terms describe scattered light with shifted frequencies from the Rayleigh line and are called Stokes and anti-Stokes Raman scattering. The frequency shift is called the Raman shift and is characteristic to the molecule but

independent of the exciting light. It is easy to see from eq. (1.6) that the occurrence of Raman scattering requires

$$(d\alpha/dQ)_0 \neq 0 \qquad (1.7)$$

in other words, there must be a polarization change with the vibration if the vibration is to be Raman active.

The quantum theory for Raman scattering states that the vibrational energy of a molecule is quantized and the degree of freedom or the number of normal vibrations is 3N-6 for non-linear molecules and 3N-5 for linear molecules, where N is the number of atoms in the molecule. The energy of each of these vibrations can be expressed as

$$E_{vi} = h\nu_i(v+1/2) \qquad v=0,1,2,3,.... \qquad (1.8)$$

where ν_i is the vibrational frequency and v is the vibrational quantum number. When a molecule in vibrational ground state (v=0) interacts with a photon with energy $h\nu_0$, it is excited to a virtual state $h\nu_0$. It releases the energy "immediately" (within about 10^{-14} s) by scattering a photon. The scattered photon will possess the same energy $h\nu_0$ if the excited electron goes back to the vibrational ground state and it will have less energy $h(\nu_0-\nu_v)$ if the excited electron goes back to the first excited vibrational state. The former case is called Rayleigh scattering which has the same frequency as the incident light, and the latter case is called the Stokes Raman scattering which has a frequency equaling to $\nu_0-\nu_V$. On the other hand, if a molecule in its first excited vibrational state (v=1) is exited by a photon $h\nu_0$ and goes back to the ground state, the anti-Stokes Raman radiation with frequency $\nu_0+\nu_V$ will be observed. The frequency differences between the Rayleigh and the Raman lines or the Raman shifts are the characteristic vibrational frequencies of the molecule. According to the Boltzmann law, only a small proportion of the molecules will occupy the first

excited vibrational state at room temperature and most of them are in the ground vibrational state. Therefore the Stokes lines are much intense than the anti-Stokes lines and often used for regular measurements.

When the excitation frequency is not in the absorbing band of the molecule, the spectrum detected is called the normal Raman (NR) spectrum. If the excitation frequency is within the absorbing band, the Raman scattering is tremendously increased and is called resonance Raman (RR) scattering.

(b) SERS Effect

When a molecule is adsorbed on some specially pretreated metal surface, the Raman signal is found to be greatly enhanced by the interactions of the exciting light, the adsorbed molecule and the metal surface. The enhanced Raman spectrum is called the surface enhanced Raman scattering (SERS) spectrum. Although SERS was found on several metal surfaces, only on three types of roughened metal surfaces is a significant SERS effect shown in the electrochemical environment.[4] These metals are Ag, Au and Cu. The enhancement is up to 5 or 6 orders of magnitude in comparison to normal Raman. Ag is a very good electrode material with very high overpotential for hydrogen evolution. It has a very wide potential window available for electrochemical reactions. Au is a noble electrode material which could be used to examine electrode reactions with quite positive redox potentials. Cu is not as noble as the other two and has a very limited potential range available. The Ag surface gives a very strong SERS effect with blue and green laser excitation, but Au and Cu work well with red laser light.

Mainly there are two theories for surface enhancement.[4] One is called the electromagnetic field enhancement theory and the other the charge transfer theory. The electromagnetic field enhancement theory is based on the amplification of the electromagnetic field through the localized plasmon resonance within metal particles when an incident light satisfies the resonance condition. The resonance condition relies on the dielectric constants of the metal and the surrounding medium and the geometry of the metal particles. The charge transfer theory is based on the interaction between the molecule and the atomic scaled surface active site. The interaction forms a surface complex so that the photo-assisted charge transfers from the molecular ground state to the metal Fermi level or from the metal Fermi level to the molecule's lowest unoccupied molecular orbital (LUMO) can take place (Figure 1.1). It is the charge transfers between the metal and the adsorbed molecules that enhance the Raman signal. According to the charge transfer theory, the SERS intensity should depend on electrode potential and reach its maximum for a metal-molecule resonance condition. When the energy difference between the metal Fermi level and the adsorbed molecule's HOMO or between the adsorbed molecule's LUMO and the metal Fermi level is equal to the energy of the excitation light, this resonance condition is satisfied. Since the metal Fermi level depends on the electrode potential, the resonance can be tuned. It should be mentioned here that the intensity maxima of the two types of charge transfer show different relations with potential and exciting frequency. For example, for the molecule to metal charge transfer, the maxima will shift to more negative potential if the exciting frequency is increased, but the maxima will shift to more positive potential with the increase of the exciting frequency for the metal to molecule charge transfer.[4]

(c) Time-Resolved SERS

The non-time-resolved SERS technique can be used to study steady state chemistry at different conditions, such as pH, temperature and potential dependence. However, no kinetic information could be obtained, especially the information for short-lived transient species. Time-resolved SERS is a very powerful real-time in-situ detection technique. It allows one to follow a physical or chemical process, such as adsorption/desorption, electrochemical oxidation/reduction or surface related chemical reaction processes, by obtaining SERS spectrum in ms or even μs.

Suppose an electrochemical process undergoes an EC mechanism

$A + e^- = B$ $\qquad E^0, k^0$

$B \rightarrow C$ $\qquad k_C$

where E^0 and k^0 are the standard electrode potential and heterogeneous rate constant for the electron transfer reaction, respectively, and k_C is the rate constant of the chemical step. The SERS of the steady state at a potential more positive than E^0 corresponds to species A. The steady-state spectrum obtained at a potential more negative than E^0 is related to species C. Nothing about species B can be obtained from the steady state measurement, since all B will be converted to C at steady state, assuming the chemical step is not extremely slow. In this case, the time resolved technique makes the observation of species B possible. Time-resolved SERS technique allows one to follow the whole process, unless the reaction is finished in a few nano seconds. For example, the experimental results will show a gradually decrease in A's spectrum and an increase in C's spectrum. However, B's spectrum will increase at the beginning and then decreases after a maximum. Theoretically, the decreasing rate of A's spectrum is directly related to the rate of the electron transfer step and the rate

of the chemical step could be obtained from the intensity profiles of species B and C. It is possible to find unique bands for each species since SERS is a highly resolved vibrational spectrum. Sometimes, the well-defined spectra of species A and C can be subtracted from the mixture's spectra so that a "pure" spectrum of species B could be obtained and this in turn makes it possible to analyze the structure of the unstable species B.

For more complicated electrochemical processes time-resolved techniques become even more important in the elucidation of the kinetics and mechanisms and this will be discussed in later chapters.

Section 1.3 Interpretation of Raman Spectra

A Raman spectrum, like an IR spectrum, is of the vibrational type. It provides information about the details of the structure of the compounds examined. Therefore, it can be used for "identifying unknown substances, detecting particular atomic groups and bond types linking the atoms, defining the geometric structure of molecules, and total analysis of vibrations."[13]

A simple way to identify an unknown substance is to compare its spectrum with a library of the spectra of known compounds and select the one which has an identical spectrum as the compound examined, since only molecules with the same atomic configuration have identical spectra. However, this simple spectrum-matching method is not commonly used because libraries of Raman spectra are not yet sufficiently available for this purpose unless the unknown substances are known to be in some special categories.[13] Thus the interpretation of Raman spectra becomes very important for structure analysis of unknown substances. The interpretation of Raman spectra is based on the normal mode analysis. A non-linear molecule that consists of N atoms has 3N-6 normal vibrations. As mentioned before, the Raman shifts corresponds to the energy differences between the first excited vibrational states and ground state. The frequencies of these vibrations can be calculated for simple molecules with high symmetry, but such a calculation is not often made since it requires information on the space arrangement of the atoms within the molecule and on force constants and this kind of information is not always available for complicated molecules. However, the spectra of complicated molecules can be interpreted by using information obtained from simple molecules and empirical knowledge. The interpretation is based on the concept of localized vibrations.[13]

If, owing to the excitation of one normal vibration of the molecule, one molecular fragment oscillates much greater than other groups of atoms, then this vibration is said to be a localized vibration. This is caused by the weak coupling between this part of the molecule and other components. As a result, its vibrational frequency will be affected only slightly by the substitution on the other parts of the molecule. Thus this frequency can be chosen as a characteristic criterion for the identification of the group.[13-16] The basic structure of the complicated molecule can be built up by using empirical knowledge to put together all the information about the functional groups, the molecular weight and the empirical formula. Of course, all the information available for the compound, such as melting point, boiling point, acidic or basic dissociation constant, etc., would be helpful for the structure analysis.

It is obvious that a better understanding of the vibration modes of basic molecules with different types of symmetry will become the bases for spectral interpretation and structural analysis.[2,14] The different selection rules for the transitions allowed in each case make the difference between Raman and IR spectroscopies. For those molecules with a center of symmetry, a vibration which is IR active ($(d\mu/dQ)\neq 0$) is inactive in Raman spectrum and vice versa. In the case of molecules without a center of symmetry, a number of vibrations can appear in both spectra but their relative intensities in each spectrum are different. For example, the vibrations of strongly polar groups are more easily observed in IR, but the double and triple bonds and the carbon-skeleton vibrations are better seen in Raman.

According to quantum theory, the intensity of an infrared band is proportional to the square of the transition moment

$$\int \psi_f^* \mu \psi_i d\tau$$

where ψ_i^* is the wavefunction of the ground vibrational state and ψ_f^* the complex conjugate of the wavefunction of the final vibrational state involved in the transition. The integral must be non-zero in order for the transition $\psi_i \mu \psi_f$ to be infrared active. In group theory, this means that there must be at least one common irreducible representation contained in both the representations of product $\psi_f^* \psi_i$ and μ. The characters of the representations of the dipole moment vector for a point group are given by[14]

$$\chi_M(R) = \pm 1 + 2\cos\varphi \qquad (1.9)$$

where R is an element or operation of the point group, φ is the angle of rotation. The selection of "+" or "-" sign in the equations depends on the property of the rotation. The "+" sign is chosen for proper rotations and "-" for improper rotations which is a proper rotation followed by a reflection in a plane perpendicular to the axis of rotation. A reflection by a plane of symmetry is an improper rotation through an angle of zero degree. The characters of the representations of the product $\psi_f^* \psi_i$ are given by the direct product of the characters of ψ_f^* with ψ_i and are the same as the characters of ψ_f^* since ψ_i is totally symmetric to the point group and its characters are all unity. Thus it is necessary in an IR active vibration that the representation of the vibration contains at least one irreducible representation common to the dipole moment vector.

Similarly a Raman allowed transition requires that the representation of the vibrations involved contains at least one irreducible representation common to the polarization tensor. The characters of the representation of polarizability are given by[14]

$$\chi_\alpha(R) = 2 \pm 2\cos\varphi + 2\cos 2\varphi \qquad (1.10)$$

where all the symbols have the same meanings as described above.

Since the components of the dipole moment vector μ, μ_x, μ_y and μ_z transform in the same way as the components of the space vector **p**, x, y and z, and the components of the polarization tensor α, α_{xx}, α_{xy}, etc., transform the same way as the products of two Cartesian coordinates, xx, xy, etc., the selection rules are also expressed as follows.[13,14]

(1) The fundamental vibration is active in IR if the related normal vibration belongs to the same representation as one of the Cartesian coordinates.

(2) The fundamental vibration is active in Raman if the related normal vibration belongs to the same representation as one or several products of the Cartesian coordinates.

As an example, the symmetry of ethylene is given here. Ethylene belongs to point group D_{2h} which is listed in Table 1.1. The number of irreducible representations appearing in the reducible representation can be found with equation [14,17]

$$N_i=(1/h)\sum n_e\chi_\Gamma(R)\chi_i(R) \qquad (1.11)$$

where h is the order of the point group, n_e is the number of elements in each class, $\chi_\Gamma(R)$ is the character of the reducible representation for the operation (R), $\chi_i(R)$ is the character of the irreducible representation type i for the operation (R) and the summation is over all of the classes. Then the reducible representations of dipole moment and polarizability can be reduced as

Table 1.1 Characters of the Irreducible Representations of D_{2h}

D_{2h}	I	σ_{xy}	σ_{xz}	σ_{yz}	i	C_{2z}	C_{2y}	C_{2x}	
A_g	1	1	1	1	1	1	1	1	$\alpha_{xx},\alpha_{yy},\alpha_{zz}$
A_u	1	-1	-1	-1	-1	1	1	1	
B_{1g}	1	1	-1	-1	1	1	-1	-1	R_z, α_{xy}
B_{1u}	1	-1	1	1	-1	1	-1	-1	z
B_{2g}	1	-1	1	-1	1	-1	1	-1	R_y, α_{xz}
B_{2u}	1	1	-1	1	-1	-1	1	-1	y
B_{3g}	1	-1	-1	1	1	-1	-1	1	R_x, α_{yz}
B_{3u}	1	1	1	-1	-1	-1	-1	1	x
$\chi_M(R)$	3	1	1	1	-3	-1	-1	-1	
$\chi_\alpha(R)$	6	2	2	2	6	2	2	2	

$$\chi_M(R)=\chi_{B1u}(R)+\chi_{B2u}(R)+\chi_{B3u}(R)$$

or $\Gamma_M = B_{1u} + B_{2u} + B_{3u}$

which means that only those vibrations containing at least one of the three irreducible representations, B_{1u}, B_{2u} or B_{3u} are IR active.

and $\chi_\alpha(R)=3\chi_{Ag}(R)+\chi_{B1g}(R)+\chi_{B2g}(R)+\chi_{B3g}(R)$

or $\Gamma_\alpha = 3A_g + B_{1g} + B_{2g} + B_{3g}$

which means that only those vibrations containing at least one of the four irreducible representations, A_g, B_{1g}, B_{2g} or B_{3g} are Raman active.

The number of normal vibrations of ethylene is 3N-6=12. Let the stretching of the C-H bonds be v(1), v(2), v(3) and v(4), the motions perpendicular to them be y(1), y(2), y(3), y(4) and z(1), z(2), z(3), and z(4) and

the stretching of the C-C bond be V(1) and V(2) and the perpendicular motions be Y(1), Y(2), Z(1) and Z(2). Then the character of the reducible representation for the operation (R) is given by [2,14]

$$\chi(R)=(U_R-2)(1+2\cos\varphi) \qquad (1.12)$$

for a proper rotation and

$$\chi(R)=U_R(-1+2\cos\varphi) \qquad (1.13)$$

for an improper rotation, where U_R is number of atoms unshifted by the symmetry operation (R) and φ is the angle of rotation. The characters of the reducible representation of the vibrations are listed in Table 1.2 and reduced to the irreducible representations,

$$\Gamma = 3A_g + A_u + 2B_{1g} + B_{1u} + 2B_{2u} + B_{3g} + 2B_{3u}$$

Table 1.2 Characters of Normal Mode Vibrations of Ethylene

D_{2h}	I	β_{xy}	β_{xz}	β_{yz}	i	C_{2z}	C_{2y}	C_{2x}
U_R	6	6	0	2	0	0	2	0
$\pm1+2\cos\varphi$	3	1	1	1	-3	-1	-1	-1
$\chi(R)$	12	6	0	2	0	2	0	2

The wavefunctions of these normal vibrations can be obtained by projecting the internal coordinates. The projecting operator of the irreducible representation type i is given by [14,17]

$$\mathbf{P}_i = N\sum\chi_i(R)\mathbf{R} \qquad (1.14)$$

where N is a normalizing factor, **R** is a symmetry operator and the summation is over all element in the point group. For A_g symmetry the three wavefunctions are

$\Psi_{Ag}(1)=(1/\sqrt{6})\{[V(1)+V(2)]+[v(1)+v(2)+v(3)+v(4)]\}$

$\Psi_{Ag}(2)=(1/\sqrt{6})\{[V(1)+V(2)]-[v(1)+v(2)+v(3)+v(4)]\}$

$\Psi_{Ag}(3)=(1/2)[y(1)-y(2)+y(3)-y(4)]$

The other Raman active vibrations are given as follows,

$\Psi_{B1g}(1)=(1/2)[v(1)-v(2)+v(3)-v(4)]$

$\Psi_{B1g}(2)=(1/\sqrt{6})\{[Y(1)+Y(2)]-[y(1)+y(2)+y(3)+y(4)]\}$

$\Psi_{B3g}=(1/\sqrt{6})\{[Z(1)-Z(2)]-[z(1)+z(2)-z(3)-z(4)]\}$

and the IR active vibrations

$\Psi_{B1u}=(1/\sqrt{6})\{[Z(1)+Z(2)]-[z(1)+z(2)-z(3)-z(4)]\}$

$\Psi_{B2u}(1)=(1/2)[v(1)+v(2)-v(3)-v(4)]$

$\Psi_{B2u}(2)=(1/2)[y(1)-y(2)-y(3)+y(4)]$

$\Psi_{B3u}(1)=(1/2)[v(1)-v(2)-v(3)+v(4)]$

$\Psi_{B3u}(2)=(1/\sqrt{6})\{[Y(1)-Y(2)]-[y(1)+y(2)-y(3)-y(4)]\}$

and a vibration which is neither IR nor Raman active

$\Psi_{Au}=(1/2)[z(1)-z(2)+z(3)-z(4)]$

Figure 1.2 gives the normal modes of these vibrations.

As the second example, The normal modes analysis results for pyridine are summarized in Figure 1.3, [1,13,14,16,18-22] where the normal modes, their symmetries and frequencies are listed since the frequency assignment will be used later for the experiment results interpretation. Pyridine is a planar molecule belonging to point group C_{2v}. There 27 vibrational normal modes all together. These modes can be classified into bond stretching modes (ν), ring angle changing modes (α), CC bond out-of-plane motion modes (ϕ), CH bond in-plane banding modes (β) and CH bond out-of-plane banding modes (γ). There are four irreducible representations in C_{2v}: A_1, A_2, B_1, and B_2. The

characters of the dipole moment and polarizability are calculated easily according to equations (1.9) and (1.10) and given in Table 1.3 together with the irreducible character table of C_{2v} and they can be reduced according to equation (1.11),

$$\Gamma_M = A_1 + B_1 + B_2 \qquad (1.15)$$

and

$$\Gamma_\alpha = 3A_1 + A_2 + B_1 + B_2 \qquad (1.16)$$

It is obvious from equations (1.15) and (1.16) that transitions with A_1, B_1 and B_2 symmetries are allowed for IR but with A_2 symmetry are forbidden. All the transitions are symmetrically allowed for Raman.

Table 1.3 Character Table of C_{2v} Point Group

C_{2v}	I	C_2	σ_{xz}	σ_{yz}
A_1	1	1	1	1
A_2	1	1	-1	-1
B_1	1	-1	1	-1
B_2	1	-1	-1	1
χ_M	3	-1	1	1
χ_α	6	2	2	2

Section 1.4 Experimental Considerations

The time-resolved SERS techniques include one-shot and multi-exposure experiments. The one-shot experiment is suitable for those compounds which have intense SERS signal and the data acquisition time for this experiment is usually longer than milliseconds. There is no restriction on the reaction types for one-shot experiment, i.e., all reversible, irreversible and quasi-reversible reactions could be studied if they have strong SERS spectra. The multi-exposure experiment can be used to deal with those compounds with weak SERS spectra or to obtain much shorter time-resolved SERS spectra, such as in micro seconds or even in nano seconds for those compounds which have very intense SERS signals. However, one thing which has to be kept in mind is that the result of the multi-exposure experiment is obtained by co-adding several hundreds or thousands measurements; therefore, it is an average of these measurements. For a reversible experiment, the multi-shot experiment works as well as the one-shot experiment and produces true information about the chemical process. However, for the irreversible reactions, before the new measurement efforts have to be made to eliminate the effect coming from the proceeding measurements, i.e., to get rid of the products produced in the proceeding measurements. Unlike the measurements made in solution where the proceeding effect can be easily removed by flowing the solution, SERS measures the molecules adsorbed on the metal surface which can not be removed by simply flowing the solution. In order to get rid of the product produced in preceding measurement, a re-pretreating potential pulse is applied on the electrode after each measurement. This re-pretreatment ensures that every measurement starts from the same conditions so that the co-added results can reflect the real situation.

There are two configurations of the experimental setup, one for potential-initiated time-resolved SERS and the other for photo-initiated time-resolved SERS measurements. The experimental setup for a potential-initiated time resolved SERS measurement is shown in Figure 1.4. In this configuration, the perturbing signal is an electrode potential pulse which is generated by a waveform generator (175 PARC) and applied on the Ag working electrode in a specially designed three-electrode electrochemical cell through a potentiostat (173 PARC). The Raman detection system includes an Argon ion laser (Spectra Physics Model 164), a SPEX triplemate monochromator, a gated photodiode array detector (EG&G PAR Model 1455), a detector interface (OMA, EG&G PARC Model 1461), a Macintosh computer and some photo lenses. The laser light is focused first by a focusing lens, which then irradiates the working electrode surface with an angle about 45 degrees. The scattering light is collected in the right angle and focused onto the entrance slit of the triplemate by two lenses with large diameter and short focal length. The photodiode array detector mounted on the triplemate is gated by a pulse amplifier (EG&G PAR Model 1304) which is in turn controlled by the Macintosh computer through the detector interface. The detector pulsewidth (data acquisition time), time delay and number of repeating cycles is set through a computer program, MacOMA. The synchronization of the potential pulse and the detector pulse is made by triggering the waveform generator and the detector interface with another signal generator which determines the recycle time.

Figure 1.5 shows the configuration of the experimental setup for a photo initiated time-resolved SERS measurement. Compared to the configuration given in Figure 1.4, another nitrogen pulsed laser is added to the system and

the waveform generator and the signal generator are taken out. For the photo initiated experiment, the nitrogen laser light pulses are used as pumping pulses to initiate the reaction and the Argon CW light as a probing light to measure the time-resolved SERS spectra; the electrode potential is set to a constant value. The choice of frequencies of laser light and the electrode potential depends on the compounds measured and other experimental conditions such as pH value and electrode materials. Furthermore, the frequencies and the electrode-potential are also correlated to each other. The choice of the experimental conditions is very important. In order to get the best experimental results, the following principles have to be kept in mind: (1) an electrode potential is chosen at which the pumping light can induce a photoelectrochemical reaction but the probing light can not; (2) the electrode potential is chosen within the region required by (1) to get the best surface enhancement effect.

In the photo initiated time-resolved SERS experiments, the nitrogen laser pulse works as both a reaction initiator and a master controller. Its pulsed light is focused on the working electrode to initiate the photoelectrochemical reaction and a small fraction of the pulses is used to trigger the OMA controller interface to synchronize the detection. The probing light is focused on the same point as the pulse light and its focus spot is a little bit smaller than that of the pulse light to make sure that only signal coming from the photolysed area are measured. The electrode potential is kept at a fixed value throughout the experiment. As in the potential initiated experiment, the detector pulsewidth (data acquisition time), time delay and number of repeating cycles are controlled through a MacOMA program.

Section 1.5 A Brief Review of the Applications of Time-Resolved Raman Spectroscopy in Chemistry and Biochemistry

Time-resolved Raman spectroscopy, especially time-resolved resonance Raman spectroscopy, has been used to study organic compounds, inorganic complex, and important biological molecules. For example, bacteriorhodopsin (bR), which is a protein contained in the cell membrane of halobacterium halobium which converts visible light into chemical energy, was studied by the time-resolved resonance Raman spectroscopy using sample-flowing[23] and pico-second pulsed laser techniques,[24] respectively. These experimental results further confirmed the mechanism of the photocycle proposed by other researchers[25-28],

$$bR_{570} + h\nu \rightarrow K_{610} \rightarrow L_{550} \rightarrow M_{412} + H^+ \rightarrow O_{640} \rightarrow bR_{570}$$

The configurations of retinal and b-carotene isomers in the lowest-excited triplet-state were studied by time-resolved Raman spectroscopy with direct flash- photolysis.[29] Two kinds of triplets, "all-trans-like" triplet and "9-cis-like" triplet, were detected.

Time-resolved resonance Raman spectroscopy was also used in detection of the intermediates of cytochrome c oxidase during the catalytic reduction of oxygen.[30] Cytochrome c oxidase is an enzyme with dual functions: catalysis for reduction of molecular oxygen to water and proton transfer coupled with electron transfer.[31] The spectra of the photo-reduced intermediates in both aerobic and anaerobic conditions were obtained by comparing the spectra with cell spinning and without cell spinning. The oxygenated intermediate during the

catalytic reduction of oxygen was detected by using a Mixed Flow Transient Raman Apparatus and a CW laser.

Since most biological molecules absorb UV light and therefore produce very intense resonance Raman signal, UV resonance Raman has been found very useful in probing biological molecules. A very general application of Raman spectroscopy in the study of biological molecules was made by T. G. Spiro and co-workers,[32] where the fourth harmonic line of a YAG laser (266 nm) and the first, second, and third anti-Stokes H2-shifted lines (240, 218, and 200 nm) are employed as the probing wavelengths. Good quality spectra were obtained at these wavelengths for proteins, and their constituent peptide, phenylalanine, tyrosine, and tryptophan chromophores, and also for nucleic acids and the nucleotides. Probing in different absorption bands selectively excites some of the Raman bands, which give rise to intense signals, and makes the spectra look different. The pH value of the solution and isotopes of the solvent were also found to have effects on the resonance Raman spectra of some biological compounds. The time-resolved study was focused on the hemoglobin,[33,34] and myoglobin,[35,36] photodynamics. Nanosecond and even picosecond Raman spectra were measured and a T-like quaternary structure was found to be formed within 7 ns of the photolysis of hemoglobin CO complex.

The resonance Raman technique was also used to study an enzyme-substrate intermediate.[37] The stimulated anti-stokes Raman line of hydrogen, 238 nm, which was generated by the fourth harmonic of the YAG laser, was used as the probing light in order to get the best resonance effect and to avoid the influence of the aromatic residues on the spectrum. A micro-mixing-flowing

device was designed to mix the enzyme with the substrate and drive the sample flowing slowly through a micro Raman cell to avoid decomposing of the sample.

Horseradish peroxidase (HRP) is one of the hemoproteins which contain protoheme IX at the active site. It catalyzes the oxidation of various substrates by using peroxide as oxidant.[38,39] The reaction mechanism is proposed as

$$PFe(III) + H_2O_2 \rightarrow comp(I)$$

$$comp(I) + AH \rightarrow comp(II) + A\cdot$$

$$comp(II) + AH \rightarrow PFe(III) + A\cdot$$

Recent time-resolved resonance Raman spectroscopic studies on the native HRP, heme-substituted, magnesium-substituted HRPs,[40,41] and O^{18} isotope-substituted HRP,[42,-45] showed that a Fe(IV)=O bond was formed in the intermediate comp(II). The frequency of the Fe=O stretching vibration depends on the heme substitutes and the pH value of the buffered solution.

Time-resolved resonance Raman spectroscopy was used to study the first excited singlet state of trans-stilbene[46-50] which is transitional state during the stilbene cis-trans isomerization and the observed singlet state Raman bands have been assigned according to normal-coordinate calculations.[51]

Time-resolved resonance Raman spectroscopy is also a very important technique in the studies of photochromism. Some compounds can change their colors upon irradiation of UV light and this behavior could be used as optical recording media for image and data storage and retrieval systems. The photochromic processes have been studied by time-resolved resonance Raman spectroscopy and more information about the structure of the transient species and the photochromic mechanisms of these compounds have been

obtained.[52]

Another very interesting application of time resolved Raman spectroscopy is the measurement of the dynamics of energy-partitioning among different vibrational modes, one of them being under resonance excitation.[53-55] The experiment is based on the simple relationship between the integrated spontaneous Raman band signal I_i and the average vibrational energy ε_i stored in the ν_i mode being probed

$$I_i^{AS} = A\varepsilon_i/h\nu_i$$

for the anti-Stokes bands and

$$I_i^{S} = B(1+\varepsilon_i/h\nu_i)$$

for the Stokes bands. The molecules were excited by CO_2 laser radiation and the Raman spectrum was probed by the second harmonic of Nd:YAG laser and recorded by both photon-counting and multichannel systems. The time resolution was 10 ns. The experiment found that during the collision the molecular energy redistributes among all the modes and transfers from the high-frequency modes to the low-frequency modes.[55]

Section 1.6 Research Work in this Thesis

In this thesis, the adsorption, electroreduction and electrooxidation of several compounds are to be investigated by time-resolved SERS, electrochemistry and digital simulation. The main purpose of this research is to demonstrate the power of time-resolved SERS combined with fast electrochemical techniques for the study of electrochemical processes. The method proves especially ideal for the detection of short-lived intermediates, identification of products, and the investigation of kinetics of adsorption and electrochemical processes. Although the compounds studied are not very complicated, the techniques developed here can be easily applied to many kinds of inorganic, organic, surface catalytic and biological systems. In Chapter II, the electrochemical reduction-oxidation processes and the photo-assisted under-potential reduction of 4-nitrobenzoic acid (PNBA) are investigated by time-resolved SERS, cyclic voltammetry (CV) and digital simulation. Time-resolved SERS spectrum corresponding to each stage on the cyclic voltammogram are recorded by multi-channel detection technique and are compared with the spectra of the authentic compounds. A transient spectrum is observed by ms time-resolved SERS when coupled with a double electrode potential step technique. The kinetics and possible mechanism of the electroreduction of this nitro compound are also discussed according to the CV, time-resolved SERS and digital simulation results. In Chapter III, IV and V, the adsorption, protonation and electrochemical reduction of 4-cyano-pyridine (4-CNPY), 4-pyridinecarboxaldehyde (ALPY), 4-(hydoxymethyl)pyridine (HMPY) are studied mainly by time-resolved SERS and cyclic voltammetry. The time resolution is increased from 10 ms to 100 μs and 10 μs which illustrates that faster electrochemical processes can be followed. The SERS spectra obtained

are discussed in some detail according to the band assignments. The stable products are identified with the authentic compounds and the unstable intermediates are discussed according to the proposed mechanisms.

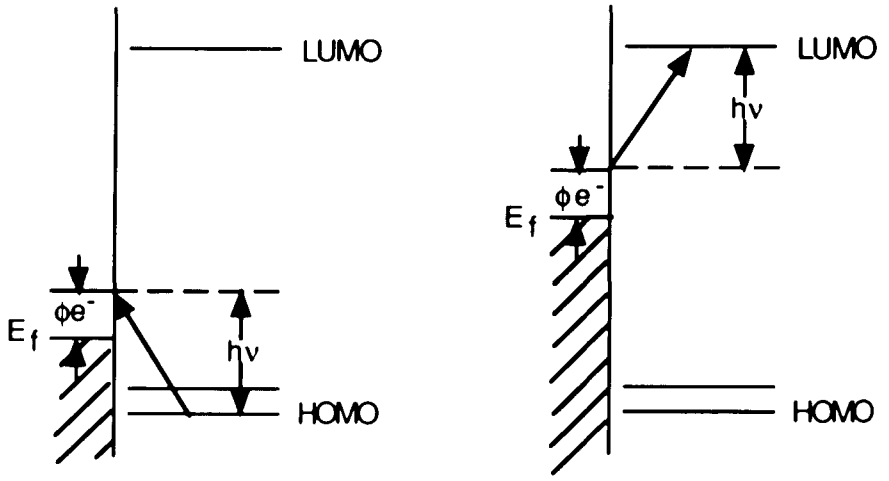

Fig. 1.1 Schematic diagram of the quantum theory of surface-enhanced Raman scattering. E_f: Fermi level of a Ag metal; LOMO: the lowest occupied molecular orbital; HUMO: the highest unoccupied molecular orbital.

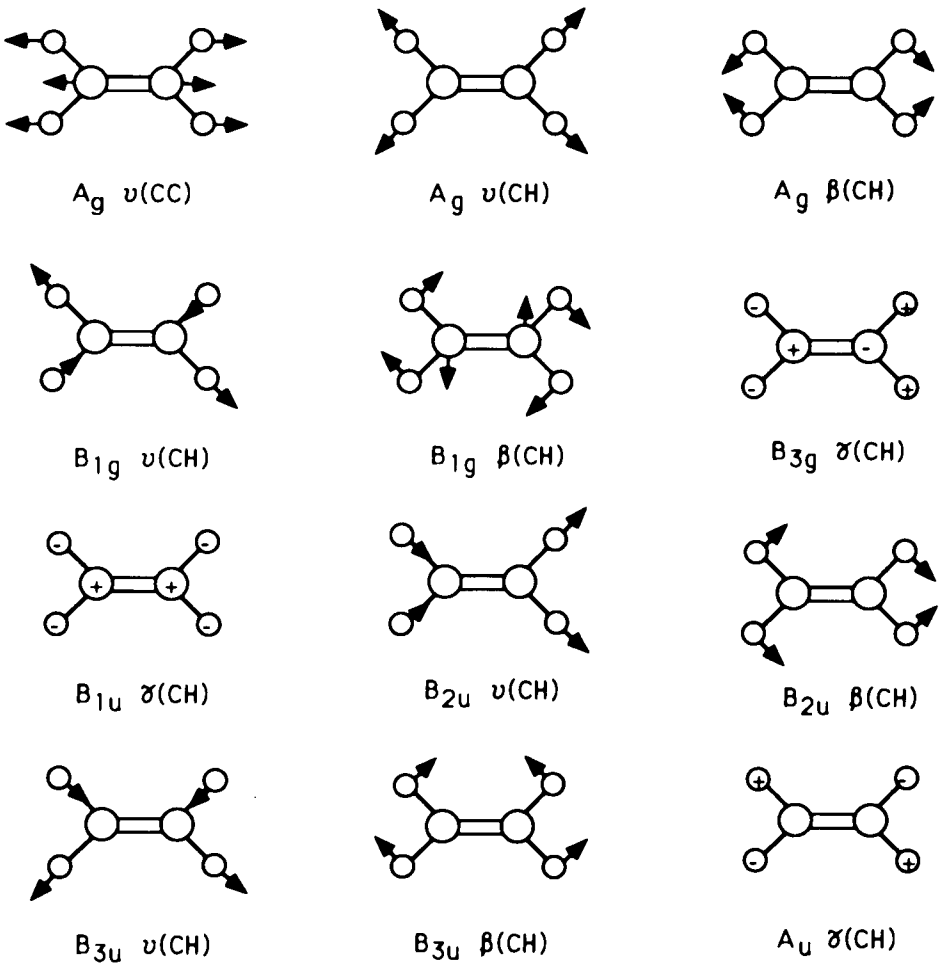

Fig. 1.2 The 12 normal mode vibrations of an ethylene molecule.

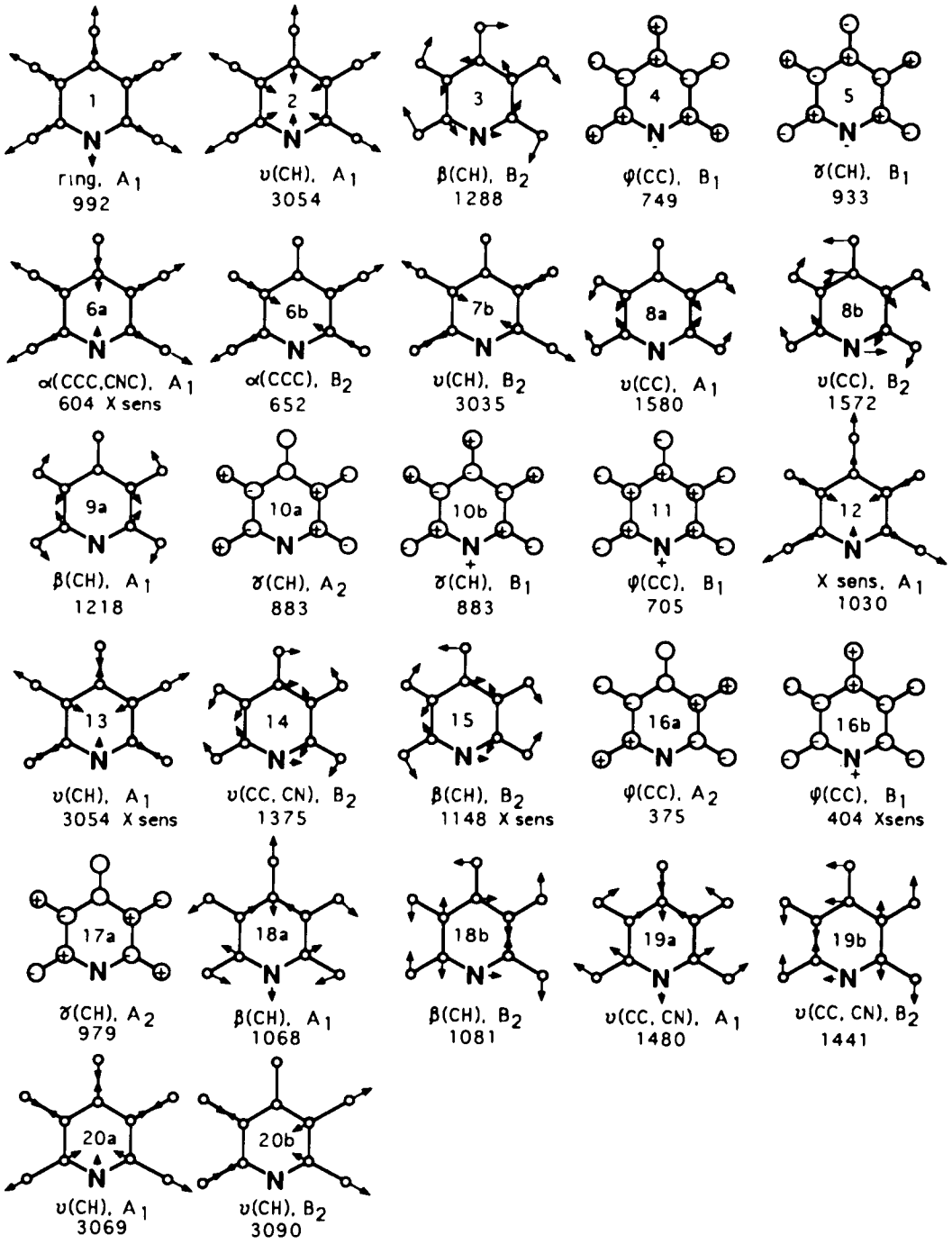

Fig. 1.3 The 27 normal mode vibrations of a pyridine molecule.

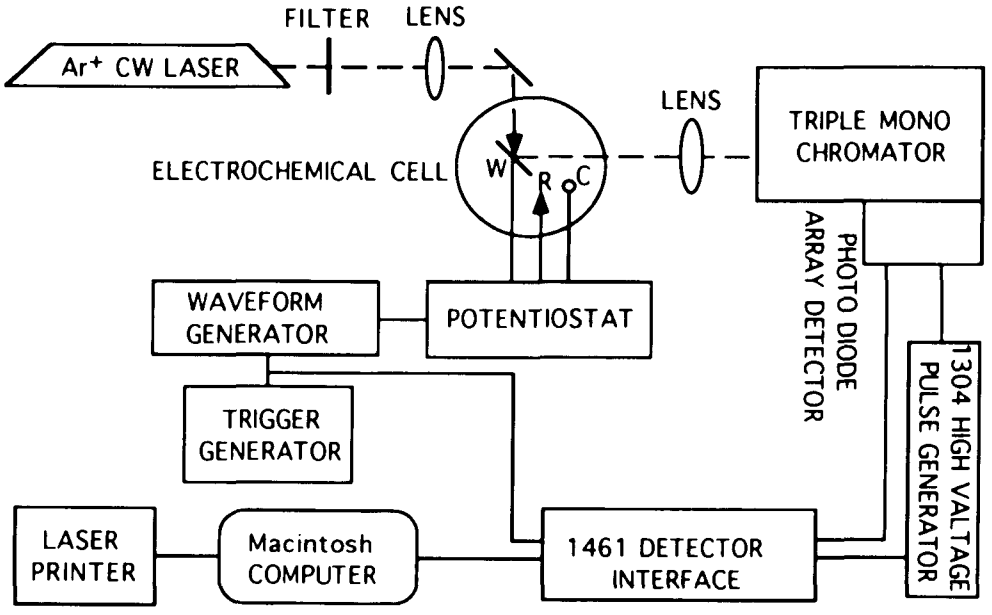

Fig. 1.4 Experimental setup of a potential-initiated time-resolved surface enhanced Raman spectroscopic measurement.

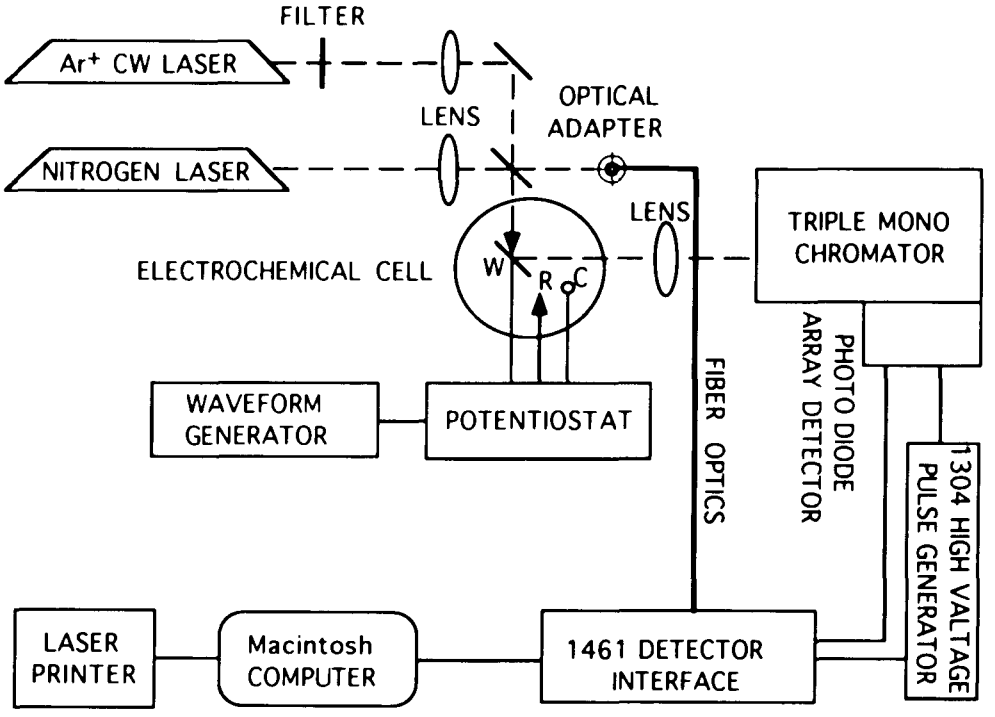

Fig. 1.5 Experimental setup of a photo-initiated time-resolved surface-enhanced Raman spectroscopic measurement.

Chapter II

Time-Resolved SERS, Cyclic Voltammetry, and Digital Simulation of the Electroreduction of p-Nitrobenzoic Acid

Section 2.1 Introduction

Investigations of the electrochemical reduction processes of aromatic nitro-compounds have a long history in the chemical literature having been discussed as early as 1908.[1] More recent reviews of this rather involved electrochemistry can be found in several books which cover electroorganic mechanisms,[2-6] and several fairly recent experimental studies have been made.[7-12] The mechanism of electrochemical nitro reduction is complicated by a dependence on pH and cathode material.[2-6,12] In alkaline medium, intermediate products such as nitroso and hydroxylamine compounds are found which can react chemically to produce an azoxy compound which may be further reduced to azo and hydrazo compounds and eventually reduced to an amino compound.[2-6]

Considering the complicated nature of this electrochemistry, the use of an in situ spectroscopic probe such as Raman spectroscopy certainly would aid in mechanistic elucidation. Thus normal Raman spectra as well as the surface enhanced Raman spectra (SERS) of these compounds have been obtained on silver and gold electrodes.[13-20] We have recently investigated the electroreduction of p-nitrobenzoate using the SERS technique and found, in the presence of the laser excitation, a time dependency in the spectra even at potentials positive to the electrochemical reduction wave.[17] This behavior was attributed to a photoinduced reduction process involving electrode reactions following an initial laser induced photolysis step. Our dynamic studies were performed at fixed potential on the time scale of seconds to minutes and the details of the mechanism could only be presumed. Other investigations of the electroreduction of nitro compounds have been carried out by time-resolved

SERS on a similar time scale in order to identify products or intermediates;[18-19] however, again only the long-lived or stable intermediates were detected since the time scale was in seconds.

Recently, we have shown it is possible, using time-resolved SERS (TRSERS) triggered with an electronically controlled shutter,[23] to detect an unstable intermediate with a lifetime of less than a 100 ms at a Ag electrode by applying a reduction-oxidation double potential step to a system containing p-nitrobenzoate. We now investigate this chemical system from the point of view of the overall electrode process occurring in cyclic voltammetry. We present some spectra of intermediates and products whose band positions were previously summarized[23] in order to discuss the nature of the electrochemical process which produces the unstable intermediate, assigned as the p-nitrosobenzoate radical anion. A related unstable intermediate, the nitrobenzene radical anion, had been detected in earlier studies during electroreduction using an ESR method in aqueous solutions[9,21,22] and with both CV and ESR methods in anionic and nonionic micelles.[10] In fact, the nitrosobenzene radical anion has also been detected by ESR during the electroreduction process of nitrobenzene on a gold electrode[11]. The SERS technique is, in addition to ESR, a method for the in situ investigation of transient radical (as well as non radical) species generated electrochemically, and it allows structural elucidation along with a rapid dynamic response for species directly at the electrode surface.

In the present work, we again utilize TRSERS methods employing a triggered shutter to further elucidate the mechanism of electrochemical and photoelectrochemical reduction of p-nitrobenzoic acid (PNBA) on Ag, by obtaining rapid scan OMA SERS spectra at various potentials (times) on fast CV

sweeps. The use of TRSERS method as the electrode potential is swept shows that nitroso and hydroxylamine species are formed by electrode reactions in different regions of the potential scan and that on the third half-cycle of the voltammogram, the chemical reaction of these two species affects the features of the voltammogram. Thus, the TRSERS method during CV scans allows us to identify the chemical nature of processes occurring as the potential is scanned. This information along with the morphology of the CV curve is used to elucidate the overall reduction mechanism as a function of electrode potential. A digital simulation of the CV curves was also run in order to confirm the mechanism and estimate heterogeneous rate constants and formal electrode potentials for individual electrochemical steps along with the rate constants for the homogeneous chemical steps.

Section 2.2 Experiment

All spectra were excited with a Spectra Physics Ar^+ model 164 laser and recorded with a Spex 1877 Triplemate spectrometer with an intensified Tracor Northern photodiode linear array (TN-1223-2I) and a model TN-1710 Tracor Northern optical multichannel analyzer (OMA). A grating of 1800 groves per mm gave a spectral coverage of about 900 cm^{-1} with a band pass of around 2 cm^{-1} at 19,436 cm^{-1}. The electrode potential was controlled with an EG&G PARC model 173 potentiostat and EG&G PARC model 179 waveform generator. The experiment was initiated by simultaneously triggering an electronic shutter, the waveform generator, and the OMA. A potential ramp of a given number of cycles could be applied to the electrode and up 16 spectra measured by the OMA at various set times on this potential waveform. The response time of this system was limited by a 7 ms response time of the electronically controlled shutter and a 10ms minimum dwell time for recording of a single spectrum.

PNBA was reagent grade and used without further purification. All salts, acids and bases were also reagent grade and all dilutions were made with deionized-distilled water. P-hydroxylaminobenzoic acid (PHABA) was synthesized according to the literature[24] and the product recrystalized three times in distilled water. P-nitrosobenzoic acid (PNSBA) was prepared[25] by using Tollens' reagent to oxidize PHABA with a molecular ratio 5:2. After acidification with concentrated HCl, the product was extracted into ether and from ether into a basic aqueous solution. In both electrochemical and SERS studies, the pH value of the solutions was adjusted to 11 by adding NaOH in order to increase the solubility of PNBA. Sodium sulfate was used as supporting electrolyte, since the SERS intensity observed for PNBA was much larger when

sulfate or nitrate was used as the electrolyte.[17] All electrode potentials are quoted versus the saturated calomel electrode, SCE.

The 488 nm line of the Ar^+ laser with a power of 150 mW was used for both photochemically excitation and probe beams and a filter was used to remove the laser plasma lines.

In slow potential sweep experiments, the CV curves were drawn directly by an X-Y recorder. For the fast potential sweep experiments, the data were collected and stored on a diskette using a digital oscilloscope (Model 206, Nicolet Instrument Corporation) and subsequently plotted on the X-Y recorder. Both smooth and roughened Ag electrodes were used in the CV experiments for comparisons. The smooth electrode was obtained by mechanical polishing with various grades of alumina down to 0.3μ. The roughened electrode was obtained electrochemically by pretreating a polished Ag electrode in 0.05M PNBA aqueous solution containing 0.1M Na_2SO_4. Two oxidation-reduction cycles (ORCs) were applied where the electrode potential was jumped from 0.0V to +0.5V for 2 seconds and then returned to 0.0V again. All SER spectra were taken on roughened electrodes.

Section 2.3 Results and Discussion

(a) Cyclic voltammetry

CV curves taken with 5 mM PNBA solution on a smooth Ag electrode show, at moderate potential scanning rates, two cathodic waves, A and B at about -0.65V and -1.2V with an anodic wave, C, at about -0.3V (Fig. 2.1a). The first cathodic peak, A, has been assigned[3-5] to a four-electron reduction of the

nitro compound to a hydroxylamine compound, reaction (2.1), and the second cathodic wave, B, to a further two-electron reduction to an amino compound, reaction (2.2)

$$Ar\text{-}NO_2 + 4e^- + 4H^+ = Ar\text{-}NHOH + H_2O \qquad (2.1)$$

$$Ar\text{-}NHOH + 2e^- + 2H^+ = Ar\text{-}NH_2 + H_2O \qquad (2.2)$$

The cathodic peak current for wave A is diffusion controlled on the smooth Ag electrode since the peak current is linearly dependent on the square root of scan rate. On a roughened Ag electrode(Fig. 2.1b), the CV curve under the same conditions has the same general shape as on the smooth electrode except for the shoulder on the rise of peak A. This shoulder may be a prepeak caused by an adsorbed species. Although the main peak A is shifted by about 110 mV in the positive direction, it is still diffusion controlled also being linearly dependent on the square root of scan rate. We have explained the shift in overpotential to a catalytically activate surface sites on the roughened Ag surface.[17] On the other hand, the peak potentials of peaks C and D do not shift on the roughened electrode, and the overall morphology of the CV curves is similar enough on both the smooth and rough Ag electrodes to conclude that, with the exception of adsorbed species, the same type of electrode mechanism is occurring in the two cases.

The anodic wave C (Fig. 2.1) is still present when the potential sweep is reversed before the second cathodic wave B develops, and it corresponds to oxidation of p-hydroxylaminobenzoate, which is formed during the first negative-going sweep, to p-nitrosobenzoate in a process involving two electrons. SERS spectral evidence for these assignments is presented below. The anodic wave C becomes lower as the switching potential is changed to

more positive values and it disappears if the switching potential is more positive than -0.45V which is right at the foot of the first cathodic wave, indicating that it is coupled to this wave. Thus PNBA is electrochemically stable in the potential region from 0.0V to about -0.45V.

A new reduction peak, D, appears in Fig. 2.1 at about -0.35V on the second negative-going potential scan which is paired with the anodic peak C and is thought to be the reduction of newly formed nitroso compound.

$$Ar\text{-}NO + 2H_2O + 2e^- = Ar\text{-}NHOH + 2OH^- \qquad (2.3)$$

However, the cathodic peak D is smaller than the anodic peak C when slow potential scanning rates are used, e.g., 100 or 200 mV/s, (see Fig. 2.1 and Fig. 2.2). In higher PNBA concentration (50mM), the cathodic peak D nearly disappears (Fig. 2.2). On the other hand, this peak increases with the increasing scan rate (Fig. 2.3) and becomes nearly equal to C when the scan rate exceeds 10 V/S. In the lower PNBA concentration (curve I and II, Fig. 2.3), the peak current ratios are higher than in higher PNBA concentrations (curve III, Fig. 2.3). These results are interpreted as indicating that the nitrosobenzoate molecules are consumed by a chemical reaction which is much faster in high PNBA concentrations than in low PNBA concentrations. According to many authors,[1-5] the chemical reaction taking place in the basic media (reaction (2.4)), is a coupling of nitroso compound with hydroxylamine to produce an azoxy compound.

$$Ar\text{-}NHOH + Ar\text{-}NO = Ar\text{-}N(\rightarrow O)=N\text{-}Ar + H_2O \qquad (2.4)$$

A possible qualitative explanation for the difference between the low and high PNBA concentration solutions involves the condition that the chemical

reaction occurs only in the solution and not on the electrode surface. Thus, only the free molecules can undergo such a reaction but not the absorbed molecules. In low PNBA concentration solutions, the current is small so that a small amount of product is obtained during the potential sweep. On the roughened surface some of the product will be adsorbed and only a small amount can diffuse into solution and undergo the chemical reaction. When the potential sweep is reversed, the adsorbed nitroso molecules are reduced again and the cathodic wave D is observed with the intensity slightly lower than that of the anodic wave C. In high PNBA concentration solutions, the larger current produces a larger amount of product. Only a small portion of the products can be adsorbed on the electrode surface due to the limited available electrode surface area, while most of the product diffuses into the solution. In this case, a larger proportion of nitroso molecules are consumed by the chemical reaction. Therefore, when the potential sweep is reversed, the reduction wave of the nitroso compound becomes much smaller than the oxidation wave. If the potential sweep is fast enough, there is not enough time for the chemical reaction to proceed and a pair of peaks, C and D, nearly symmetric in height is obtained.

A similar explanation can be made to account for the difference in the current ratios between the roughened and the smooth electrodes. Since the current is larger, because of increased area, on the roughened electrode than on a smooth electrode, but the volume of the reaction zone near the electrode surface is the same, the concentration of the product of the electrochemical reaction in this zone is also higher for the roughened electrode. Thus the chemical reaction proceeds to a larger extent.

(b) SERS Spectroscopy

In order to identify the species produced during the electrochemical process, spectra of the authentic p-hydroxylaminobenzoic acid, a possible intermediate product, were taken at different potentials in both acidic(Fig. 2.4c) and basic media (Fig. 2.4a,b). In both cases, the spectra are the same in a potential region from -0.5V to -1.0V, with three main bands at 847, 1364 and 1600 cm^{-1}. A representative spectrum at -0.5V and pH=11 is shown Fig. 2.4a. The oxidation of hydroxylamine compound occurs at potentials more positive than -0.3V. The spectrum obtained at -0.2V in basic media shows two prominent bands at 1277 and 1329 cm^{-1} and a shoulder band at 1095 cm^{-1} (Fig. 2.4b); however, the former two bands are very weak and the 1095 cm^{-1} band does not appear on the spectrum in acidic media (Fig. 2.4c). According to literature,[2-5] the chemical coupling reaction between nitroso and hydroxylamine compounds proceeds quickly in basic media but does not occur in acidic media. We assign the 1095/1277/1329 cm^{-1} bands to the chemical product, the azoxy compound. Approximately the same bands were found by Gao et al[18,19] in nitrobenzene reduction and assigned to azoxybenzene. The other bands in Fig. 2.4b,c can be attributed to the oxidation product, p-nitrosobenzoate, as discussed below.

SERS spectra were rapidly recorded(0.1s dwell time) at various potentials(times) on a potential waveform from 0.0V to -0.45V, back to 0.0V, and finally returned to -0.45V, (Fig. 2.5). Although the first reduction wave of PNBA starts from -0.45V with a peak located at about -0.6V on the voltammogram, the SERS spectra obtained during the initial negative-going potential sweep in an experiment with a scan rate of 0.1V/S show that the reduction reaction occurs at the potentials much more positive than -0.45V. Several new bands have begun

to grow as soon as the potential is more negative than -0.2V (Fig. 2.5). We have attributed this under-potential reduction to a laser induced photolysis effect.[17] Our interpretation of this effect is that the dynamic electric field of the exciting laser light is superimposed on the static electric field of the metal electrode at the Fermi level making photoemitted electron transfer possible.[17] The initial spectrum at 0.0V shows only four major bands at 866, 1115, 1350 and 1600 cm^{-1} which represent the starting species, PNBA.[17] When the potential is swept to values more negative than -0.2V, several new features begin to appear at 926, 1145, 1372, 1395 and 1454 cm^{-1} which can be attributed to the nitroso compound by comparison with the spectrum of p-nitrosobenzoate prepared from the hydroxylamine compound.[23] The 1145/1395 cm^{-1} pair of bands was assigned, in nitrobenzene reduction,[18] to the nitrosobenzene phenyl ring-nitrogen (C-N) bond and the N-O bond stretching vibrations, respectively.

According to the reduction mechanism proposed from purely electrochemical studies,[1-6] the first reaction step should be a four-electron reduction of the nitro group to hydroxylamine, but from our spectral investigations in the presence of laser light, the first reduction product detected is the nitroso compound. It seems likely that the nitro compound is undergoing a two-electron reduction to the nitroso compound directly at the potentials more positive than -0.45V in the presence of the laser light. On the other hand, the spectra obtained during the positive potential sweep from -0.45V to 0.0V, e.g., the top spectrum at -0.35V in Fig. 2.5a, show much more rapid growth in these new bands. This means that more nitroso compound is produced during the positive-going potential sweep than during the initial negative-going sweep, and this nitroso compound would come from the oxidation of hydroxylamine which forms during the initial negative-going sweep. According to the CV

results, the nitroso compound produced photoelectrochemically can be further reduced to hydroxylamine electrochemically at potentials more negative than -0.35V. However, in this potential region we do not observe well-defined SERS bands for the hydroxylamine compound. This result is because the hydroxylamine bands are not well isolated from those of the nitro and nitroso compounds[23] and the overall spectrum of hydroxylamine is so weak that it is covered by those of the other two species.[18]

An investigation of the changes in relative intensities of the newly growing bands during the entire three half-cycle potential sweep shows that the 926, 1454 cm^{-1} bands have approximately the same growth behavior as the 1395 cm^{-1} band (see Fig. 2.6a,b,c). In the initial sweeping stage, all three bands grow slowly with increase in the negative-going potential (Fig. 2.6a). When the potential is swept back in the positive direction from -0.5V to 0.0V, the intensities of the 1454 and 1395 cm^{-1} increase even more rapidly (Fig. 2.6b), while during the third stage, they all decay with the negative-going potential (Fig. 2.6c). This similar trend among the 926, 1395 and 1454 cm^{-1} bands supports the conclusion that they belong to the same species, the nitroso compound. On the other hand, three other bands at 1175, 1277 and 1329 cm^{-1} do not show the same dependence. They begin to appear on the first sweep in the positive potential direction and continue to grow on the following sweep in the negative potential direction. Gao et. al.[18,19] found bands at 1274 and 1324 cm^{-1} to be characteristic of azoxybenzene, and thus it is clear that we can assign the features at 1175, 1277 and 1329 cm^{-1} to an azoxy compound. The formation of azoxy compound is good evidence for the existence of hydroxylamine during the under-potential reduction process since azoxy compound is a product of the chemical combination in solution of nitroso

compound with hydroxylamine.[3-12] The azoxy compound could also be formed in the initial negative-going sweep, but there is no spectral evidence for its existence during this period for the 100 mV/s scan rate. This is most likely a kinetic effect since at a slower scan rate of 2 mV/s, a 1277 cm^{-1} band for azoxy compound is observed (Fig. 2.7) in the initial negative-going sweep.

According to the above discussion, the mechanism of the photoinduced under-potential reduction process occurring in the potential range from -0.2V to -0.5V can be envisioned as follows: first, the PNBA undergoes a two-electron reduction (2.5) to p-nitrosobenzoic acid with the help of the photolysis effect.

$$Ar\text{-}NO_2 + 2e^- + 2H_2O = Ar\text{-}NO + 2OH^- \qquad (2.5)$$

Then, the nitroso compound can be further reduced to the hydroxylamine compound by picking up two more electrons at the electrode surface at potentials more negative than -0.35V

$$Ar\text{-}NO + 2H_2O + 2e^- = Ar\text{-}NHOH + 2OH^- \qquad (2.6)$$

Furthermore, the chemical coupling reaction (2.7) between the p-nitrosobenzoate and p-hydroxylamine in the solution phase produces the azoxy compound which can replace the hydroxylamine and adsorb on the Ag electrode surface.

$$Ar\text{-}NHOH + Ar\text{-}NO = Ar\text{-}N(\rightarrow O)=N\text{-}Ar + H_2O \qquad (2.7)$$

When a very slow potential scan rate, such as 2 mV/s, is used, a steady state can be reached at each potential level. The SERS obtained in such a situation represent the stable species on the electrode surface at each potential. Fig. 2.7 shows the steady-state SERS during a very slow potential sweep from

0.0V out to -0.8V and back to -0.5V, with a scan rate of scan rate of 2 mV/s. The strongest spectrum was detected at -0.3V and the new bands come as early as at -0.1V. The 847, 926, 1138, 1277, 1395 and 1454 cm^{-1} bands are stable in the potential region from -0.2 to -0.6V, although their relative intensities change with potential. The 1138 cm^{-1} band is caused by an overlap of the 1130 cm^{-1} band with the 1145 cm^{-1} band. These bands show that the nitroso and azoxy compounds are formed and are electrochemically stable in this potential region. When the potential is more negative than -0.6V, all the bands corresponding to the nitro, nitroso and azoxy compounds decay quickly and only one major band at 1364 cm^{-1} and three weak bands at 847, 866 and 1600 cm^{-1} are left. This spectrum can be attributed to the p-hydroxylamine compound, since the authentic p-hydroxylamine compound shows three bands at 847, 1364, and 1600 cm^{-1}. As the potential sweep is reversed, the recovery of the lost bands begins at -0.5V and these bands then become more and more intense with positive-going potential, indicating that more nitroso and azoxy compounds are produced during this sweep.

However, if the potential is swept very fast, the reactions are controlled by kinetics. Fig. 2.8 shows the SER spectra obtained by real-time detection during a fast CV experiment where the potential is swept from 0.0V to -1.0V, with a scan rate of 1.0V/s. The spectra in the potential region from 0.0V to -0.5V on the initial negative-going sweep do not show significant development of bands for the nitroso or azoxy compound. When the potential is swept past the first four-electron reduction peak, the spectrum of hydroxylamine is obtained. The spectrum shows only two major bands at about 1364 and 1600 cm^{-1}. The 866 cm^{-1} band becomes very weak and the 1115 cm^{-1} PNBA band totally vanishes from the spectrum. The 1364 cm^{-1} band seems to be a result of overlapping of

the 1350 and a newly growing 1372 cm^{-1} bands. Two new bands at 1145 and 1454 cm^{-1} first appear at -0.5V when the potential sweep is reversed. As the potential reaches -0.3V, a large number of bands develop. Among these bands, the 926/1145/1395/1454 cm^{-1} bands represent the nitroso compound and the 1095/1175/1277/1329 cm^{-1} bands represent the azoxy compound. This result is in agreement with the CV experiment where an anodic peak arises at about -0.3V, which corresponds to the formation of the nitroso compound from the hydroxylamine. The assignment of 1454 cm^{-1} band is somewhat difficult, since it may belong to either nitroso or azoxy compounds. According to Gao at. al.,[18,19] both the azoxy and azo compounds show strong bands in this region. When the potential is swept in negative direction again, all bands increase in intensity at first and then decay, but no new bands arise. At last, when the potential reaches to -0.9V, the 1364 cm^{-1} band again becomes the major band. Thus the 1372 cm^{-1} bands can be assigned with confidence to hydroxylamine according to these experiment results.

The time dependences of some SERS bands taken in a square wave experiment are shown in Fig. 2.9. In this three level potential experiment, the potential is stepped from 0.0V to -0.5V, held for 5s, stepped back to 0.0V for 5s, and finally again stepped to -0.5V for 5s, Fig. 2.9. A spectrum is taken every one second throughout this waveform with an integration time of 0.1s. The relative intensities of the 926, 1145, 1277, 1395 and 1454 cm^{-1} bands (relative the 1350 cm^{-1} band of PNBA) are given in the figure. It can be seen that except for the 1277 cm^{-1} band, all other bands show a similar potential dependence. This further confirms the conclusion that the 926/1145/1395/1454 cm^{-1} bands belong to the same species, p-nitrosobenzoate, which is produced rapidly as the potential returns from -0.5V to 0.0V and is consumed when the potential is

stepped to -0.5V again. The 1277 cm^{-1} band corresponds to the azoxy compound, and a similar change in intensity is not observed for this band as the potential goes to -0.5V again, since this potential is not negative enough for the reduction of the azoxy compound under the experimental conditions.

The following section describes an experiment where a short-lived intermediate in the electrochemical redox reaction of PNBA is detected by ms time-resolved SERS. The experimental apparatus used in these experiments is identical to that previously described[17] with the addition of an electronically controlled shutter with a response time of 7 milliseconds, used to initiate the detection procedure, which itself is illustrated in Fig. 2.10. A potential pulse (-0.9V vs. SCE) is applied to the electrode for a period of 200ms to reduce PNBA to the hydroxylamine compound, and the potential is relaxed to -0.2V during which the time resolved surface enhanced Raman spectrum is recorded by means of a gated detection scheme, which samples the spectrum by an optical multichannel analyzer (OMA) at various intervals (Fig. 2.10).

Fig. 2.11 shows the time-resolved SERS spectra for the potential excitation experiment in 0.05M PNBA with 0.1M Na_2SO_4 as supporting electrolyte at pH 11. The electrode potential is jumped from zero to -0.9V for 200 ms duration then back to -0.2V. The time-dependent SERS were taken at t_1, when the potential returned from -0.9V to -0.2V (see Fig. 2.10). The time interval between successive spectra was 10ms. At the pumping potential, -0.9V, the main species on the Ag electrode surface should be the hydroxylamine compound according to our proposed cyclic voltammetry reduction scheme[17]. The first spectrum obtained after the potential pulse returns to -0.2V shows one intense band at 1364 cm^{-1} and two weaker bands at 866 and 1600 cm^{-1}. These same bands are also found at -0.9V during the potential excitation and

are nearly identical to those bands of the authentic hydroxylamine compound, PHABA (see Fig. 2.4), confirming that PHABA is formed at -0.9V. Several new peaks at 996, 1095, 1115,1130, 1145, 1175, 1233, 1277, 1325, 1350,1395, 1454, and 1580 cm^{-1} start to appear 30 ms later. The final spectrum most likely corresponds to a mixture including nitro, nitroso and azoxy compounds. Some of these bands at 866, 1115 and 1350 cm^{-1} belong to the nitro compound which continues to diffuse onto the surface of electrode after the electrochemical reduction ceases. The bands at 1130, 1145, 1395 and 1454 cm^{-1}, represent the formation of the nitroso compound (see Fig. 2. 4), while the bands at 1095, 1277 and 1325 cm^{-1} are close to bands found in the spectrum of azoxybenzene at 1098, 1273, and 1325 cm^{-1} [18,19] and represent the product of the chemical coupling reaction between the nitroso and the hydroxylamino compounds. The bands representing the azoxy compound appear nearly at the same time and the same rate as those of the nitroso compound (see Fig. 2.12a). This result is consistent with the conclusion drawn from electrochemistry that a rapid chemical reaction, which consumes the nitroso molecules, follows the formation of nitroso compound. However, the assignment of all of the bands due to the azoxy compound is difficult because some of the bands assigned to nitroso compound overlap with the azoxy compound.

Transient bands are found at 966, 1233 and 1580 cm^{-1}. These bands appear slightly earlier than those bands for the final products and then disappear about 70 ms later. The experimental curves of the intensities of the transient 1233 and 1580 cm^{-1} bands versus time are shown in Fig. 2.12b. These transient bands must correspond to some kind of intermediate. A reasonable interpretation suggests that this intermediate is a free radical anion,

$Ar\text{-}NO^-$, produced during the electrochemical oxidation of the hydroxylamine compound:

$$Ar\text{-}NHOH + 2OH^- = Ar\text{-}NO^- + 2H_2O + e^- \quad (2.8)$$

$$Ar\text{-}NO^- = Ar\text{-}NO + e^- \quad (2.9)$$

The life-time of this species on the Ag electrode surface is about 70ms. ESR studies also provide evidence for the existence of nitroso radical anion but the life-time of this free radical in solution is much longer, about two minutes.[11] The shorter life-time in our experiment is understandable since the species is not free in solution but is situated in the electrical double layer at the Ag surface.

The 1580 cm^{-1} band of the transient species may be assigned as the benzene ring stretching mode. The resonance effect of the free radical with benzene ring would tend to stabilize the radical and thus cause a shift of the ring stretch band from 1600 to 1580 cm^{-1}. Furthermore, the transient band at 1233 cm^{-1} may be related to the carbon-nitrogen vibration since the resonance effect favors the double bond structures and the carbon-nitrogen single bond vibration band is located at about 1145 cm^{-1}.

(c) Digital Simulation of the Electrode Process

A set of electrode reactions and coupled chemical steps which model the overall electrode process can be proposed from the nature of the CV curves and the TRSERS results taken on triangular sweep potential scans. A digital simulation of the CV curves for a smooth electrode was implemented and compared with experimental results on a smooth electrode. This is a

reasonable approach because although the SERS results were obtained on a roughened electrode, comparison between the CV curves on the smooth and roughened electrodes (e.g., see Figs. 1a and 1b) show the same qualitative features. Although, there is definitely adsorption behavior on the roughened Ag electrode, evident for peak A (Fig 1b), it does not appear on the smooth electrode, and thus was not included in the digital simulation model. Furthermore, the other peaks which were simulated (C and D) show up in exactly the same place on both the smooth and roughened electrodes indicating that the species identified by SERS in these potential regions are most likely to also be involved in the electrode process on the smooth electrode. Additionally, it should be noted that the SERS results are also influenced by a photoinduced process; however, as we have previously pointed out[17], the same intermediates and products are involved in electrochemical and photochemical reduction of arylnitro compounds.

The digital simulation of the CV curves was carried out with a General Program of Simulation (GPS)[26] which is a later version of the program of Rieger and Gosser[27] written in FORTRAN for digital simulation of electrochemical current-potential curves. This program utilizes an expanding space grid for computational efficiency and Runge-Kutta solution of chemical kinetics for mechanistic generality. It is available from one of the authors (DKG) upon request. Because of the coupled fast chemical steps, each half-cycle of the potential scan cycle of the CV took about one-half hour to simulate on an Apple Macintosh II or a DEC VAX 11/780, about ten minutes on a faster Celerity 1260D computer, and about four minutes on a Cray Y-MP for a 0.2V/s scan rate. These results only indicate CPU time for the Macintosh since the other machines were used in a time-sharing mode and also the code was not

optimized for speed on the supercomputer. As the scan rate is lowered, the time for simulation goes up. For example, at 0.05V/s it took three hours to simulate, the complete CV curve shown in Fig 15 on a Macintosh II.

The CV curves were simulated for potential scans between -0.1V and -1.0V. One point is output for every one mV in the potential scan. All diffusion coefficients were assumed to be equal with D= $1x10^{-5}$ cm^2/s. In this potential range, the electrode process involves four electrons and four protons. Since the solution is alkaline, water is taken as the proton source, and all hydrolytic reactions are assumed to be fast with respect to electrode reactions and, therefore, to be at equilibrium. Under these conditions, a direct 2 e^-, $2H^+$ reaction behaves exactly as a system modeled with two successive one electron transfers(ET) with symmetry factor, α, equal to 0.5.[28] The reduction of nitro compound to nitroso compound is modeled in this way with two ET steps (2.10) and (2.11) followed by an irreversible chemical step (2.12). It should be mentioned that this process could also be modeled by one ET step followed by a disproportionation and then loss of water. However, this more complicated mechanism would not markedly influence the shape of the CV curve, and since we do not have evidence of the single electron adduct species, we have assumed a mechanism with the direct two-electron transfer. The E^o for each ET step involving hydrolytic action is formulated in terms of a Nernst equation for only those species which exchange electrons. Also, the standard heterogeneous ET rate constant, k^o, is an apparent constant which depends on pH and acid dissociation constant.

$$Ar\text{-}NO_2 + e^- + H_2O \xrightarrow{E_1^0, k_1^0} Ar\text{-}NO_2H + OH^- \qquad (2.10)$$

$$Ar\text{-}NO_2H + e^- + H_2O \xrightarrow{E_2^0, k_2^0} Ar\text{-}NO_2H_2 \qquad (2.11)$$

$$Ar\text{-}NO_2H_2 \xrightarrow{k_{c1}} Ar\text{-}NO + H_2O \qquad (2.12)$$

The reduction of the nitroso to hydroxylamine also involves two electrons and two protons. In this case we take as the first step in this reduction a simple one ET reaction (2.13) to form the nitroso free radical anion, AR-NO$^-$. Using TRSERS in a potential step experiment,[23] we have obtained evidence for the existence of this species as unstable intermediate at the electrode surface during the electrochemical oxidation of p-hydroxylaminobenzoate to p-nitrosobenzoate. The experiment shows three transient bands at 996, 1233, and 1580 cm^{-1} with a life time of 70 ms which we assigned to this species.[23] The last ET step (2.14) must involve one electron and two water molecules (2 protons) to form the p-hydroxylaminobenzoate. Finally we include an irreversible condensation reaction (2.15) between hydroxylamine and nitroso compounds to form azoxy which accounts for the SERS observation of this compound and the nature of peak labeled D in the CV curves.

$$Ar\text{-}NO + e^- \xrightleftharpoons{E_3^0, k_3^0} Ar\text{-}NO^- \qquad (2.13)$$

$$Ar\text{-}NO^- + e^- + 2H_2O \xrightleftharpoons{E_4^0, k_4^0} Ar\text{-}NHOH + 2OH^- \qquad (2.14)$$

$$Ar\text{-}NO^- + Ar\text{-}NHOH \xrightarrow{k_{c2}} Ar\text{-}N(O)=N\text{-}Ar + H_2O \qquad (2.15)$$

Because the finite difference program for this mechanism requires so much computation time, it is not practical to use an optimization procedure to obtain the estimated parameter set. Instead, we have used a trial and error

procedure which involved around 500 computer simulations. We systematically varied the parameter set to arrive at a best fit set by (i) visually observing the effect of these changes on the deviations between the simulated CV curve and experimental points, especially in regions where the current rises up to the peak potentials, and (ii) by making sure that the final optimized parameter set accurately simulated the CV curves as a function of scan rate. The results of this procedure are the following parameter set :

E_1^0= -0.27V, k_1^0 = 1.08x10^{-5} cm s^{-1}, α_1 = 0.5

E_2^0= -0.27V, k_2^0 = 1.08x10^{-5} cm s^{-1}, α_2 = 0.5

E_3^0= -0.34V, k_3^0= 0.0600 cm s^{-1}, α_3 = 0.63

E_4^0= -0.32V, k_4^0 = 0.0165 cm s^{-1}, α_4 = 0.63

k_{C1} = 500 s^{-1}

k_{C2} = 4.5 s^{-1}

To some extent the first six parameters are decoupled from the remaining eight parameters since the former determine the position and shape of peak A (Fig. 2.1) and the rest of the set determine the characteristics of peaks C and D.

We have also tested the validity of parameter set by showing that variations in their values do have measurable effects on the simulated peak potentials and peak currents. Thus, in order to produce a shift of ± 3mV in the peak potential for peak A, the values of k_1^0 and k_2^0 need to vary from 0.8 x10^{-5} to 1.3 x10^{-5} cm/s. This same variation in the peak potential of C can be obtained when the value of k_3^0 is varied from 0.04 to 0.10 cm/s or k_4^0 is varied from 0.015 to 0.019 cm/s. A ± 3% variation in the peak current of peak A is obtained when

k_{C1} is varied between 300 and 1000 s^{-1}. Finally, a ± 5% variation in the peak current ratio of peak D to peak C is found when the value of k_{C2} is varied from 3.5 to 5.5. Thus, the simulated data seem to be fairly sensitive to the parameter values with the exception of k_{C1}. The value we have obtained for the rate constant for this irreversible step is in the nature of a lower bound, since larger values will not substantially effect the simulated curve but do make the computation time prohibitive.

Some simulated cyclic voltammograms are shown in Fig. 2.13. Note for these curves, the potential axis has been reversed. The simulation results are qualitatively consistent with the experimental results obtained in 5 mM PNBA solution on a smooth Ag electrode(Fig. 2.1). Fig. 2.14a, b show the dependences of peak potentials, Ep_A, Ep_C, Ep_D and Ep_C-Ep_D for the simulated and the experimental results as a function of the potential scan rate. Fig. 2.14c is a comparison of experimental and simulated peak current ratios, i_D/ i_C also as a function of scan rate. This peak ratio is especially sensitive to the chemical rate constants in the electrode process. It can be seen that there is reasonably good agreement in all cases between simulated and experimental results.

Experimental data points and a continuous simulated curve for a 0.05V/s are shown in Fig. 2.15. The open circles are used for the experimental data on the first cycle and open triangles are used for the last half-cycle for less confusing presentation. The background current from the pure supporting electrolyte has been subtracted from the experimental current obtained with p-nitrobenzoate. Even so it can be seen that on the first negative-going scan, the simulation is flat and well below the experimental points. This is probably because the experimental data include residual reduction current from impurities either on the solid Ag electrode or in the p-nitrobenzoate solution

which is not represented in the simulation. The background current must be irreversible because it does not show up as much on the positive-going scan where the fit is quite good. At the reversing potential, a small amount of charging current can also still be seen, probably due to an uncompensated charging current in the presence of the p-nitrobenzoate. The simulation predicts the absolute value of the main peak current to within about a 3% error, even using the geometric area for the true surface area of the electrode, approximate diffusion coefficients, and neglecting correction for charging and background current which is found in the presence of the p-nitrobenzoate solution. In fact, the agreement of the simulated and experimental current is good, especially in the important parts of the voltammogram which contain all the information about the mechanism: the wave shapes, peak potentials and peak currents.

Section 2.4 Conclusion

The electrochemical reduction of arylnitro compounds is a rather complex process. The investigation of the electrode process of p-nitrobenzoate by OMA recording of SERS spectra during cyclic voltammetric scans indicates the existence of the p-nitrosobenzoate, p-hydroxylaminobenzoate and azoxy-benzoate compounds as intermediate and product species. These species, for which we provide SERS spectral evidence, have all been considered in mechanisms of arylnitro reduction based on the classical techniques of organic electrochemistry[2-6]. Almost all of the SERS bands found in our time-resolved spectra can be assigned to these compounds. In our original investigation[17], we concluded that the time dependent SERS bands found at fixed electrode potential between -0.2V and -0.5V were due to a product which was either p-

aminobenzoic acid or azodibenzoate. Analysis, herein, of SERS spectra taken as a function of potential scan shows that the time dependent spectra in our original investigation are mainly due to a mixture of bands from the starting nitro compound and the p-nitrosobenzoate intermediate with possibly one or two bands coming from the azoxy product compound.

The digital simulation of this rather complicated CV mechanism on a smooth Ag electrode indicates that in the dark the first step in the reduction process for p-nitrobenzoate can be modeled as an EC process with a two-electron two-water(proton) irreversible reduction to a species which loses a water molecule in a following chemical step to form the nitroso compound. Because of the irreversibility of the ET steps, a current for this process is not seen anywhere near the E^o of the two-electron reduction on the initial negative-going CV scan. At more negative potential the overpotential drives the formation of the nitroso compound which is than reduced in much faster ET steps to the hydroxylamine compound so that only a four-electron process is observed. On the return scan the oxidation of hydroxylamine to nitroso is relatively facile. When the scan is reversed again, the nitroso can be reduced to hydroxylamine at more positive potentials because a high overpotential for nitro reduction is not necessary. However, the nitroso and hydroxylamine can condense to form an azoxy compound, and this reaction makes the overall process an ECEC mechanism. In the presence of laser light, a photoinduced process stimulates the formation of the nitroso compound so that it is observed in a so-called underpotential (-0.1V to -0.5V) region.

Weaver and coworkers[18] have pointed out that SERS data will be most important for elucidation of the overall electrode process in CV when adsorbed species are rapidly interconverted to solution species. This situation appears to

be true in the present case because "product" peaks C and D appear in the same place for the rough and smooth electrodes, indicating that the adsorption which only appears to affect peak A on the rough electrode does not alter the overall mechanism very much when considering the smooth electrode system. Thus we have not included adsorbed species in our model of the electrode process but have used SERS identification for chemical species involved in the mechanism. The very good agreement of the experimental and simulated results is taken as impressive evidence for the validity of the proposed mechanism. Furthermore, these results show the utility of coupling electrochemical measurements, in situ vibrational spectroscopic measurements, and digital simulation for the elucidation of the mechanisms of complex electrode processes.

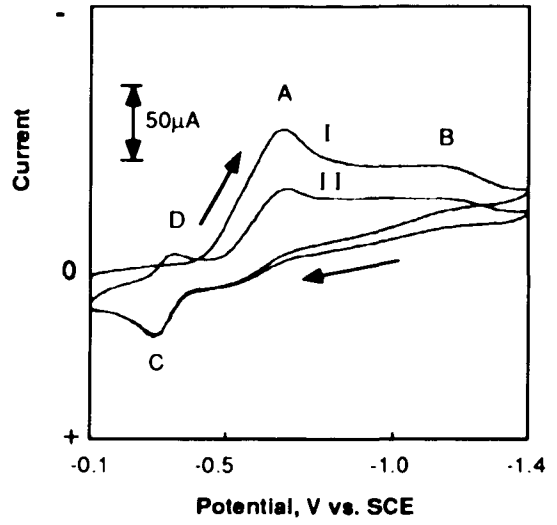

(a)

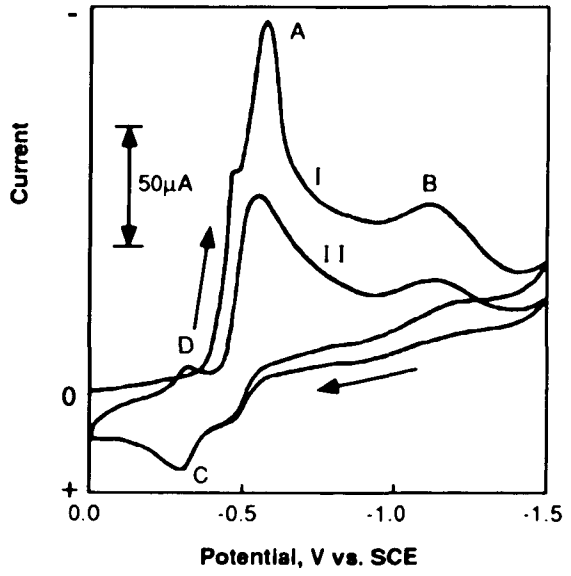

(b)

Fig. 2.1 (a) Cyclic voltammogram of PNBA on a smooth Ag electrode. (b) Cyclic voltammogram of PNBA on a roughened Ag electrode. Pretreatment for the roughened electrode is the same ORC pretreatment used in TRSERS measurements (see text); Solution: 5.0 mM PNBA in 0.1M Na_2SO_4; geometric surface area of electrode: 0.0154 cm^2; Scan rate: 200 mV/s; Curve I is the first cycle and curve II is the second cycle; The arrows indicate potential scan directions.

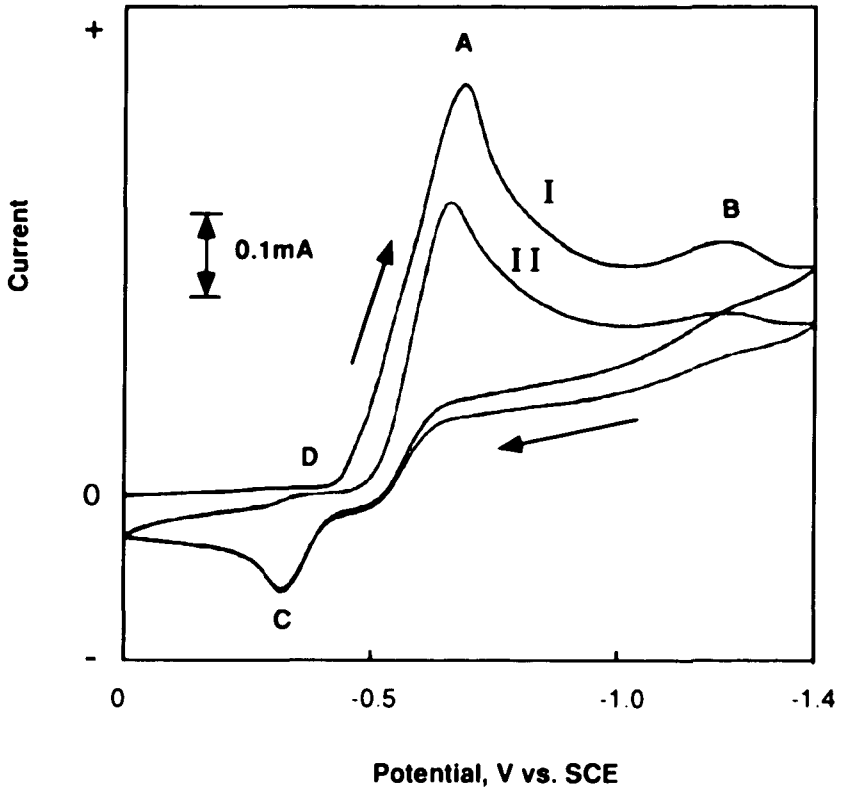

Fig. 2.2 Cyclic voltammogram of PNBA on a smooth Ag electrode at increased concentration. Solution: 50 mM PNBA in 0.1M Na_2SO_4; geometric surface area of electrode: 0.0154 mm^2; scan rate: 100 mv/S; Curve I is the first cycle and curve II is the second cycle; The arrows indicate potential scan directions.

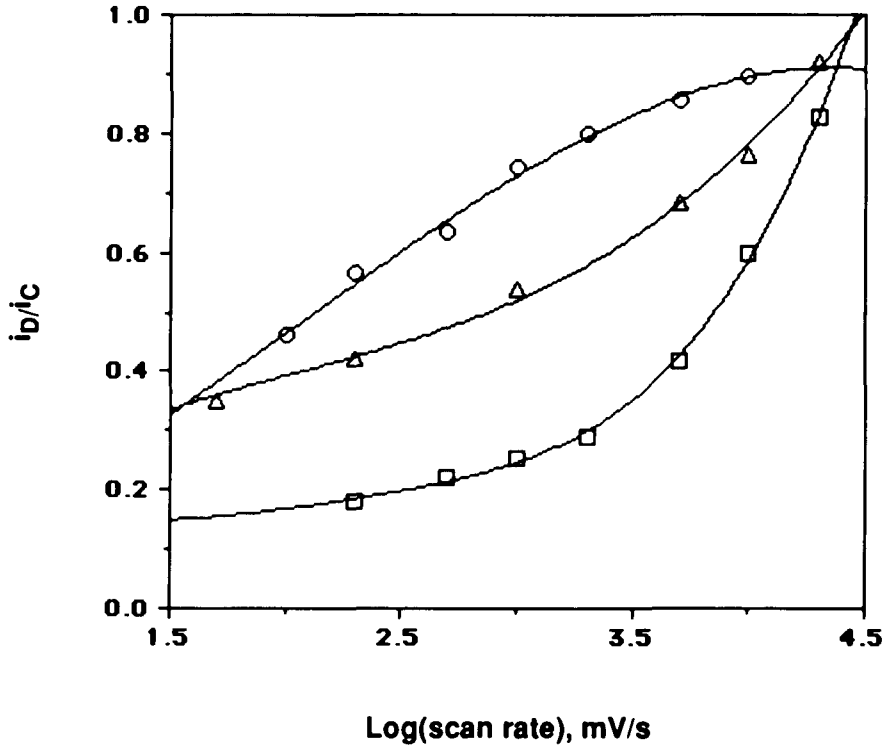

Fig. 2.3 The dependence of the ratios of peak currents, i_D/i_C, on the potential scan rate. The subscript refers to a particular peak. Supporting electrolyte: 0.1 M Na_2SO_4. Curve I (□): 5.0 mM PNBA on a smooth Ag electrode. Curve II (Δ): 5.0 mM PNBA on a roughed Ag electrode. Curve III (O): 50 mM PNBA on a roughed Ag electrode

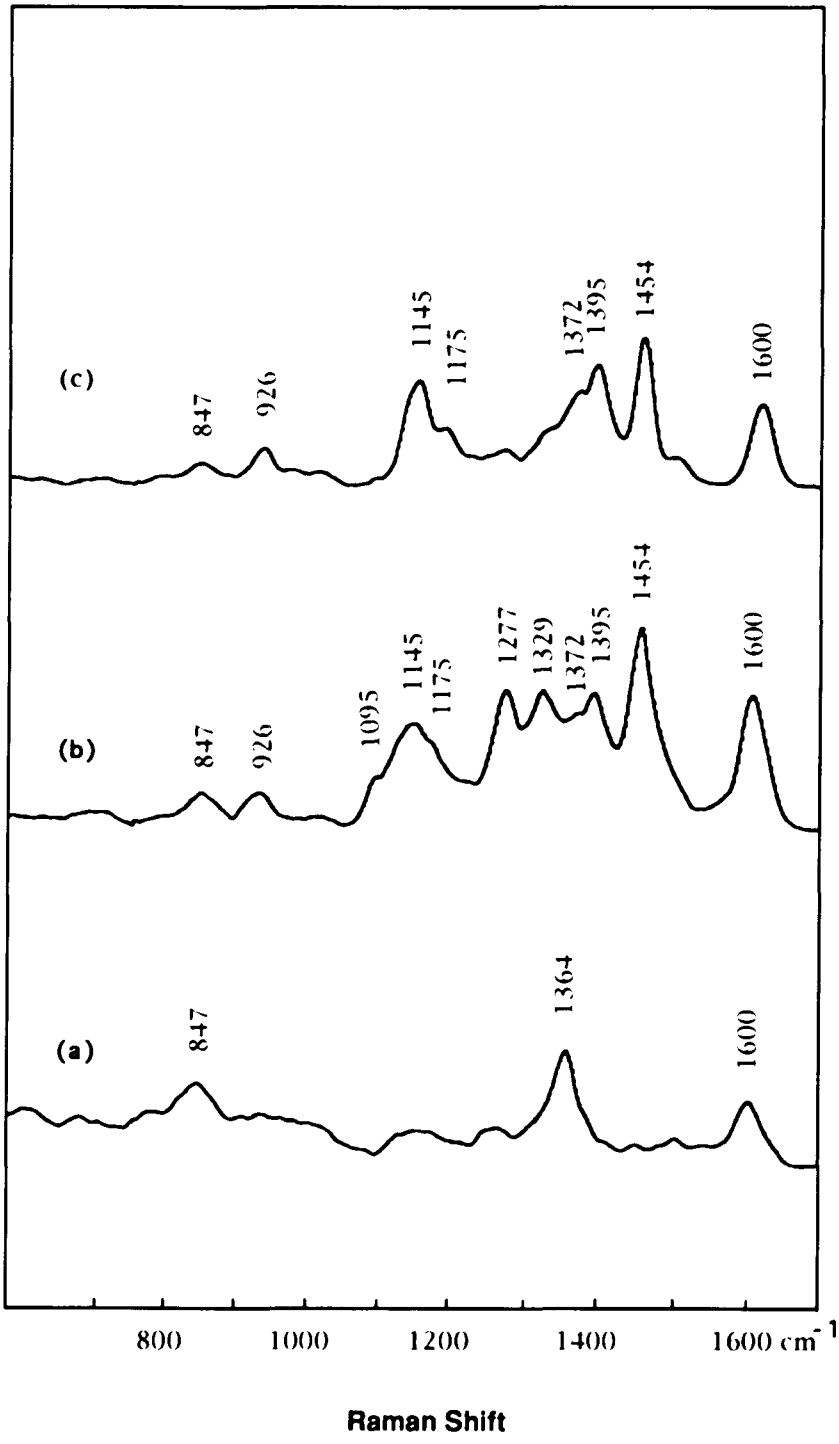

Fig. 2.4 SERS Spectra of the authentic p-(hydroxylamino)benzoic acid in 0.1M Na_2SO_4 at different potentials and pH. (a) pH=11.0 at -0.50V; (b) pH=11.0 at -0.2V; (c) pH=3.7 at -0.2V.

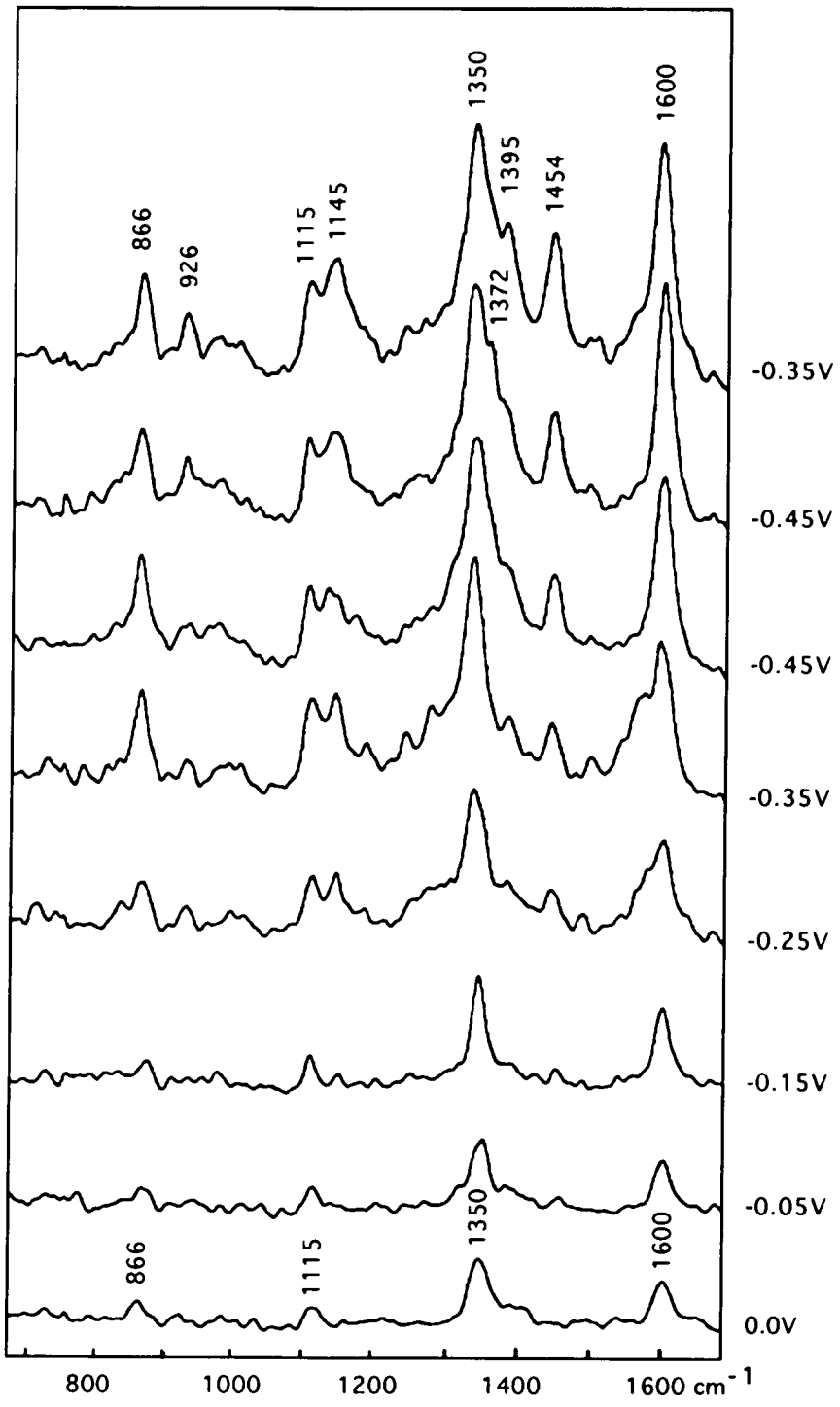
866
926
1115
1145
1350
1372
1395
1454
1600
-0.35V
-0.45V
-0.45V
-0.35V
-0.25V
-0.15V
-0.05V
0.0V
800
1000
1200
1400
1600 cm-1
Raman Shift

Fig. 2.5(a)

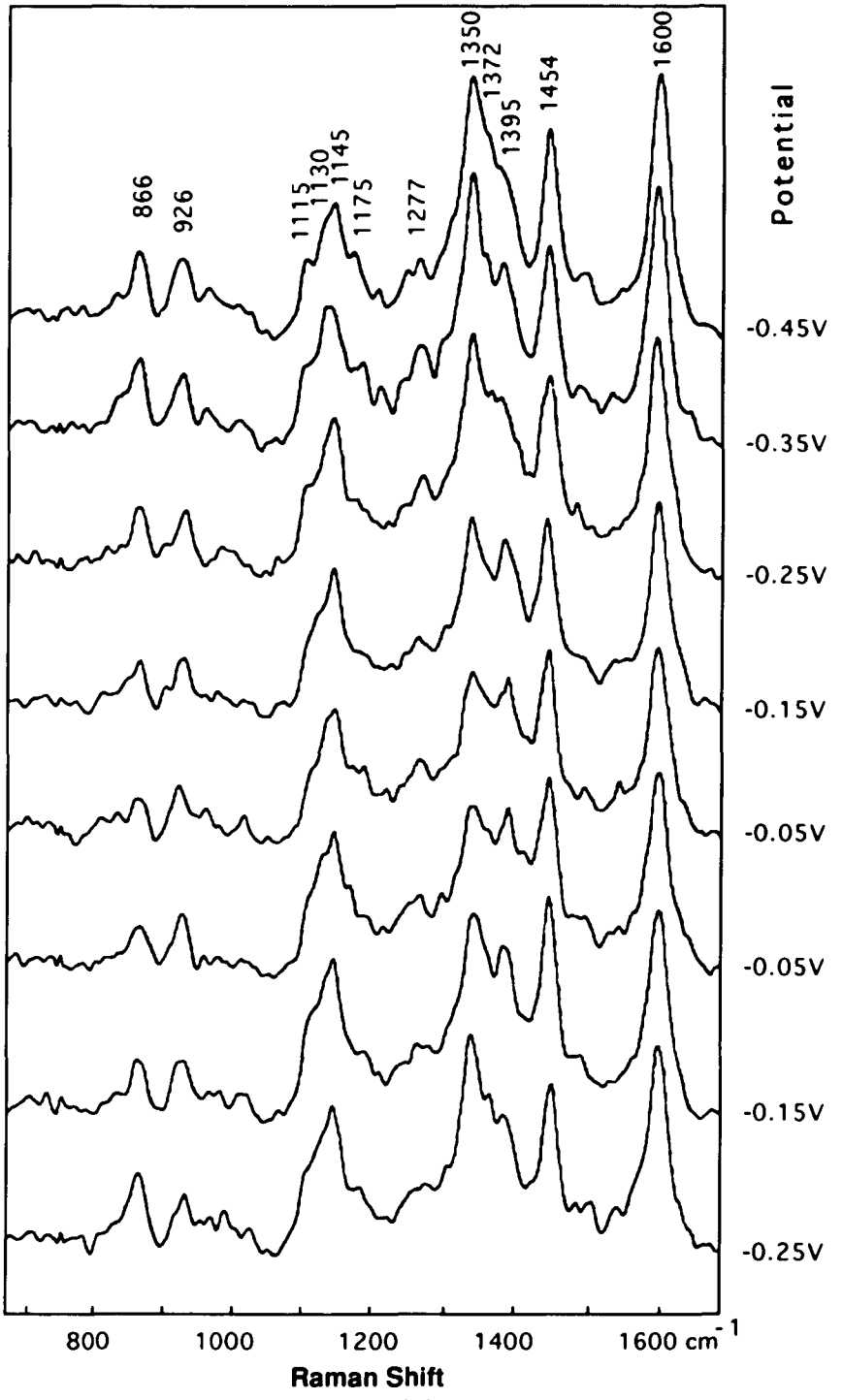

Fig. 2.5(b)

Fig. 2.5 SERS spectra obtained in 50 mM PNBA on a roughened Ag electrode during a CV experiment. (a) & (b): 0.0V to -0.45V to 0.0V to -0.45V. Dwell time of spectra: 100 ms. Potential scan rate: 100 mV/s.

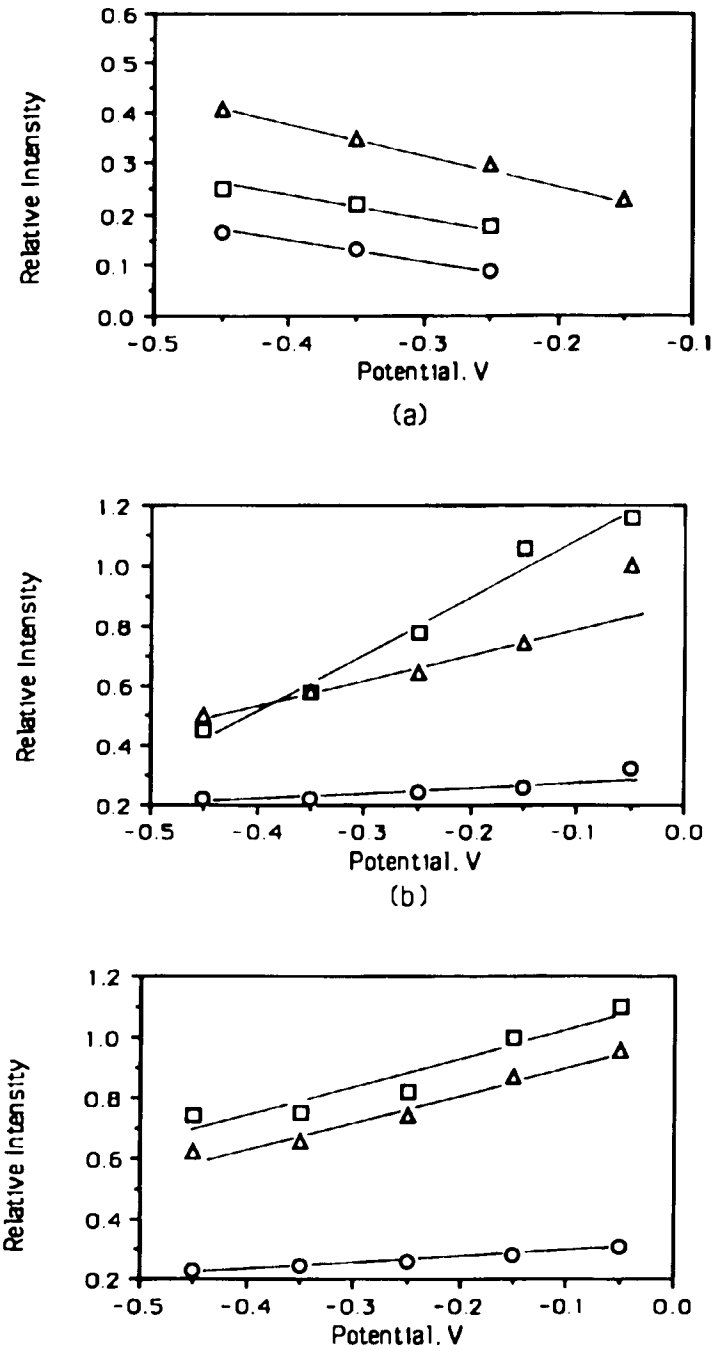

Fig. 2.6 The dependence of relative intensities of some SERS bands on potential. Potential scan rate: 100 mV/s. a) the initial negative-going scan: from 0.0V to -0.5V; b) the reverse positive-going scan: from -0.5V to 0.0V; c) the second negative-going scan: from 0V to -0.5V. (O): 926 cm^{-1}; (Δ): 1395 cm^{-1}; (□): 1454 cm^{-1}.

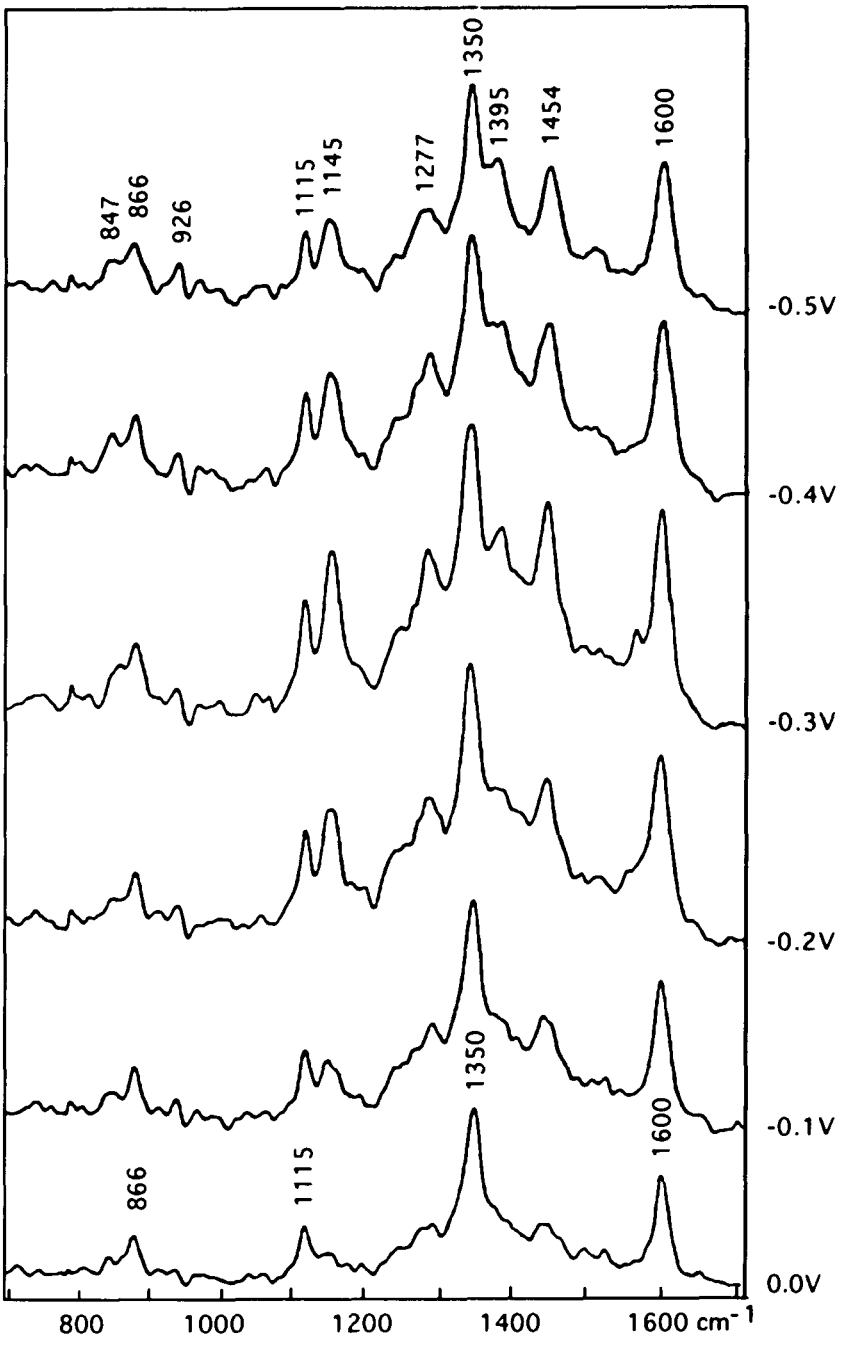
847
866
926
1115
1145
1277
1350
1395
1454
1600
-0.5V
-0.4V
-0.3V
-0.2V
-0.1V
0.0V
866
1115
1350
1600
800
1000
1200
1400
1600 cm-1
Raman Shift

Fig. 2.7(a)

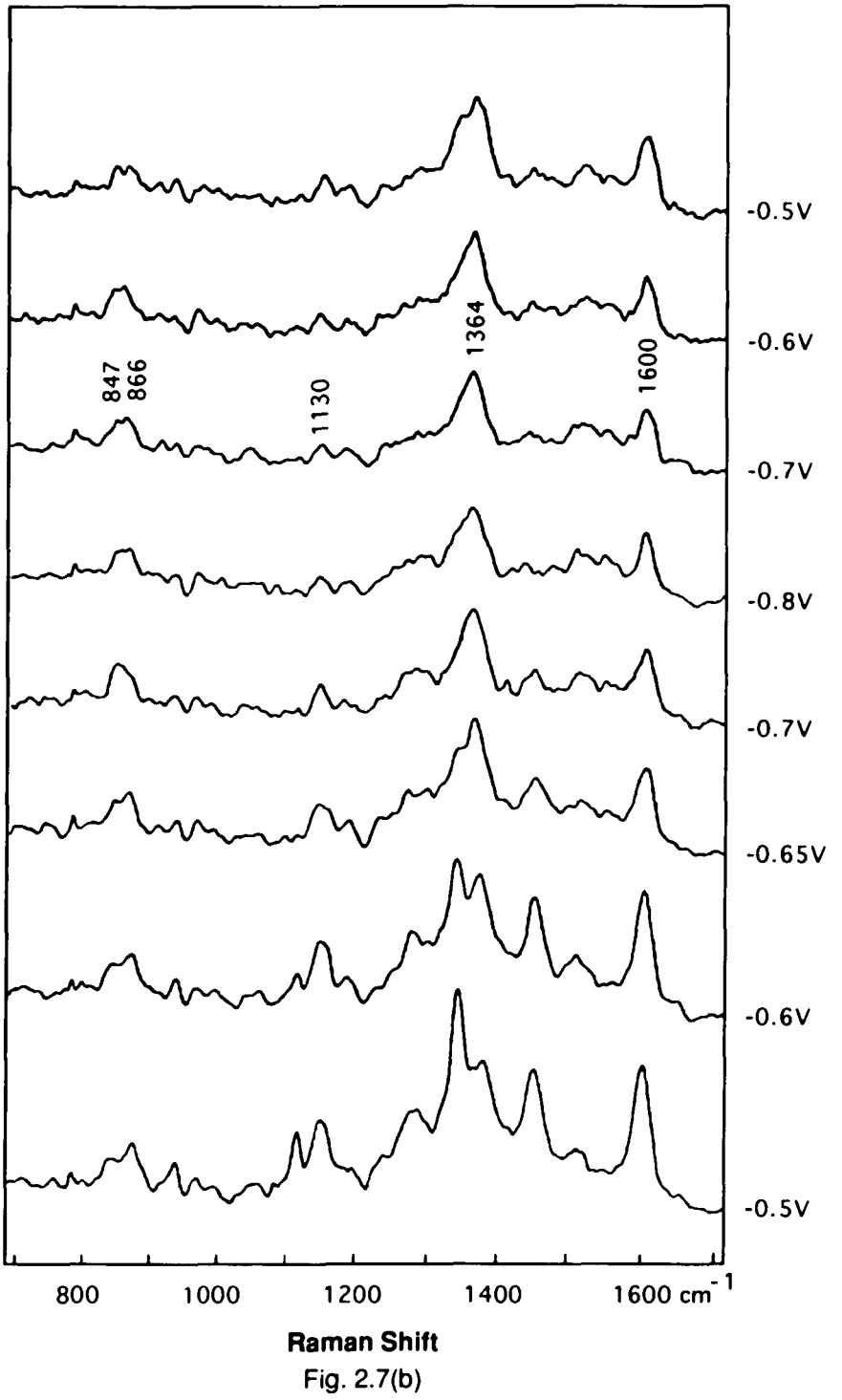

Fig. 2.7(b)

Fig. 2.7 The SERS spectra on a roughened Ag electrode taken during a slow potential scan CV experiment. (a) & (b) 0.0V to -0.8V to -0.5V. Dwell time : 1s; Potential scan rate: 2 mV/s. Solution: 50 mM PNBA in 0.1 M Na_2SO_4, pH=11.

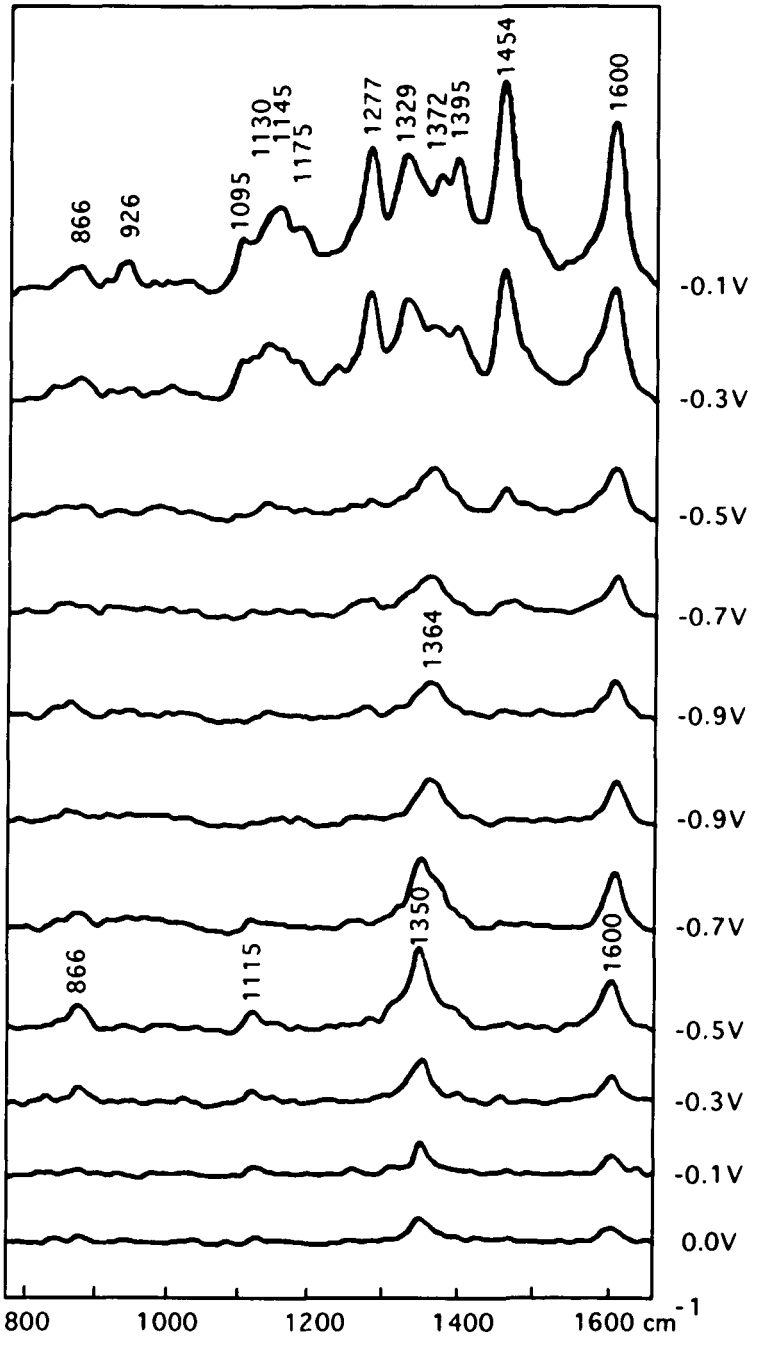
866
926
1095
1130
1145
1175
1277
1329
1372
1395
1454
1600
-0.1V
-0.3V
-0.5V
-0.7V
1364
-0.9V
-0.9V
1350
-0.7V
866
1115
1600
-0.5V
-0.3V
-0.1V
0.0V
800
1000
1200
1400
1600 cm-1
Raman Shift

Fig. 2.8(a)

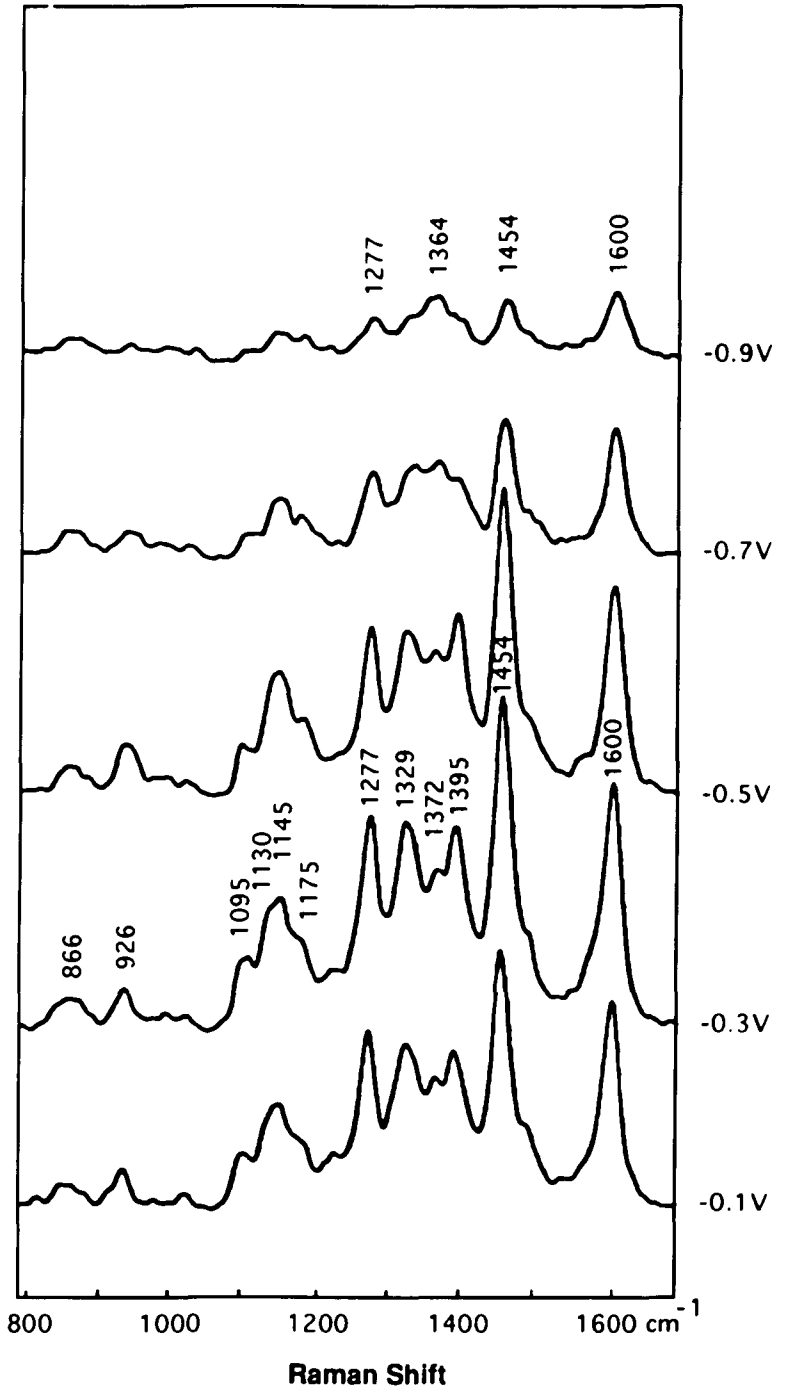

Fig. 2.8(b)

Fig. 2.8 SERS spectra taken during a fast potential scan CV experiment with real time detection.(a) & (b) 0.0V to -0.9V to 0.0V to -0.9V. Scan rate: 1.0 V/s. Dwell time: 60 ms. Solution and electrode: Same as in Fig. 2.7.

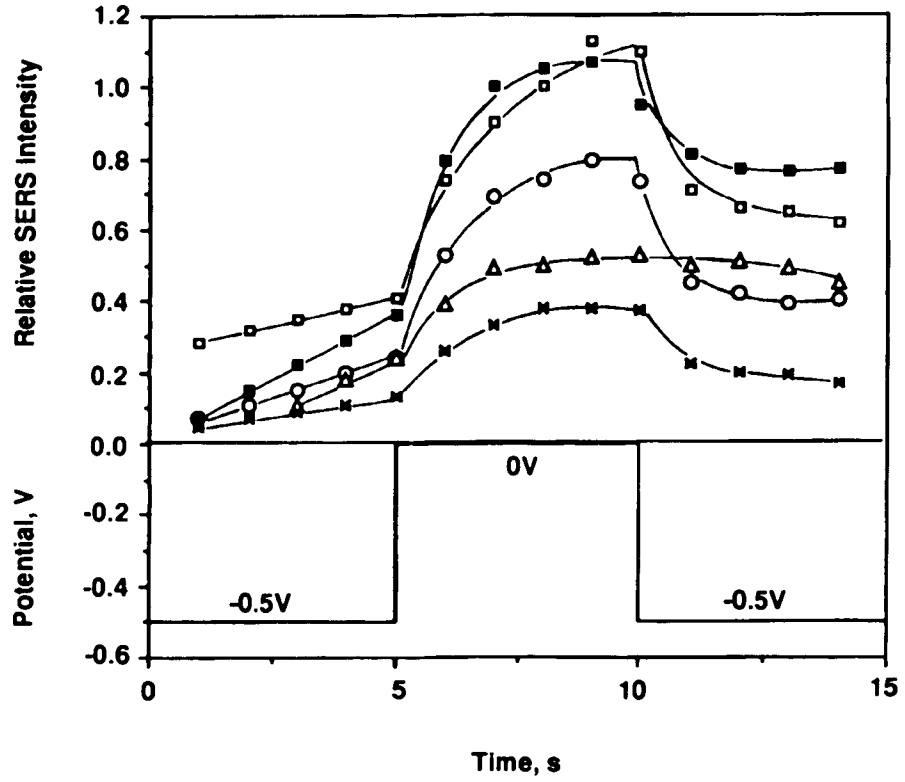

Fig. 2.9 The dependence of the relative intensities of some SERS bands on both potential and time. The band intensities are relative to the 1350 cm-1 band of PNBA. The time-resolved SERS spectra were taken in a potential square wave experiment. Irradiation with 120 mW of 488 nm laser light. Dwell time for each spectrum is 100 ms. The electrode was roughened by two oxidation reduction cycles (ORC) with a pulse of 0.0V to +0.5V vs. SCE for one second. Both ORC pretreatment and TRSERS measurement are in 50 mM PNBA aqueous solution with 0.1M Na_2SO_4 as electrolyte. pH=11.

×---- 926 cm^{-1}; □---- 1145 cm^{-1}; ▲---- 1277 cm^{-1}; ■---- 1395 cm^{-1}; ○---- 1454 cm^{-1}

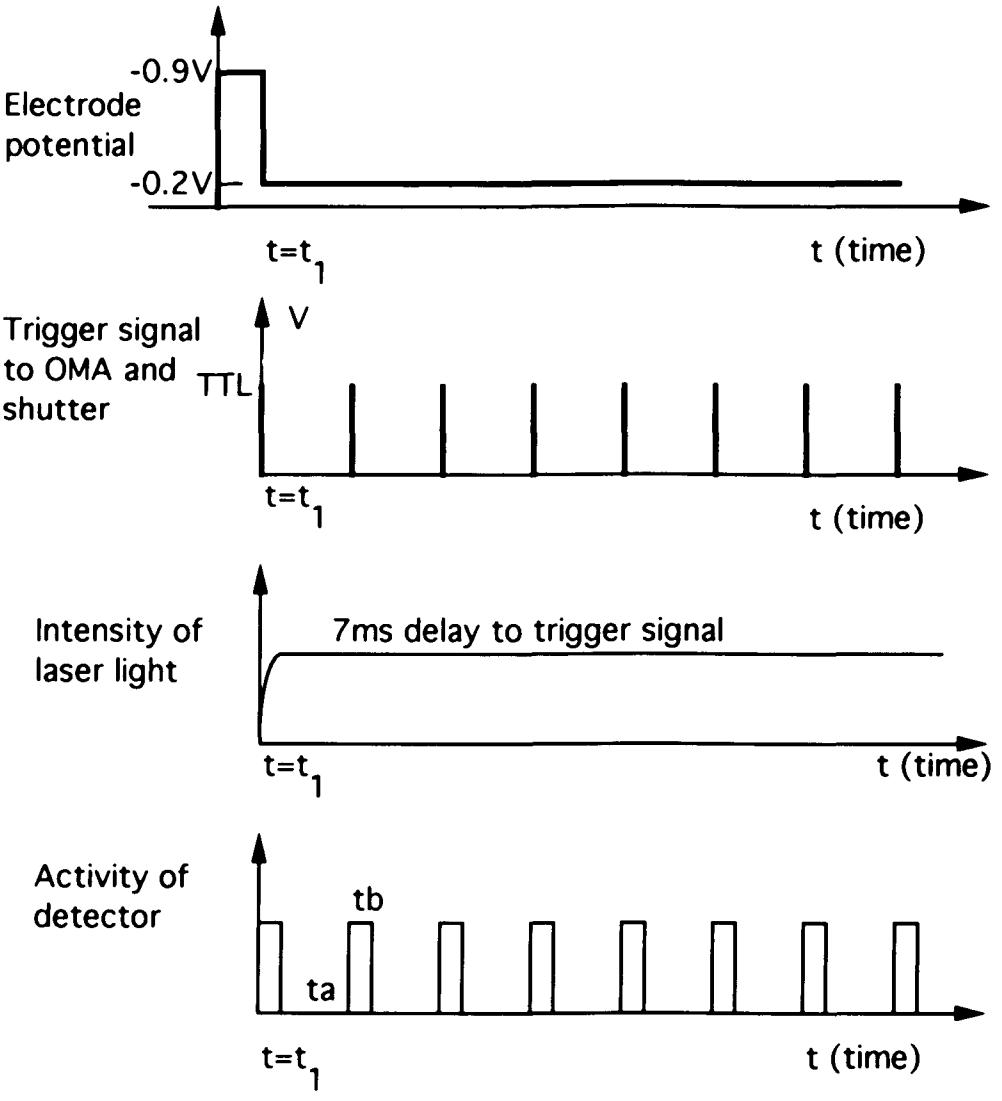

Fig. 2.10 Time-Resolved SERS detecting process for an electrochemical excitation experiment. A potential pulse (-0.9V) is exerted on the electrode for a period t1 (200 ms) to reduce PNBA to its hydroxylamine compound, the first product, then the potential returns to -0.2V and an unstable intermediate is generated during this process. Following the exciting potential pulse each TTL trigger generated by a waveform generator enables a SERS detection. ta is delay time between spectra and tb is integration time of SERS spectrum.

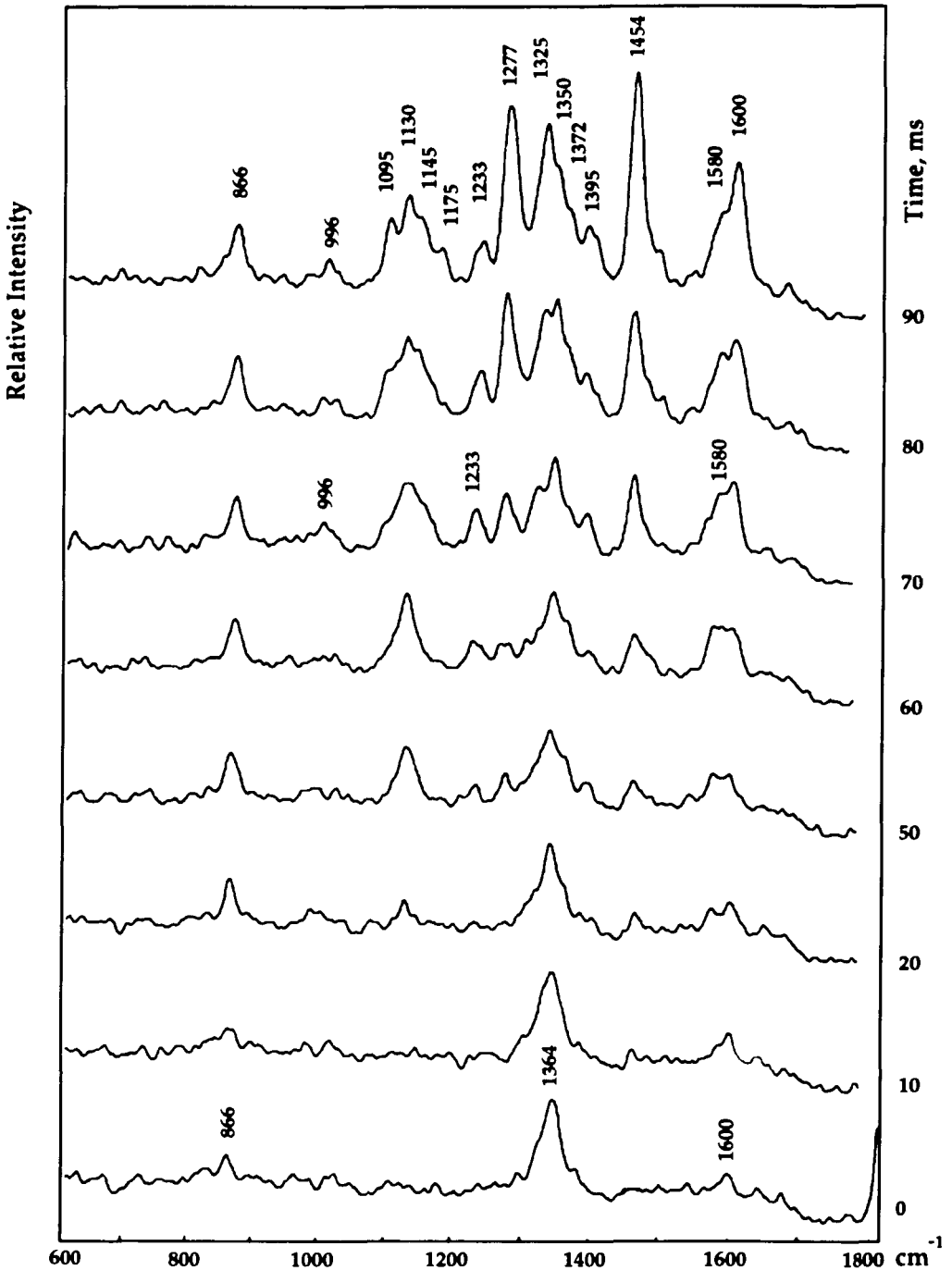
Relative Intensity
Time, ms
866
996
1095
1130
1145
1175
1233
1277
1325
1350
1372
1395
1454
1580
1600
1364
600
800
1000
1200
1400
1600
1800
cm-1
0
10
20
50
60
70
80
90

Fig. 2.11(a)

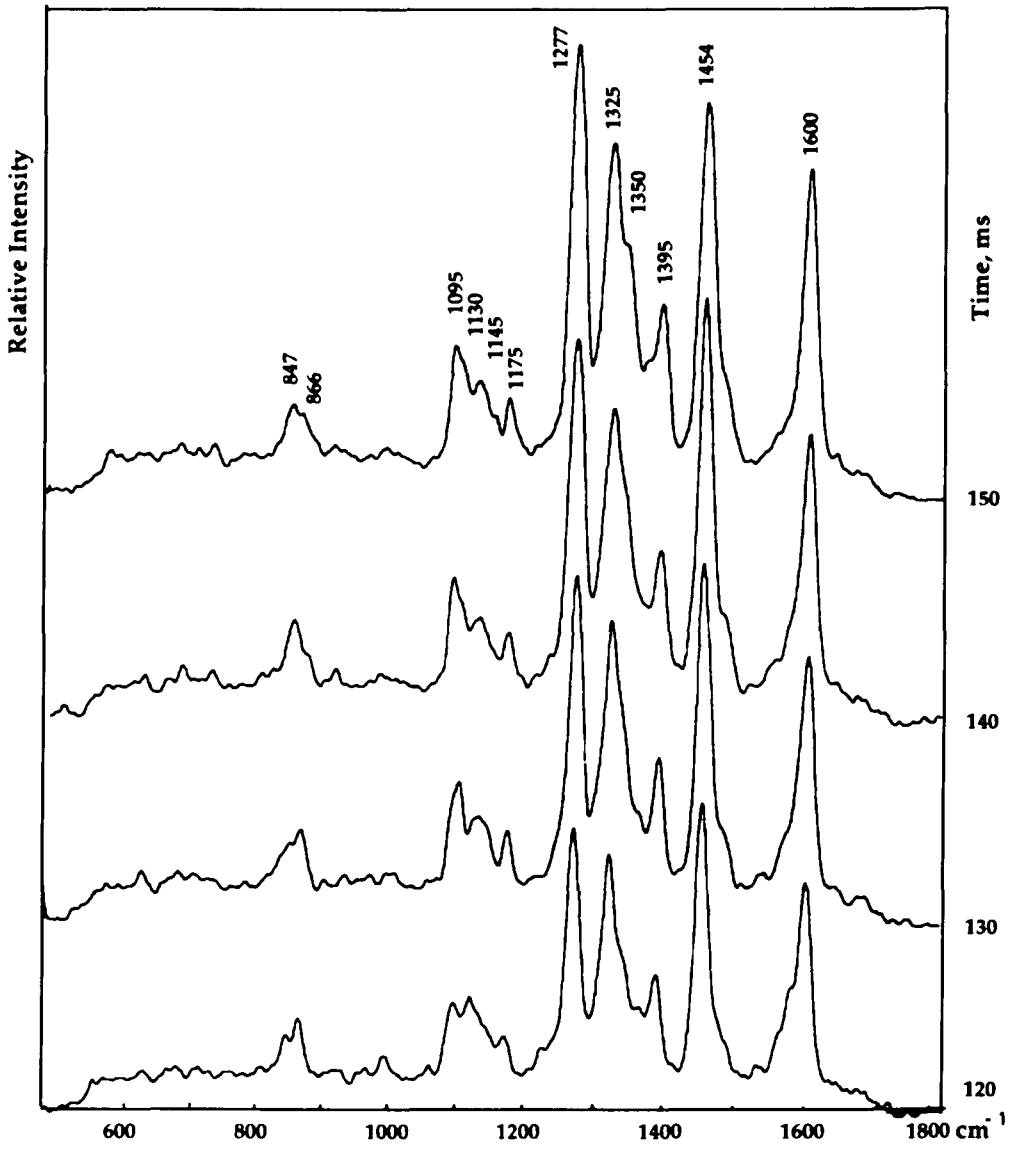

Fig. 2.11(b)

Fig. 2.11 Time-resolved SERS spectra of PNBA on a roughed Ag electrode. Excitation potential pulse from 0.0V to -0.9V with 200 ms pulse width duration followed by a step to -0.2V. Irradiation with 120 mW of 488 nm laser light. (a) Time: 0-90 ms, (b) Time:120 -150 ms.

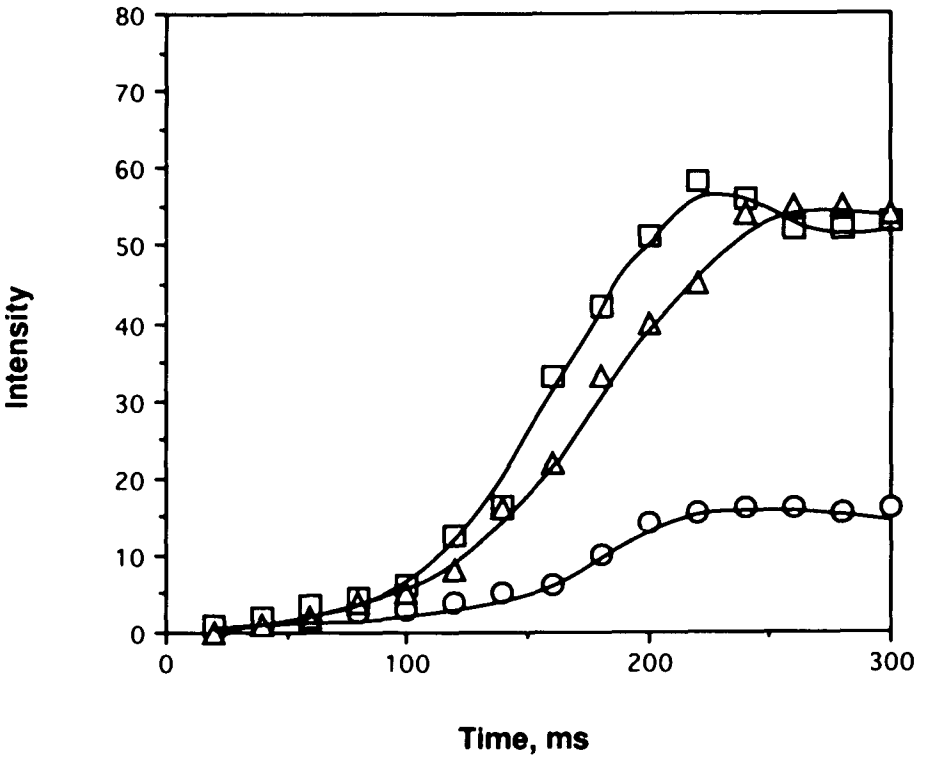

Fig. 2.12(a)

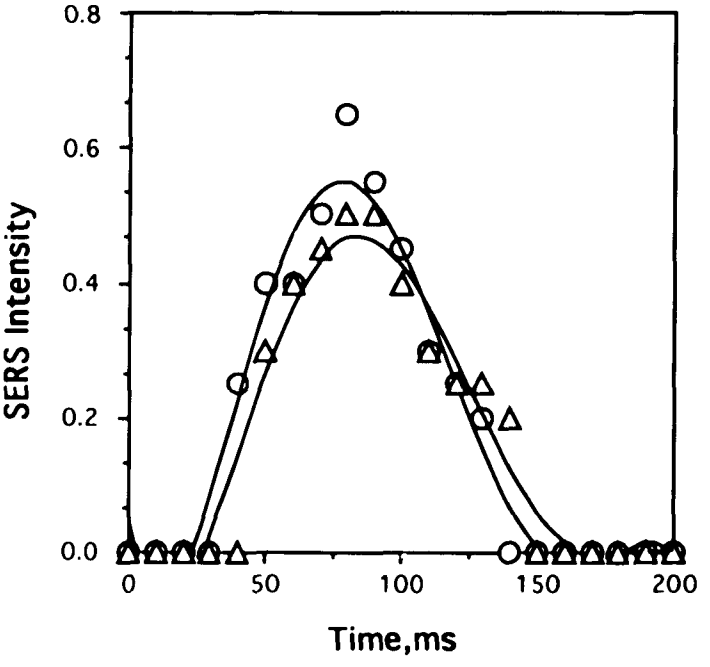

Fig. 2.12(b)

Fig. 2.12 Time dependence of intensities of some SERS bands in a potential pulse excitation experiment.

(a) Bands plotted: Δ---1277 cm^{-1}; O---1395 cm^{-1}; □---1454 cm^{-1}.

(b) Bands plotted: O---1233 cm^{-1} , Δ---1580 cm^{-1}

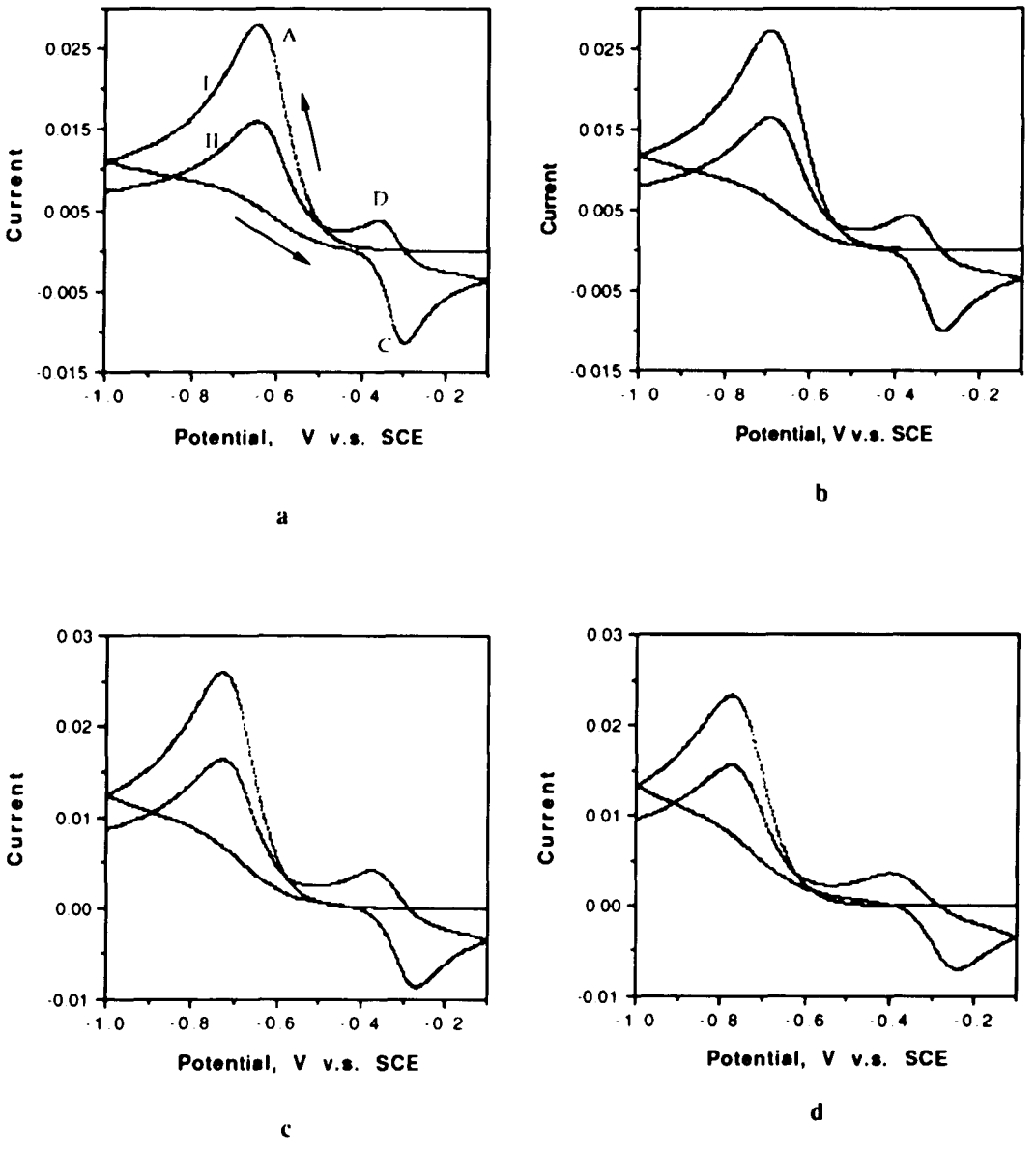

Fig. 2.13 Simulation results of cyclic voltammograms for the PNBA electrochemical reduction process as a function of scan rate. See text for the parameters. Scan rate: a)100 mV/s; b)500 mV/s; c) 2.0 V/s; d) 10.0V/s.

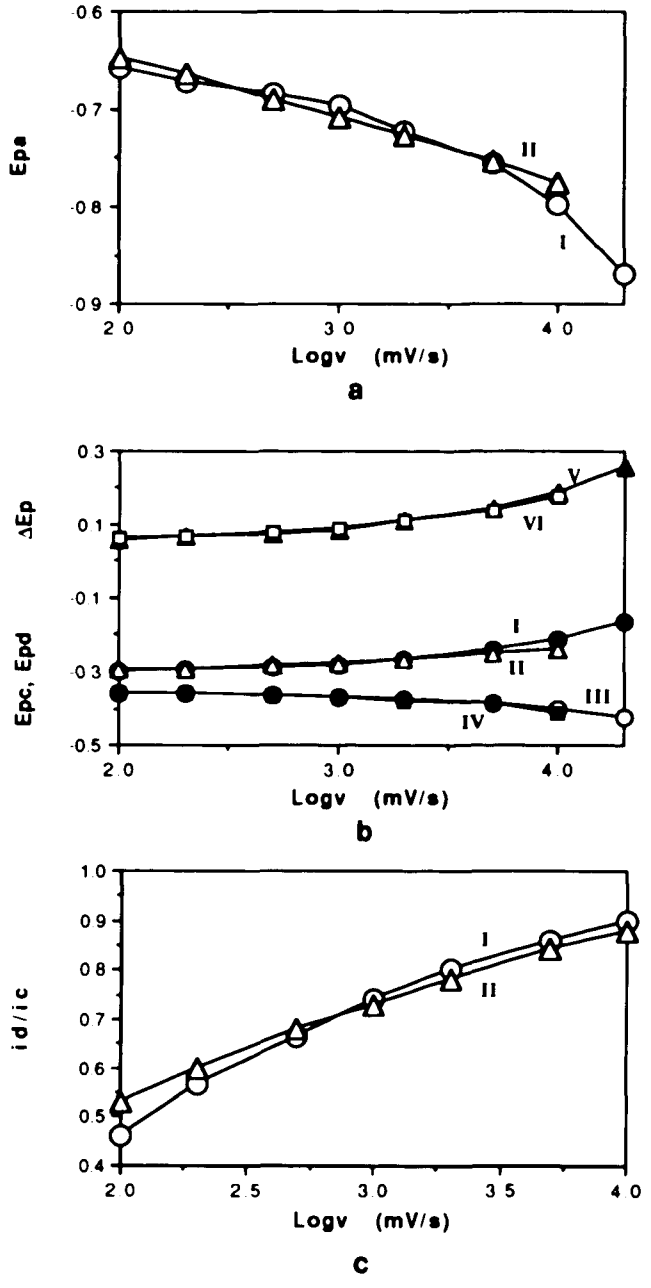

Fig. 2.14 a) The dependence of peak potential, Epa, on potential scan rate in 5.0 mM PNBA on a smooth Ag electrode. Curve I (O): Experimental results; Curve II (Δ): Simula-tion results. b) The dependence of peak potentials,Epc and Epd, on potential scan rate in 5.0 mM PNBA on a smooth Ag electrode. Curve I(●): experimental result for Epc; Curve II(Δ): simulation result for Epc; Curve III(O): experimental result for Epd; Curve IV(■): simulation result for Epd; Curve V (▲): experimental Epc-Epd; Curve VI(❑): simulated Epc-Epd. c) The dependence of the ratio of peak currents, i_d/i_c, on potential scanning ratein 5.0 mM PNBA on a smooth Agelectrode. (O): Experimental result; Curve II (Δ):Simulation result.

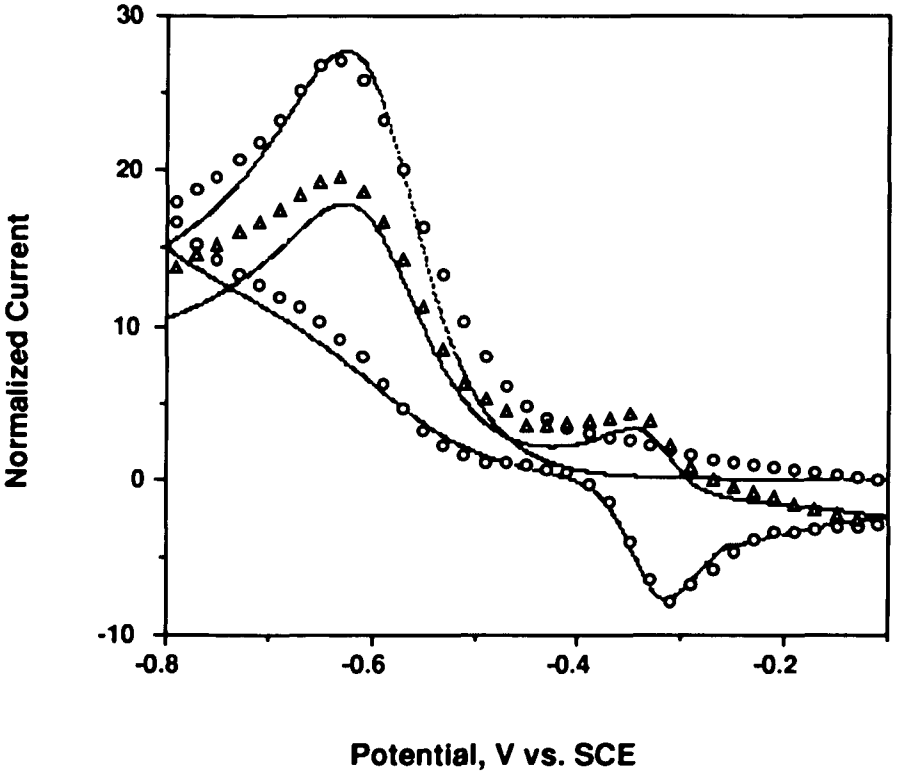

Fig. 2.15 Comparison of a simulated CV curve with experimental points. Scan rate: 50mV/s. Solution concentration of PNBA: 2.0 mM . Geometric surface area of the electrode: 0.0154 cm^2 Solid line --- simulated CV curve; ° --- experimental points on first cycle. ▲---- experimental points on second cycle. The simulated current is related to the experimental current in microamps by the factor : (surface area of the electrode) x (the square root of scan rate) x (the bulk concentration in moles/cm^3) x100. Dividing the experimental current by this factor gives the points used for comparison with the simulated current.

Chapter III

SERS Study of 4-Cyanopyridine Adsorption and Electroreduction Process on a Silver Electrode

Section 3.1 Introduction

As a sensitive surface probe, surface enhanced Raman spectroscopy (SERS) has enabled us to obtain information about species on a SERS active surface.[1,2] It has been used to investigate the adsorption process of molecules on a Ag surface[2-5] and the electrochemical oxidation/reduction process of organic compounds[2,6-11] and inorganic compounds.[12] Intermediates which are stable at special potentials have been observed by steady-state SERS measurements. [6-10,12] However, little information about short-lived intermediates and kinetics have been obtained in previous SERS studies. In this chapter, time-resolved SERS is used to study the adsorption and electroreduction of 4-cyanopyridine on a Ag electrode and kinetic information about this process is obtained.

Current-potential curves suggest that on a Hg electrode, 4-cyano-pyridine, 4-CNPY, undergoes a four-electron reduction to 4-aminomethyl-pyridine in acidic buffered solutions and a two-electron reduction to pyridine and cyanide in alkaline buffers.[13,14] In situations which are neither strongly acidic nor strongly basic, the number of electrons transferred during the reduction is between two and four, i.e., both products are produced. However, what will happen on a Ag electrode in an unbuffered neutral solution? The cyclic voltammetric result shows only one reduction wave peaked at about -1.4V on a SERS active Ag electrode and the reduction product suggested in the literature[15,16] from the SERS results is pyridine. Other SERS studies also indicate that the orientation of the adsorbed species are affected by the solution concentration, the electrode potential and the type of sovent.[17-19]

Section 3.2 Experimental

(a) Experiment Setup and Chemicals

An Ar^+ laser was used as light source. The SERS detecting system includes a three-electrode optical-electrochemical cell with a Ag working electrode, a Pt counter electrode and a SCE reference electrode, a SPEX triplemate (SPEX INDUSTRIES, INC.) mounted with a diode-array photodetector (EG&G PARC, model 1455XC) which is controlled by a Macintosh Plus computer through a detector interface (EG&G PARC, model 1461). The frequency resolution of this system is two wavenumbers per diode channel. The potential on the working electrode is controlled by a potentiostat (EG&G PARC, model 173) and a waveform generator (EG&G PARC, model 175). 4-Cyanopyridine (98%), 4-amino-methylpyridine (98%), 4,4'-bipyridyl hydrate (98%) and 4-pyridinecarboxaldehyde (98%) were purchased from the Aldrich Chemical Company, Inc. and pyridine from Mallinckrodt, Inc.. 4-Cyanopyridine was recrystalized from distilled water before use. All solutions were made with distilled water containing 0.1M reagent grade KCl.

(b) Experimental Procedure

The adsorption and electroreduction of 4-cyanopyridine (4-CNPY) on a Ag electrode were studied by both potential dependent surface-enhanced Raman spectroscopy (PD-SERS) and time resolved surface-enhanced Raman spectroscopy (TR-SERS). The 488 nm line of the Ar^+ laser was used as a probe

beam. The power of laser output was about 200 mW with about 80 mW reaching the electrode surface. Before SERS spectra were taken, the Ag electrode was polished and then pretreated by oxidation-reduction cycles (ORCs) in-situ in solutions with Raman active compounds or ex-situ in solution with only pure 0.1M KCl. The dwell time for each spectrum varied from hundreds of microseconds to several seconds. Sometimes, in order to check if the cause of changes in SERS spectra is due to an electrochemical effect or a laser induced photo-electrochemical effect, the SERS spectrum at a given potential was taken at a surface point which had been irradiated by the laser light for a long time and compared with the spectrum obtained from a new point on the electrode surface which had not been irradiated before the SERS measurement. The experimental results were saved on a floppy diskette, and then could be analyzed or plotted on a laser printer.

Section 3.3 Results and Discussion

(a) Concentration Dependence of 4-CNPY SERS Spectra

Fig. 3.1 shows SERS spectra of 4-cyanopyridine (4-CNPY) at -0.4V in 0.1M KCl at different concentrations. Basically, two types of spectra were found which can be related to either a dilute or a concentrated CNPY solution condition, respectively. One type of spectrum, A, corresponds to a simple 4-CNPY molecule or a monomer and the other type of spectrum, B, most likely to a dimer or an aggregate species. In dilute solution which contains 1.0 mM CNPY and 0.1M KCl, the monomer type spectrum A, curve (a) on the bottom in Fig. 3.1, shows two very strong bands at 1605 and 1008 cm^{-1}, three strong

bands at 1502, 1410 and 1214 cm^{-1} and three weak bands at 1372, 1261 and 1064 cm^{-1} in the spectral window. The dimmer or aggregate type spectrum B, curve (d) or (e) at the tope of Fig. 3.1 obtained in concentrated CNPY solutions, e.g., 10 or 20 mM CNPY, shows four very strong bands at 1600, 1520, 1208 and 970 cm^{-1}, two strong bands at 1261 and 1006 cm^{-1}, one medium strong band at 1450 and several weak bands at 1472, 1430, 1064 and 847 cm^{-1}. These two types of spectra share some of the Raman bands, such as the 1600, 1208 and 1006 cm^{-1} bands. However, the 1502 and 1410 cm^{-1} bands distinctively belong to the monomer spectrum, while the 1520, 1261, 970 and 847 cm^{-1} bands to the spectra in more concentrated solutions, which are possibly related to the dimer or aggregate. The SERS spectra obtained in medium concentrations, such as 2.5 and 5.0 mM CNPY, show a combination of bands from the two distinct types.

In order to assign the SERS bands, normal Raman spectra of both 4-CNPY solid and solutions were taken and are listed in Table 3.1 along with the assignments.[20-22] Four bands in the C-H stretch region are detected for the solid, but only one at 3068 cm^{-1} which is the total symmetric A_1 mode has strong intensity. It seems that most of the A_1 mode vibrations produce intense bands in Raman spectra.

The normal Raman spectra of 4-CNPY in both acetone and ethanol solutions show fewer bands than that of solid. However, the spectrum in ethanol shows two additional bands at 1002 and at about 1600 cm^{-1} with very strong intensities. These two bands are very close to the two original ν(CC) bands which are located at 992 and 1596 cm^{-1} and are considered to belong to the

same vibrations but of a protonated species since the pyridine ring nitrogen is basic and there are protons available in ethanol.

It is evident, by comparison with the normal Raman spectra of 4-CNPY, that all strong monomer SERS bands except 1410 cm^{-1} belong to A1 symmetry and are attributed to the symmetric in-plane type of vibrations.[20-22] Even the 1410 cm^{-1} band which has B2 symmetry is also an in-plane asymmetric stretch. However, many distinctive SERS bands of the putative dimer or aggregate are related to so-called out-of-plane γ vibrations. For example, both the 970 and 847 cm^{-1} bands are assigned to the γ(CH) modes. These facts indicate that the type A spectrum corresponds to the monomer species which adsorbs on the Ag electrode surface vertically, while the putative dimer or aggregate spectrum corresponds to a species which is oriented parallel or partly parallel to the electrode surface. Additional evidence for this conclusion is that the relative intensity of CN triple bond stretching with frequency at 2239 cm^{-1} decreases with increasing 4-CNPY concentration. The vertical orientation of the CN triple bond produces the most intense band and the parallel orientation the weakest.[23] Thus, the concentration of the species taking a parallel or partly parallel orientation increases with the bulk 4-CNPY concentration. The relative intensity of the 970 cm^{-1} band to the adjacent 1006 cm^{-1} band shows a strong concentration dependence and it increases with 4-CNPY concentration. A linear relationship is found between this relative intensity and the square of concentration when concentration is smaller than 0.01M (Fig. 3.2). This linear relationship is consistent with the formation of the dimer as the bulk concentration increase.

When the electrode is pretreated ex-situ in a solution containing only

0.1M KCl and then dipped into a 0.02M 4-CNPY solution, the putative dimer or aggregate spectrum is also observed. An interesting phenomenon is that in 2.5mM CNPY solutions, type A spectrum is observed after the first two-ORC pretreatment and the combination of types A and B is obtained after another two ORCs. This suggests that in this particular situation the dimer or aggregate is probably formed on the electrode surface when the ORCs produces more adsorption sites for attraction of 4-CNPY molecules from solution.

If the dimer or aggregate does exist, at least on the electrode surface, one of the possible orientations is that one of the CNPY molecules adsorbs on the Ag electrode surface vertically through the pyridine ring nitrogen and the other CNPY molecule orientates parallel. However, if this is true, the spectrum for the vertically adsorbed species should be always more intense than or at least have the same intensity as the spectrum for the parallel oriented species. In fact, in concentrated solutions the spectrum with intense out-of-plane bands overwhelms the vertically oriented spectrum. It seems more likely that the two adjacent 4-CNPY molecules lie face to face but with two cyano groups in the opposite directions so that their dipole moments compensate each other. Two possible orientations for such a dimer on electrode surface are either a face-to or a tilted orientation. In both situations the out-of-plane vibration bands could be observed with strong intensities. However, it seems that the tilted orientation is more reasonable, since, although the dipole moments are canceled out in the dimer, the electrode surface still feels a local dipole moment of the molecule attached on it. Of course, the local dipole moment will be much weaker than the dipole moment of the individual CNPY molecule because it is partially canceled by the dipole moment of the other molecule in the dimer. This model can also be thought as an aggregate when the surface concentration of the dimers is

very high.

(b) Time Dependence of 4-CNPY SERS Spectra at Various Potentials Where Electrolysis Does Not Take Place

The time-dependent SERS spectra of 4-cyanopyridine were taken and studied in neutral aqueous solutions with 0.1M KCl as supporting electrolyte. The pretreatment was performed by starting from a variety of different potentials and stepping to +0.3V for 2 seconds then returning to the starting potential in solutions containing 0.01M 4-CNPY with laser light shining on the electrode surface. Right after the pretreatment pulse, the SERS spectra were taken consecutively.

The result obtained at -0.1V (Fig. 3.3) shows only three major bands at about 1019, 1191 and 1598 cm^{-1} right after the pretreatment pulse. Many new bands grow up with time, and these new bands are located at 850(m), 967(vs), 1138(w), 1205(vs), 1262(m), 1445(m), 1464(w), and 1520(vs) cm^{-1}. The original 1019 cm^{-1} band shifts to 1006 cm^{-1} and the 1598 cm^{-1} band shifts to 1603 cm^{-1}. With the growth of the band intensities, the background also increases. Additionally, the cyano triple bond stretching band at 2239 cm^{-1} shows a decrease in intensity simultaneously with time.

According to Green and Harrison,[20] all of the three bands observed initially belong to A_1 symmetry, the totally symmetric vibration modes, and are assigned to the ring, β(CH), and ν(CC) vibration modes, where β(CH) is the in plane bending of the C-H bonds and ν(CC) is the stretch of the C-C bond. We

may assign the starting spectrum with only three major bands at 1019, 1191 and 1598 cm^{-1} to a species which interacts strongly with Ag surface, such as a surface complex. The strong interaction between adsorbed 4-CNPY molecules and the active sites of the electrode surface, which are probably silver ions, causes the ring mode (A_1) and the β(CH) mode (A_1) vibrations to shift from 1006 and 1205 cm^{-1} to 1019 and 1191 cm^{-1} respectively. Some of the intense newly growing bands can be directly assigned to the fundamental modes shared by both the monomer and the dimer (or aggregate). For example, the 967 cm^{-1} band is assigned to a γ(CH) (A_2) mode and the 1262 cm^{-1} band to a X-sens (A_1) mode,[20] where γ(CH) is the C-H out-of-plane bending and X-sens is the mode whose frequency is very sensitive to the substituent, X. The 1464 cm^{-1} band is assigned to the ν(CC, CN) (A_1) mode of the monomer, but the 1445 and the 1520 cm^{-1} bands to the ν(CC, CN) (A_1) and the ν(CC) (B_2) modes of the dimer (or aggregate), respectively.

All the phenomena discussed above can be explained by proposing that the 4-CNPY molecule stands vertically on the electrode surface with the ring nitrogen end-on immediately after the potential pretreatment and later the newly adsorbed molecules begin to cant toward the surface. The initial spectrum is similar to the SERS obtained in low concentration of 4-CNPY. The newly growing spectra represent the formation with time of the dimer or aggregate. As we discussed before, the dimer or aggregate tends to be adsorbed tilted. In this case, the out-of-plane modes tend to be more, though not exactly, perpendicular to the electrode surface. Thus, when the dimer or aggregate is formed, the intensities of the bands related to the out-of-plane modes will increase. The decrease in the intensity of the cyano band is probably due to some of the adsorbed molecules changing their orientation from vertical to tilted

so that the CN triple bond is no longer perpendicular to the surface.

At more negative potentials up to -0.6V, the new bands grow even faster. At -0.4V (Fig. 3.4), the initial bands are at 1006, 1198 and 1606 cm^{-1}, and the 1019 cm^{-1} band does not show up at this potential. This is similar to the 1025 cm^{-1} band in pyridine's SERS spectrum,[2] which only shows up at very positive potentials. The newly growing bands at about 1211(vs), 1415(m), and 1510(s) cm^{-1} are seen even in the first spectrum right after the pretreatment. With time some other bands at 970(sh), 1068(w) and 1262 cm^{-1}(m) are observed. At -0.6V (Fig. 3.5), except for the three major bands at 1006, 1198 and 1606 cm^{-1}, two new bands at 1411 and 1506 cm^{-1} appear at the beginning and then shift with time to 1416 and 1521 cm^{-1}. Another new band appears at 1451 cm^{-1} after about one and half minutes. If Fig. 3.4 and Fig. 3.5 are compared, It can be seen that the starting spectra are the same, but the final spectra are quite different. For example, the spectrum at -0.6V in Fig. 3.5 shows two strong bands at 1521 and 969 cm^{-1} and a medium band at 1451 cm^{-1}, whereas the spectrum at -0.4V shows two bands at 1510 and 1415 cm^{-1} instead. These latter bands are the same as those in the starting spectrum. In addition, the 970 cm^{-1} band appears as a shoulder band at -0.4V instead of a very strong band. In fact, the final spectra obtained at -0.1V and -0.6V are nearly the same as the steady-state spectra at high concentrations, though there are some frequency shifts for some bands which are probably caused by the electrode potential. Thus the dimer or aggregate is formed at these two potentials. However, the surface species at -0.4V might be a monomer rather than a dimer or aggregate since the final SERS spectrum here is more like the low concentration steady state spectrum.

The presence of laser light during the ORC pretreatments has an effect

on the SERS spectra only at special potentials. For example, at both -0.1V and -0.6V the same sets of transient SERS spectra are obtained no matter whether the laser light is on or off the electrode during the ORC. However, the SERS spectrum detected at -0.4V when electrode is pretreated in-situ in the dark is quite different from that obtained when laser light is present during the pretreatment. The spectrum looks more like the steady-state spectrum obtained at -0.6V in high concentrations (Fig. 3.1e).

This special phenomenon is probably related to the photosensitivity of AgCl at -0.4V at which AgCl formed during the oxidation half-cycle in the ORC pretreatment is more sensitive to the laser light. An intensive investigation of the laser illumination effect on the morphology of Ag surface has shown that the presence of the laser light during the ORC causes a photoreduction of AgCl and this photoreduction produces more sites for adsorption.[24] More available sites favor the adsorption of monomer and also make the adsorption process easy and faster. The SERS spectrum at -0.4V when the electrode is pretreated in the presence of laser light does reach its saturated value faster then at the other two potential values.

Experiments also show that the presence of laser light during the time elapsed between measurements has little effect on the time dependence of the spectra. This indicates that the intensity build-up is due to the absorption of molecules not the photolysis.

The ex-situ pretreatment in pure 0.1M KCl aqueous solution at potentials which are more negative than -0.3V gives rise to the same results as the in-situ pretreatment in the dark. For example, consider a Ag electrode pretreatment ex-

situ by an ORC with a final potential -0.4V, at which the AgCl formed during the positive potential pulse in the ORC has already been reduced to Ag. Then if this electrode is put into a SERS cell which contains 10mM 4-CNPY solution and the SERS spectrum is measured at the same potential, a gradually build-up of the SERS intensity with time was observed similar to the situation with in-situ pretreatment. The same phenomenon was also observed even when the electric circuit is open. In this case the buildup of the SERS intensity is solely due to the adsorption of 4-CNPY molecules since no reduction of AgCl occurs. These results indicate that the reduction of Ag atoms from AgCl may not be the reason for the time dependence of 4-CNPY SERS spectrum, i.e., it is not the rate-determining-step. The adsorption of 4-CNPY molecules and the formation of aggregates are the slow steps which control the whole process.

In conclusion, the time-dependent spectra at different potentials in 0.02M 4-CNPY solution show that after ORC pretreatments, the end-on species, a monomer, adsorbs first and then the tilted species, maybe a dimer or an aggregate, with only one exception, i.e., when electrode is pretreated in-situ at -0.4V in the presence of laser light, only the end-on monomer spectra are observed.

(c) The Electroreduction of 4-CNPY

I. Monomolecular Reactions

Electrochemically, the reduction of 4-CNPY in neutral aqueous solutions occurs at the potential more negative than -1.0V with a peak potential at about -1.35V. The mechanistic analysis for the electrochemical reduction is complicated by many possible pathways and products. The two simplest possible monomolecular processes (1) produce pyridine and CN^- and (2) 4-aminomethylpyridine, PY-CH_2NH_2 (AMPY),

$$PY\text{-}CN + 2e^- + H^+ = PY + CN^- \quad (1)$$

$$PY\text{-}CN + 4e^- + 4H^+ = PY\text{-}CH_2NH_2 \quad (2)$$

Fig. 3.6 shows a typical potential dependence of SERS spectra for 1.0mM 4-CNPY in the range from 800 to 1700 cm^{-1} at steady state. The starting spectrum corresponds to a vertically orientated 4-CNPY monomer. A new band at about 1522 cm^{-1} appears at -0.7V and it keeps growing as potential is moved further negative. The original 1501 and 1411 cm^{-1} bands begin to decrease at -0.9V and totally vanish in the product spectrum at -1.2V The original 1605 cm^{-1} band shifts to 1589 cm^{-1}, 1522 cm^{-1} to 1529 cm^{-1}, and 1008 cm^{-1} to 1002 cm^{-1}. Another new band appears at 1630 cm^{-1} and a shoulder band at about 970 cm^{-1}. The final spectrum at -1.2V can be assigned to pyridine which is produced along with cyanide by two-electron reduction of 4-CNPY. The SERS band of free cyanide was observed at -1.2V at 2190 cm^{-1} which corresponds to the stretching mode of CN^- triple bond.

Fig. 3.7 shows the SERS spectra of pyridine at -0.4V and -1.2V. The spectrum obviously depends on potential. The spectrum at -0.4V (Curve a in

Fig. 3.7) looks quite different from the product spectrum obtained at -1.2V. It shows two extremely strong bands at 1034 and 1004 cm^{-1}. However, the spectrum at -1.2V (Curve b in Fig. 3.7) is almost identical with the product spectrum at -1.2V in Fig. 3.6 except for a weak band at 1529 cm^{-1} and a small shoulder band at 970 cm^{-1}. This difference is probably caused by the formation of small amount of another compound such as a product of a bimolecular chemical coupling reaction.

II. Bimolecular Reactions

The most possible products of bimolecular reactions include 4,4'-bipyridine (BIPY), 4-pyridylmethyleneazin (AZIN) and azo-4-methyl-pyridine (AZO). The following sets of reactions show all of the possibilities,

$$2PY\text{-}CN + 2e^- = \underset{BIPY}{PY\text{-}PY} + 2CN^- \quad (3)$$

$$2PY\text{-}CN + 2e^- + 2H^+ = \underset{AZIN}{PY\text{-}CH{=}N\text{-}N{=}CH\text{-}PY} \quad (4)$$

$$PY\text{-}CH{=}N\text{-}N{=}CH\text{-}PY + 2e^- + 2H^+ = \underset{AZO}{PY\text{-}CH_2\text{-}N{=}N\text{-}CH_2\text{-}PY} \quad (5)$$

The bimolecular products could be thought to be formed through following scheme,

$$PY\text{-}CN + e^- = PY\text{-}CN^- \quad (1a)$$

$$PY\text{-}CN^- = PY\cdot + CN^- \quad (1b)$$

$$PY\cdot + PY\cdot = PY\text{-}PY \quad (3a)$$

$$PY\text{-}CN^- + PY\text{-}CN + e^- + 2H^+ = PY\text{-}CH{=}N\text{-}N{=}CH\text{-}PY \quad (4a)$$

Time-resolved SERS can be used to follow the electroreduction process of 4-CNPY. The experimental result in 20 mM 4-CNPY in the μs domain for a potential-pulse experiment is shown in Fig. 3.8, where the potential was stepped from -0.4V to -1.2V. The Ag electrode was pretreated in-situ in the dark at -0.4V in 0.02M 4-CNPY with 0.1M KCl. The starting spectrum is the same as the steady-state spectrum shown in Fig. 3.1 (d) or (e). The time-resolved SERS results show that, at the beginning, the relative intensity of the 1450, 1262 and 970 cm^{-1} bands decreases, but the 847 cm^{-1} band increases. No new bands were found in the first 2,500 μs. After about 2,500 μs, two new bands appear at 1417 and 1472 cm^{-1} and the original 1520 cm^{-1} band gradually shifts to 1530 cm^{-1}. Although no transient bands were found in the 10 ms time window, the decrease of the intensity of three initial bands in the first 2,000 μs can be related to the formation of 4-CNPY anion by one electron reduction. The final spectrum represents new species generated by electrode reactions. These could belong to any one or a number of possible products.

The steady state SERS spectra in concentrated solutions (Fig. 3.9), show changes at -1.0V, as predicted from the CV results. The original bands at 1471 and 847 cm^{-1} begin to increase at -1.0V, but the 1450 and the 1261 cm^{-1} bands begin to decrease. Two new bands appear at 1426 and 1417 cm^{-1} at -1.1V and keep growing no matter whether potential stays there or is moved further negative. The product spectrum obtained at -1.2V is the same as that in time-resolved SERS experiment. It contains two very strong bands at 1416 and 1208 cm^{-1}, five strong bands at 1600, 1530, 1003, 989 and 966 cm^{-1}, two medium strength bands at 1471 and 847 cm^{-1} and two strong shoulders at 1590 and 1426 cm^{-1}. The 1630 cm^{-1} band which is present in the 1.0 mM product spectrum does not appear in this spectrum. The SERS spectra are lost

if potential is made more negative than -1.2V. Even at this potential, the total intensity of spectra is much weaker than at more positive potentials and fades with laser light. The intense spectra were obtained at a new point on the Ag electrode surface which had not been irradiated by laser light. The major difference between the spectra in concentrated solutions and those in dilute solutions is that four bands at 1470, 1426, 1416 and 847 cm^{-1} appear more intensive in the former case (Fig. 3.9). This indicates that besides pyridine, at least another product is produced in the concentrated solutions. Most likely it is an azo compound which comes from a bi-molecular process. The assignment will be made later by ruling out other possible products by comparison of spectra.

III. Concentration Dependence of the Electroreduction Products

The reduction product spectra of 4-CNPY on a Ag electrode in different CNPY concentration solutions at -1.2V are shown in Fig. 3.10, which evolved as the potential was swept very slowly (0.33V/s) from -0.4V to -1.2V. As mentioned above, two types of product spectra, one of which is related to pyridine and the other to an azo compound, are obtained in dilute (1.0 mM) and concentrated (20.0 mM) solutions, respectively. Similar to the spectra of the starting species shown in Fig. 3.1, the product spectra in intermediate concentrations are the combinations of these two types of spectra with different weighing factors. The ratio of the azo over pyridine increases with 4-CNPY bulk concentration.

It is hard to tell whether or not pyridine is present in the product spectra in very concentrated solutions, since the pyridine spectrum is weak at -1.2V and

may be covered by the intense azo spectrum. However, in medium concentrations, both pyridine and azo spectra are present in the product spectra (Curve b in Fig. 3.10). The 1630 cm^{-1} band is exclusive for pyridine at -1.2V and its intensity relative to the azo spectrum decreases with the increase of 4-CNPY concentration. Thus, it is certain that even in concentrated solutions, pyridine is still one of the products of 4-CNPY reduction. This is in agreement with Furukawa's conclusion.[16]

There seems to be a one to one correspondence between the starting species and the products, that is, the 4-CNPY monomer produces pyridine and the dimer or aggregate gives rise to the azo compound. This can be seen by comparing the spectra in Fig. 3.1 with those in Fig. 3.10. However, in an intermediate concentration, 2.5 mM 4-CNPY, we can obtain both azo and pyridine depending on experimental conditions. If the potential is stepped to -1.2V from -0.4V directly, the product spectrum (Curve b in Fig. 3.11) is quite different from that obtained when potential is changed very slowly (Curve b in Fig. 3.10). In this potential step experiment, only the pyridine spectrum is observed rather than a combination of the pyridine and azo spectra.

Another deviation from the one to one correspondence is shown in an experiment when 4-CNPY is only present on the electrode surface (Fig. 3.12). The Ag electrode can be modified by pretreating with ORCs in 0.02M 4-CNPY solution. The modified electrode is then washed and placed in a solution which contains only supporting electrolyte, 0.1M KCl. The initial SERS spectrum of this system at -0.4V (Curve a in Fig. 3.12) is primarily the same as the in-situ experiment in 0.02 M 4-CNPY solution (Curve e in Fig. 3.1). However, the product spectrum in the experiment with the modified electrode at -1.2V (Curve

b in Fig. 3.12) is different from that observed in the in-situ experiment in 0.02 M 4-CNPY (Curve e in Fig. 3.10). It is, however, similar to the product spectrum in 1.0 mM 4-CNPY solution (Curve a in Fig. 3.10), which looks like pyridine. This indicates that an aggregate on the surface is probably necessary but not sufficient for producing the azo compound. In other words, the product obtained in concentrated solutions is not just from a simple mono-molecular reaction such as electron transfers or surface product reacting with solvent, or a reaction between the surface produced species. Otherwise, the product spectrum observed in the experiment with the modified electrode should be the same as the spectrum obtained in the in-situ experiment. It seems more likely that the product produced in concentrated solutions comes from a bi-molecular reaction in which the solution species plays an important role. On the other hand, pyridine can be produced from both 4-CNPY monomer as shown in the experiment in 1.0 mM 4-CNPY solution, and from an aggregate as in the potential step experiment in 2.5 mM CNPY solution and in the modified electrode experiment. One thing common to all situations where pyridine is the major product is that there is little possibility of a chemically coupling reaction between the electrode product species, probably a radical or radical anion, and the solution species, 4-CNPY molecules. For example, in the modified electrode experiment, only the adsorbed species can be involved in the electrochemical reduction process. In very dilute solutions such as 1.0 mM, the chemical coupling reaction is minimized because of the low concentration of solution species. For the potential step experiment in 2.5mM 4-CNPY solution, since the potential is stepped to a very negative value immediately, the radicals reduced on the surface would be further reduced to the final reduced product before it reacts with a solution species. It should be point out that this result can be obtained only in low 4-CNPY concentrations. If the potential step experiment is

done in a concentrated 4-CNPY solution, such as 0.01M or 0.02M, the azo type spectrum is observed and overwhelms the pyridine spectrum.

Monitoring of the SERS spectra in the region from 1800 to 2600 cm^{-1} shows that only one band is located at about 2239 cm^{-1} at -0.6V and at more positive potentials. Another band appears at about 2090 cm^{-1} when the potential is more negative than -1.0V, which is exactly the same frequency as that of cyanide ion surface species, CN^-. The relative intensity of this band decreases with the increase of 4-CNPY bulk concentration. Similar results are obtained in the experiment with the modified electrode which is pretreated in 20 mM 4-CNPY. In this experiment, the CN stretch band of 4-CNPY at 2240 cm^{-1} is hardly observed, but the CN^- ion stretch band at 2090 cm^{-1} in the product spectrum is much more intensive than in the concentrated 4-CNPY solutions. Therefore, one obvious fact is that, along with pyridine, cyanide is produced during the electrochemical reduction, and the efficiency of producing cyanide decrease with 4-CNPY concentration. This suggests that the product in concentrated solutions probably comes from a process which does not produce cyanide. For such a process which involves two reactant molecules without producing cyanide, azo-4-methylpyridine would be our first choice for the product.

As a summery, the following conclusions can be drawn from the analyses above: 1) The electrochemical reduction products in dilute solutions is pyridine and cyanide; 2) The major reduction process in concentrated solutions involves a bi-molecular reaction between an electrode generated species and a solution species, and this reaction either does not produce or produces only very little cyanide; 3) Azo-4-methylpyridine is probably the major product in concentrated

solutions; 4) Azo-4-methylpyridine is formed after 2.5 ms in the time-resolved SERS experiment.

IV. Product Identification

Besides pyridine and 4-aminomethylpyridine, there are several other possible products from the monomolecular process, such as 4-(iminomethyl)-pyridine (abbr. IMPY), 4-pyridinecarboxaldehyde (ALPY) or its reduction product, 4-(hydroxymethyl)pyridine (HMPY).

$$PY\text{-}CN + 2e^- + 2H^+ = PY\text{-}CH{=}NH \quad (6)$$

IMPY

$$PY\text{-}CH{=}NH + H_2O = PY\text{-}CHO + NH_3 \quad (7)$$

ALPY

$$PY\text{-}CHO + 2e^- + 2H^+ = PY\text{-}CH_2OH \quad (8)$$

HMPY

For the bimolecular process, 4-pyridyl(4-pyridylmethylene)amine (PPMEA), 4-pyridyl(4-pyridyl-methyl)amine (PPMA) are also possible,

$$2PY\text{-}CN + 2e^- + H^+ = PY\text{-}N{=}CH\text{-}PY + CN^- \quad (9)$$

PPMEA

$$PY\text{-}N{=}CH\text{-}PY + 2e^- + 2H^+ = PY\text{-}NH\text{-}CH_2\text{-}PY \quad (10)$$

PPMA

If the hydrolysis is possible, 4-aminopyridine would also be produced,

$$PY\text{-}N{=}CH\text{-}PY + H_2O = PY\text{-}NH_2 + PY\text{-}CHO \quad (11)$$

In order to further identify the products, SERS spectra of several authentic compounds were taken in conditions similar to that for the 4-CNPY

reduction. Table 3.2 gives all the experiment results. The spectrum of 4-(aminomethyl)-pyridine looks very much like that of 4-CNPY in concentrated solutions. It shows three very strong bands at 1605, 1206 and 1006 cm^{-1} and three strong bands at 1532, 1262 and 971 cm^{-1}. However, unlike 4-CNPY, the SERS spectrum of 4-AMPY is almost independent of potential. The strong 1262 cm^{-1} band in 4-AMPY spectrum does not exist in the product spectra in dilute 4-CNPY solutions and is very weak in concentrated solutions. In addition, the two very strong bands at 1416 and 1469 cm^{-1} in the product spectrum of the 4-CNPY reduction do not appear in 4-AMPY spectra. Therefore, 4-AMPY is ruled out as a product or at least as a major product in the reduction process of 4-CNPY under our experimental conditions.

One can find phenylmethyleneamine type molecules in Beilstein's Handbook,[25] but 4-pyridinemethyleneamine is not commercially available. Fortunately 4-pyridinecarboxaldehyde (ALPY) is available and its SERS spectra have been taken at various electrode potentials. The spectrum of 0.01M ALPY in 0.1M KCl at its equilibrium potential, -0.2V, show three very strong bands at 1605, 1207, and 1005 cm^{-1}, three strong bands at 1531, 1260 and 970 cm^{-1} and seven weak bands at 1460, 1423, 1325, 1088, 1056, 868 and 842 cm^{-1}. Among these bands, only two of them, located at 1531 and 1325 cm^{-1}, are unique for ALPY. All the others have their corespondents in the 4-CNPY spectrum although the 868 cm^{-1} band only shows up in IR, not in the Raman spectrum. A significant change in the spectrum occurs at -0.6V. When the potential is more negative than -0.6V, the spectrum remains the same. It corresponds to the electroreduction product of ALPY, 1,2-bis(4-pyridyl)ethane (see Chapter IV). Compared to the ALPY spectrum at -0.2V, the spectrum found between -0.6V and -1.2V is quite complicated. The three original bands at 1605,

1207 and 1005 cm^{-1} remain very strong, but the first band shifts to 1601 cm^{-1}. Three strong new bands appear at 1561, 1538, 1505 cm^{-1} and a shoulder band at 1480 cm^{-1}. The relative intensities of the 1423, 1325, and 868 cm^{-1} bands become intense and the 868 cm^{-1} band shifts to 878 cm^{-1}. Three original bands at 1531, 1460 and 970 cm^{-1} disappear from the spectrum. The spectrum of 1,2-bis(4-pyridyl)ethane is quite different from the product spectra of 4-CNPY reduction. Thus neither ALPY nor 1,2-bis(4-pyridyl)ethane can be the reduction product of 4-CNPY. According to eqns. (7) and (11), ALPY is one of the hydrolysis products of IMPY and PPMEA. Since ALPY is not formed, the other two compounds, ammonia and 4-aminopyridine will not be formed either. Thus, all the possible monomolecular reduction products, except IMPY, have been eliminated. Even IMPY can also be eliminated as the products for two reasons. i). According to Baizer and Adams,[15,26] the hydrolysis of immino compounds easily occurs, thus if it exists, ALPY or HMPY should be observed. ii). Both pyridine and IMPY are two-electron reduction products of 4-CNPY and these two reactions are in parallel, thus the concentration dependences of these two reaction rates are expected to be the same. However, the product spectrum in dilute solution can be assigned to pyridine. The other product spectrum appears only in higher 4-CNPY concentrations and its relative intensity to that of pyridine increases with concentration. Thus it can not be assigned to IMPY.

Since the possibilities of the reactions shown in eqns.(2), (6)-(8) and (11) have been eliminated, besides pyridine, only five possible products are left and all of them are derived from bimolecular process. 4,4'-Bipyridine is the only compound commercially available. The BIPY spectrum shows little change in the potential region from -0.4V to -0.8V. Two very intense bands are found at about 1606 and 1292 cm^{-1}, one strong band at 1011 cm^{-1} and two medium

strong bands at about 1512 and 1230 cm^{-1}, two weak bands at 1474, 1436 cm^{-1} and two shoulder bands at 1530 and 1322 cm^{-1}. These spectra represent stable BIPY. When potential is more negative than -1.0V, the 1474 cm^{-1} band disappears. The intensities of the 1530, 1512, 1322 and 1230 cm^{-1} bands begin to increase and the 1235 cm^{-1} band shifts to 1222 cm^{-1}. Another new band at 1652 cm^{-1} appears at -1.1V. Large changes in both frequency and relative intensity occur at -1.2V. The 1606 cm^{-1} band shifts to 1594 cm^{-1}, 1530 to 1535, 1512 to 1505, 1322 to 1335, 1011 to 996 cm^{-1}. The 1652, 1594, 1535, 1505 and 996 cm^{-1} bands become very intense, but the 1292 cm^{-1} band becomes weaker. In addition, a new band appears at 1043 cm^{-1}.

When the potential is moved further negative, the 1505, 1335 and 1043 cm^{-1} bands keep increasing, but the 1652, 1535 and 1292 cm^{-1} bands decrease. In addition, the 1505 cm^{-1} band shifts to 1500 cm^{-1}. Finally the spectrum at -1.5V shows three very intense bands at 1593, 1500 and 1336 cm^{-1}, three intense bands at 1222, 1043 and 996 cm^{-1}. The 1652, 1535, and 1292 cm^{-1} bands become very weak.

When potential is swept back in positive direction, the spectrum shows a delay up to -1.2V, i.e., it remains almost the same as that at -1.5V and the spectrum which appears at -1.2V during the negative-going potential sweep, can not be recovered. At more positive potentials, the spectra observed are almost the same as those during the negative-going sweep.

This experimental result indicates that the overall reduction-oxidation process is reversible. The reduction includes two successive electron transfers. The first electron transfer is much easier than the second, or the first energy

barrier is much lower than the second barrier. As a result, the one-electron reduction intermediate, $BIPY^{\cdot -}$ radical, can be observed during the negative-going potential sweep, but not during the positive-going sweep.

Since BIPY is reduced at almost the same potential as 4-CNPY, what would happen to BIPY if large amounts of 4-CNPY exists in its vicinity. The SERS result obtained in a 0.4 mM BIPY-0.02 M 4-CNPY mixture at -0.4V is almost the same as that in pure 4-CNPY solution, except for a very strong 1291 cm^{-1} band. At -1.2V where both compounds are reduced if they are alone, 4-CNPY is reduced but BIPY isn't. The product spectrum of 4-CNPY is the same as in pure solution. BIPY spectrum shows only a small frequency shift at 1291 band.

Because the SERS experiments of BIPY in both pure BIPY and BIPY-4-CNPY mixture solutions show totally different spectra at the corresponding potentials, BIPY can not be a product in 4-CNPY reduction process.

There are only two possible mechanisms with four possible products left. They are PPMEA, PPMA, AZIN and AZO. According to Colthup et al,[27] the C-N single bond stretch frequency is at 1191-1171 cm^{-1} for the aliphatic secondary amines, 1342-1320 cm^{-1} and 1315-1250 cm^{-1} for the aromatic secondary amines. Also the C=N and the N=N double bond stretches are in the frequency ranges 1690-1620 cm^{-1} and 1450-1400 cm^{-1} respectively. Since the product spectrum in concentrated solutions shows one strong distinct band at 1417 cm^{-1}, therefore, except for AZO, none of them could be the product.

Section 3.4 Conclusion

There are two kinds of species adsorbed on the Ag electrode surface. The one which is predominant in dilute solutions is the simple 4-CNPY molecule adsorbed with an end-on orientation. The other species which plays an important role in concentrated solutions is a dimer or aggregate of 4-CNPY adsorbed in a tilted orientation. The time dependent SERS shows that, in concentrated solutions, the monomer adsorbs on the electrode surface first and then the dimer or aggregate is formed. The presence of laser light during the ORC pretreatments has some effect on the formation of dimer or aggregate at a particular potential, but it has little effect on the adsorption process during the time elapsed between measurements. The reduction product in dilute solutions is pyridine no matter which species, monomer or aggregate, is adsorbed on the electrode surface. Azo-4-methylpyridine is probably the best choice for the product in concentrated solutions and a bi-molecular process is the most likely approach in this situation. The overall reaction mechanism can be proposed as follows,

$$PY\text{-}CN + e^- = PY\text{-}CN^-$$

$$PY\text{-}CN^- + e^- + H^+ = \underset{\text{(pyridine)}}{PY} + CN^-$$

$$PY\text{-}CN^- + PY\text{-}CN + e^- + 2H^+ = \underset{\text{(AZIN)}}{PY\text{-}CH{=}N\text{-}N{=}CH\text{-}PY}$$

$$PY\text{-}CH{=}N\text{-}N{=}CH\text{-}PY + 2e^- + 2H^+ = \underset{\text{(AZO)}}{PY\text{-}CH_2\text{-}N{=}N\text{-}CH_2\text{-}PY}$$

Table 3.1 Assignments of Normal Raman and SERS Spectra of 4-CNPY

assignment	symmetry	fundamentals	solid	in acetone	in ethenol	SERS 1.0mM	SERS 2.5mM	SERS 5.0mM	SERS 10.0mM	SERS 20.0mM
CH strech	B2	3086 w	3084 w							
CH strech	A1	3068 s	3068 s	3070 s	3070 s					
CH strech	A1	3049 m	3050 m							
CH strech	B2	3030 m	3030 m							
CN strech	A1	2246 vs	2246 vs	2242 vs	2240 vs	2239 vs	2239 s	2238 m	2238 w	2238 w
ν(CC)**	A1				1600 s					
ν(CC)	A1	1596 s	1596 vs	1594 vs	1596 s	1605 vs	1602 vs	1603 vs	1602 vs	1600 vs
ν(CC)*	B2						1519 m	1520 s	1521 s	1520 s
ν(CC)	B2	1547 m	1510 w			1502 s	1505 m	1504 sh		
ν(CC,CN)*	A1							1470 vw	1471 w	1472 w
ν(CC,CN)	A1	1497 m		1488 m			1451 vw	1451 w	1449 w	1450 m
ν(CC,CN)*	B2						1430 vw	1429 vw	1429 vw	1431 vw
ν(CC,CN)	B2	(1406)†				1410 s	1408 m	1406 w	1406 vw	1406 vw
β(CH)	B2	1340 m	1340 m	1332 w		1336 w	1372 w			1345 w
X-sens	A1	1240 m	1240 m			1260 w	1260 m	1262 s	1261 s	1261 s
α(CC)	B2	(1219)†								
β(CH)	A1	1193 vs	1194 vs	1194 vs	1196 vs	1214 s	1209 vs	1208 vs	1208 vs	1208 vs
β(CH)	B2	(1081)†								
β(CH)	A1	1073 m	1078 w			1064 w	1063 w	1064 w	1064 w	1064 vw
ring**	A1				1002 vs					
ring	A1	989 vs	992 vs	992 vs	992 vs	1008 vs	1006 vs	1006 vs	1006 s	1006 s
γ(CH)	A2	979 w					970 s	970 s	970 vs	970 vs
γ(CH)	A2	941 vw	(941)							
γ(CH)	B1	(865)								
γ(CH)	B1	827 w								
X-sens	A1	774 s	778 m	776 m	778 m					
α(CC)	B1	(710)†								
α(CCC)	B2	667 s	670 s	672 m	672 m					
α(CC)	B1	559 m	562 m	564 m	564 w					
X-sens	B2	550 w	(550)							
X-sens	A1	452 m	456 m	458 s	456 m					
α(CC)	A2	(400)								
X-sens	B1	371 vw								
δ(CN)	B2	190 s								
γ(CN)	B1	145 m								

α ---- scissors motion;
β ---- in plane bending;
γ ---- out of plane bending;
ν ---- stretch;
δ ---- out of plane motion of bond.

vs ---- very strong;
s ---- strong;
m ---- medium;
w ---- weak;
sh ---- shoulder.

* assigned to the aggregate; ** assigned to the protonated molecules.

Table 3.2 SERS Bands of AMPY, ALPY and BIPY in 0.1M KCl on Ag Electrode

AMPY		ALPY		BIPY	
-0.6V	-1.2V	-0.2V	-1.2V	-0.6V	-1.2V
					1652 vs
1605 vs	1605 vs	1605 vs	1601 vs	1606 vs	1594 vs
			1561 s		
1532 s	1532 s	1531 s	1538 s	1530 sh	1535 vs
			1505 s	1512 m	1505 vs
1457 w	1454 m	1460 w	1480 sh	1474 w	
1426 w	1426 w	1423 w	1425 s	1436 w	
1372 m	1324 w	1325 w	1326 s	1322 sh	1335 m
				1292 vs	1292 m
1262 s	1262 s	1260 s	1254 s		
				1230 m	1222 m
1206 vs	1204 vs	1207 vs	1208 vs		
		1088 w	1089 w		
1057 w	1057 w	1056 w	1057 w		1043 m
1006 vs	1004 s	1005 vs	1004 vs	1011 s	996 vs
971 s	971 s	970 s			
		868 w	878 s		
		842 w	842 m		

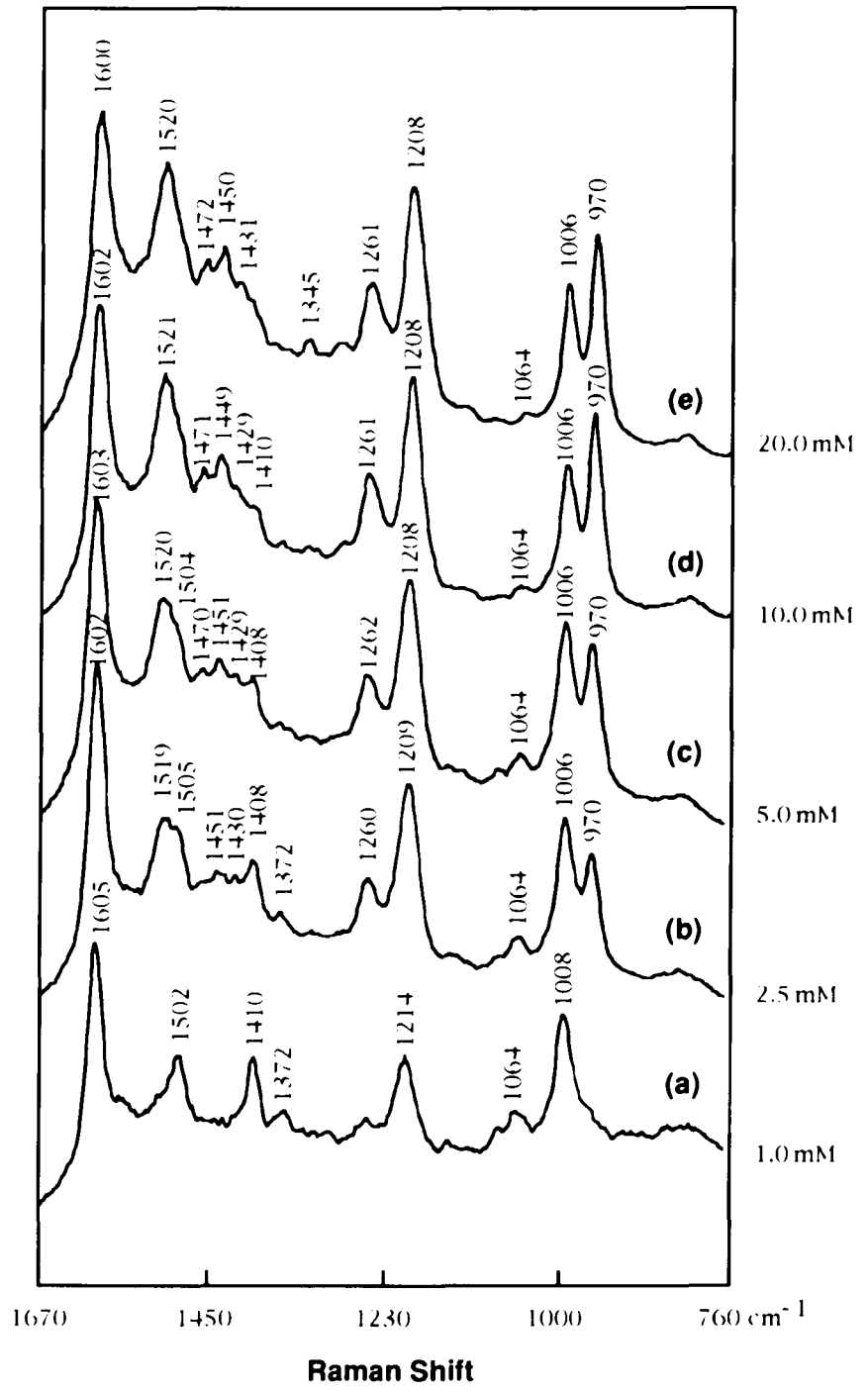

Fig. 3.1 SERS spectra of 4-CNPY in 0.1M KCl with different 4-CNPY concentrations at -0.4V. (a) 1.0 mM; (b) 2.5 mM; (c) 5.0 mM; (d) 10.0 mM; (e) 20.0 mM.

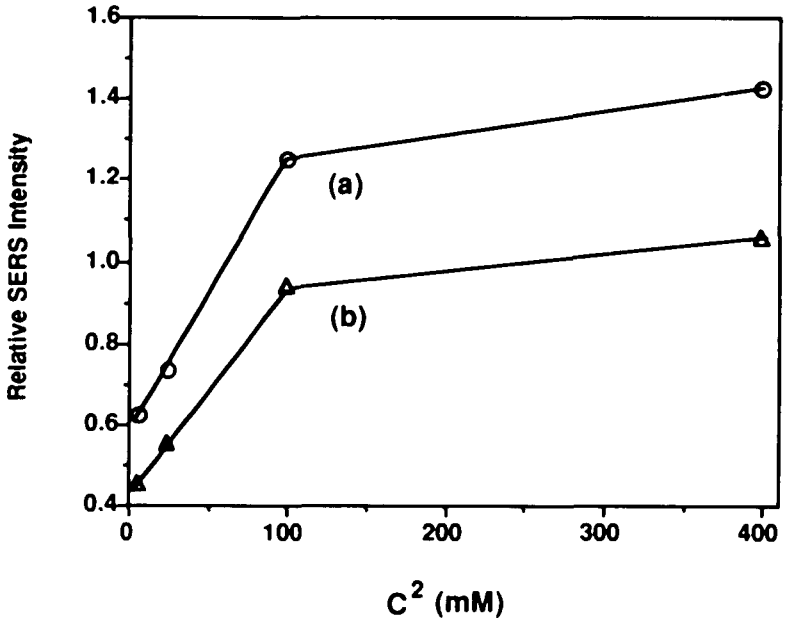

Fig. 3.2 Concentration dependence of relative SERS intensity of 4-CNPY in 0.1M KCl solutions at -0.4V. (a) bands 970/1006;(b) bands 1520/1006.

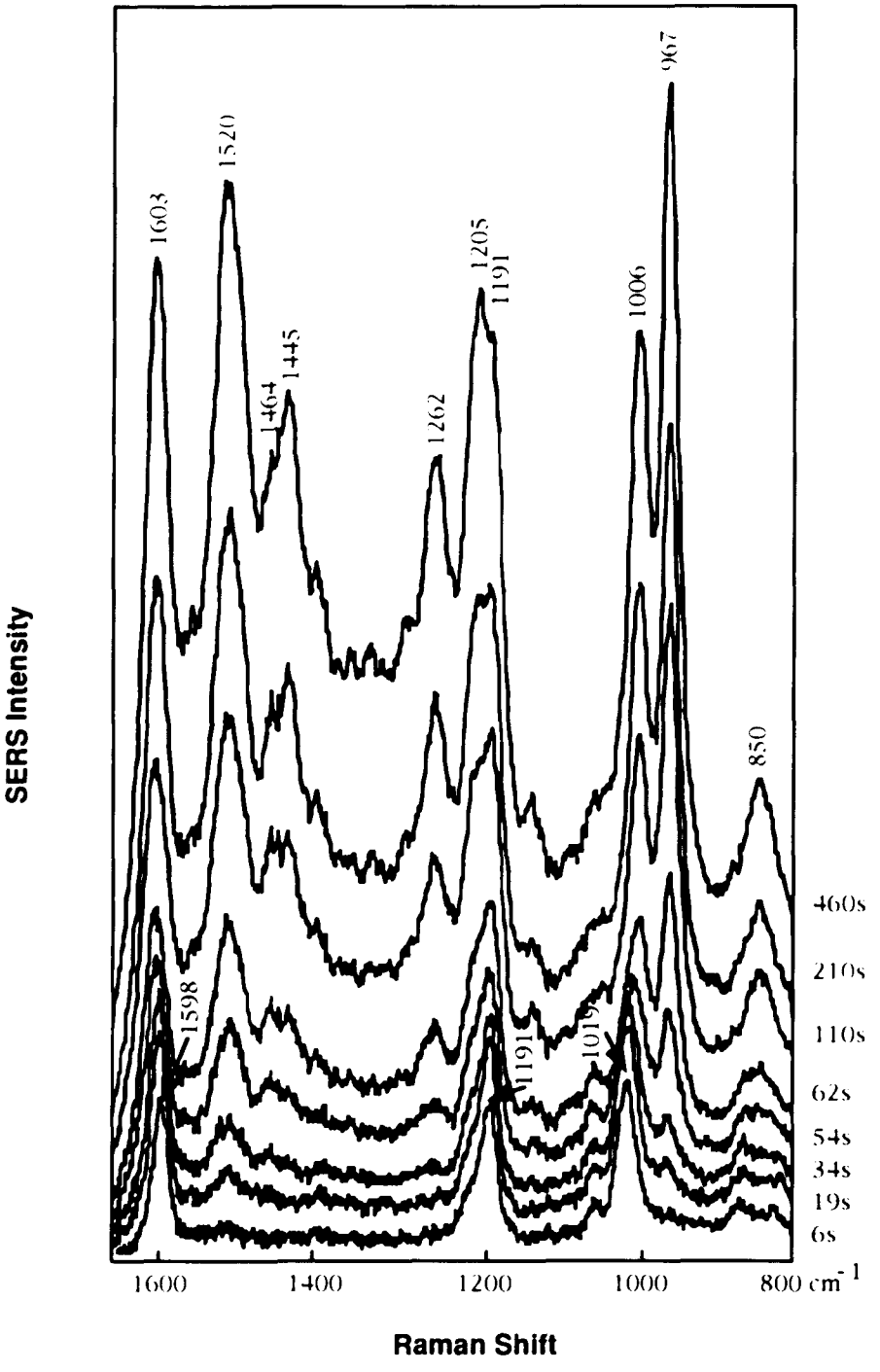

Fig. 3.3 Time dependence of 4-CNPY SERS spectra in 20.0mM 4-CNPY -0.1M KCl solution at -0.1V right after an in-situ pretreatment.

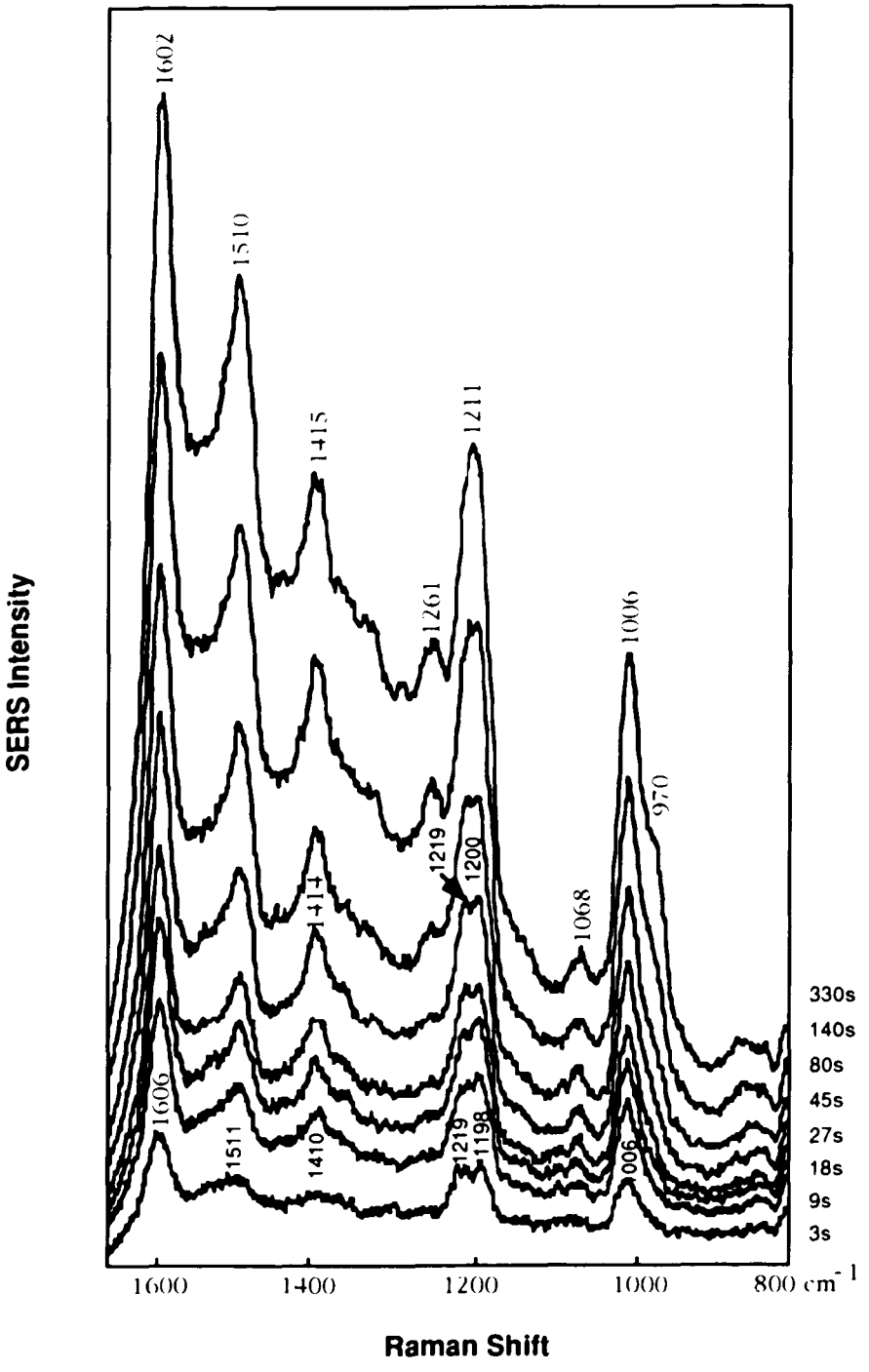

Fig. 3.4 Time dependence of 4-CNPY SERS spectra in 20.0mM 4-CNPY -0.1M KCl solution at -0.4V right after an in-situ pretreatment.

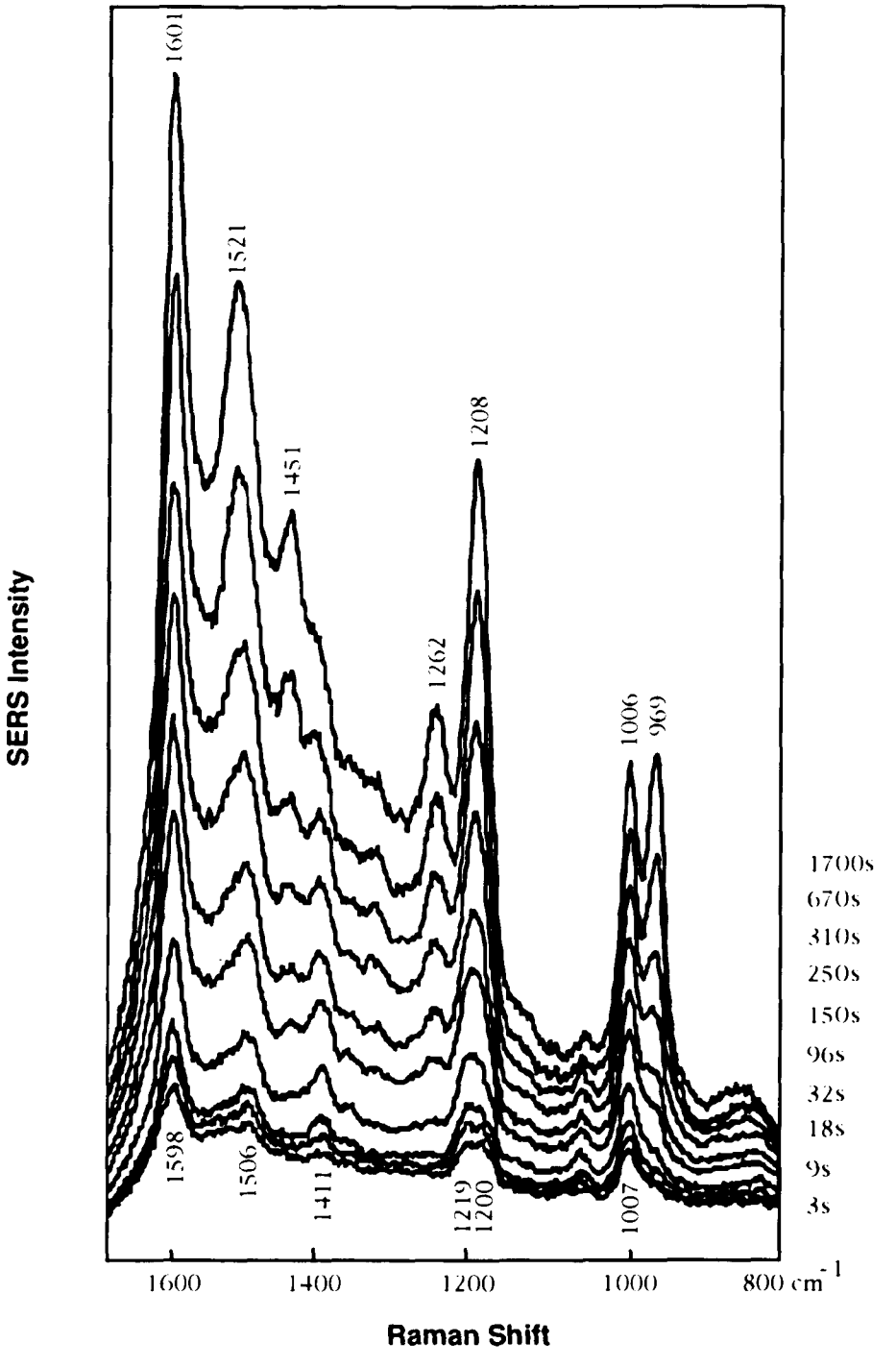

Fig. 3.5 Time dependence of 4-CNPY SERS spectra in 20.0mM 4-CNPY 0.1M KCl solution at -0.6V right after an in-situ pretreatment.

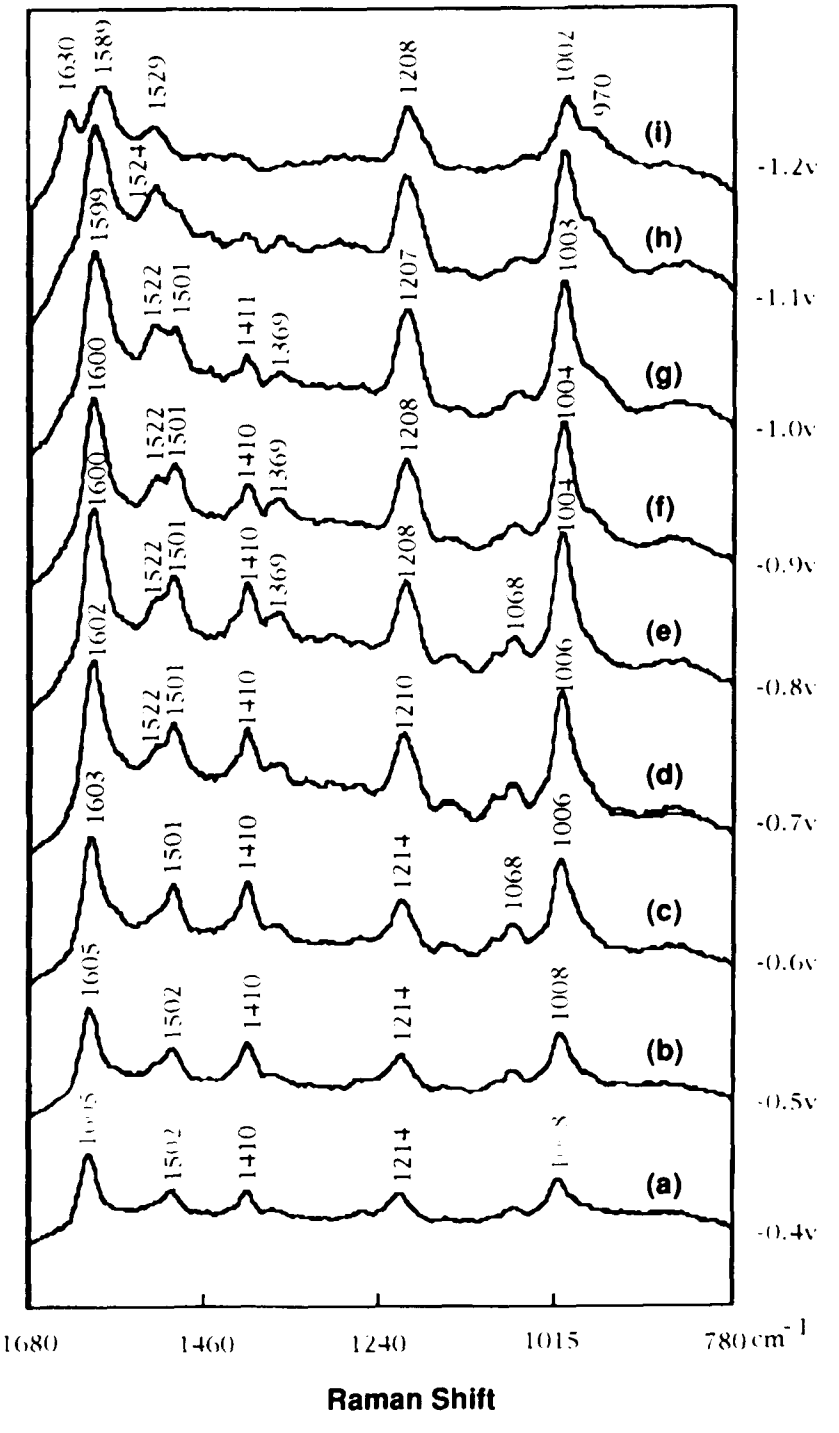

Fig. 3.6 Potential dependence of 4-CNPY SERS spectra in 1.0 mM 4-CNPY 0.1M KCl solution.

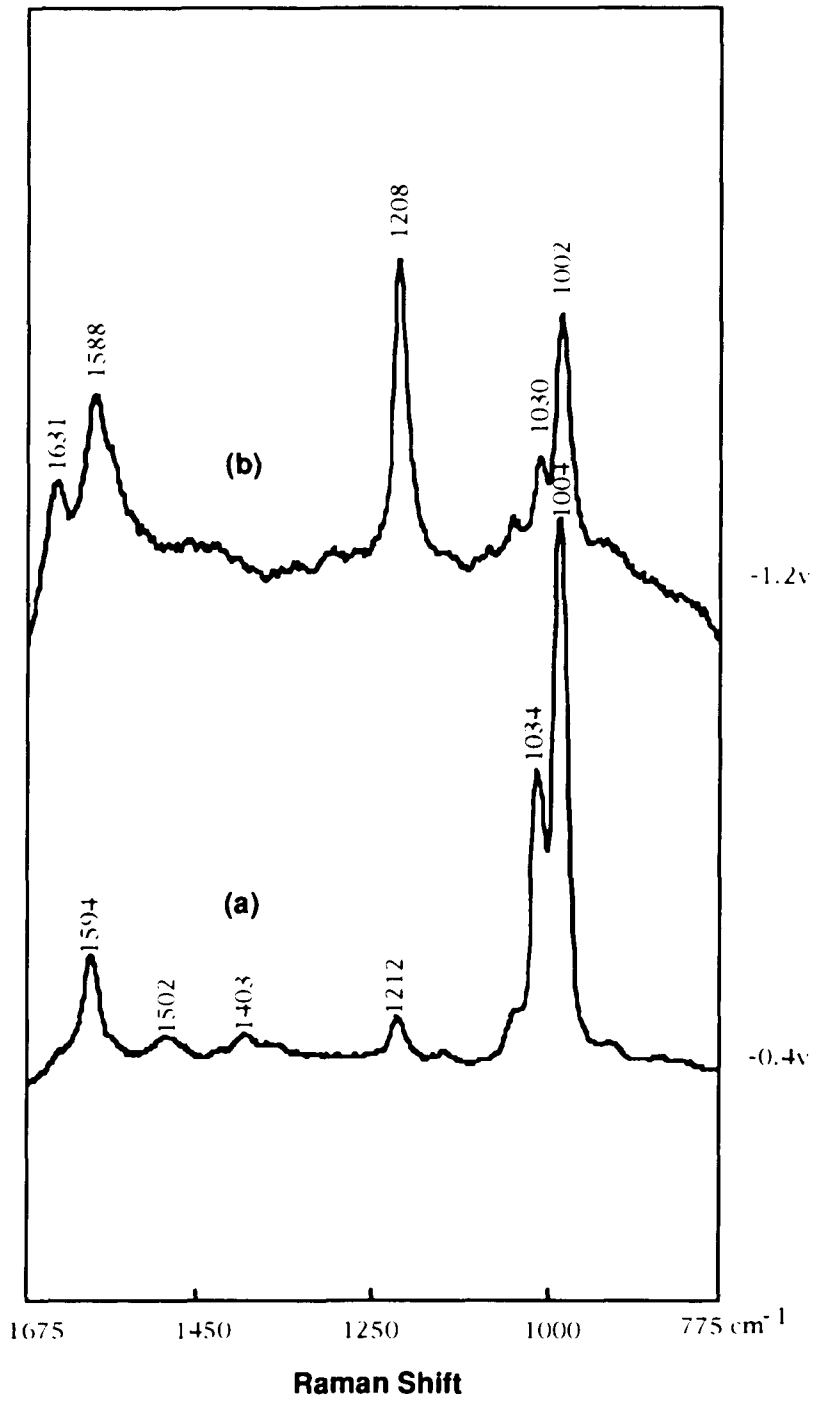

Fig. 3.7 SERS spectra of pyridine in 5.0mM pyridine-0.1M KCl at potential: (a) -0.4V; (b) -1.2V.

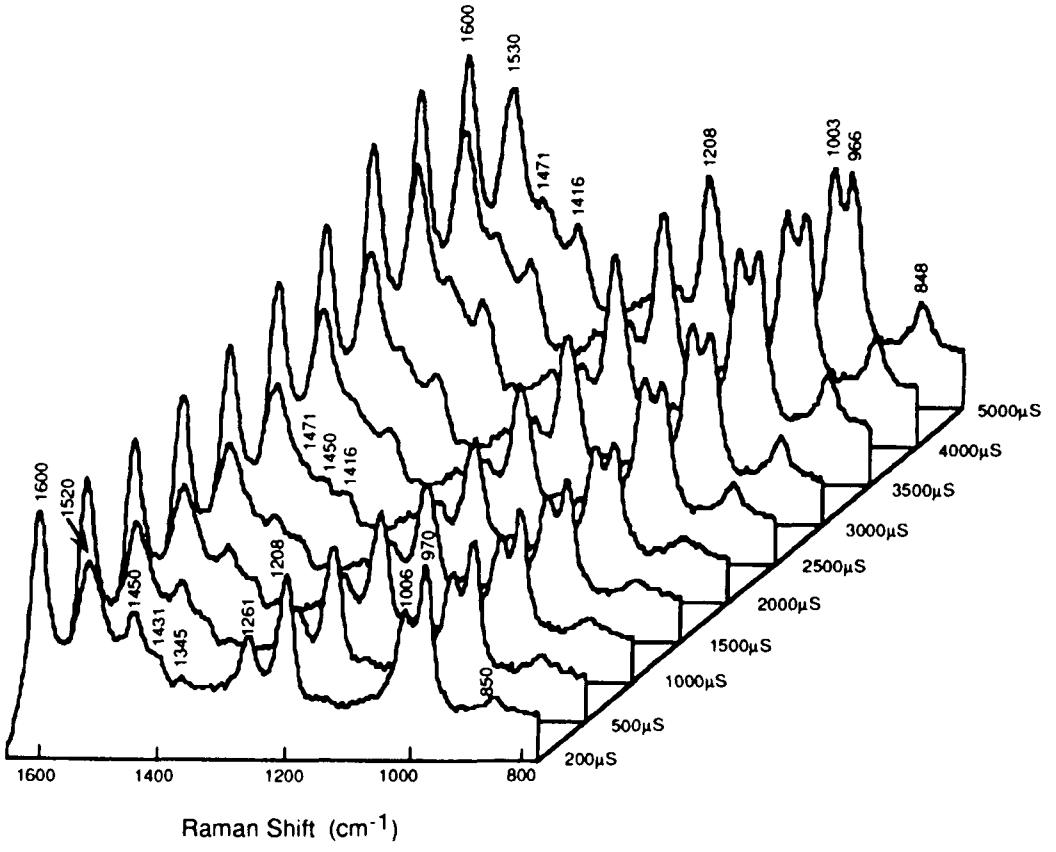

Fig. 3.8 Time-resolved SERS spectra during the reduction of 4-CNPY in 20.0mM 4-CNPY-0.1M KCl solution in a potential step experiment. Initial potential: -0.4V; final potential: -1.2V. Time scale from front to back: (1) 200 μs; (2) 500 μs; (3) 1,000 μs; (4) 1,500 μs; (5) 2,000 μs; (6) 2,500 μs; (7) 3,000 μs; (8) 3,500 μs; (9) 4,000 μs; (10) 5,000 μs.

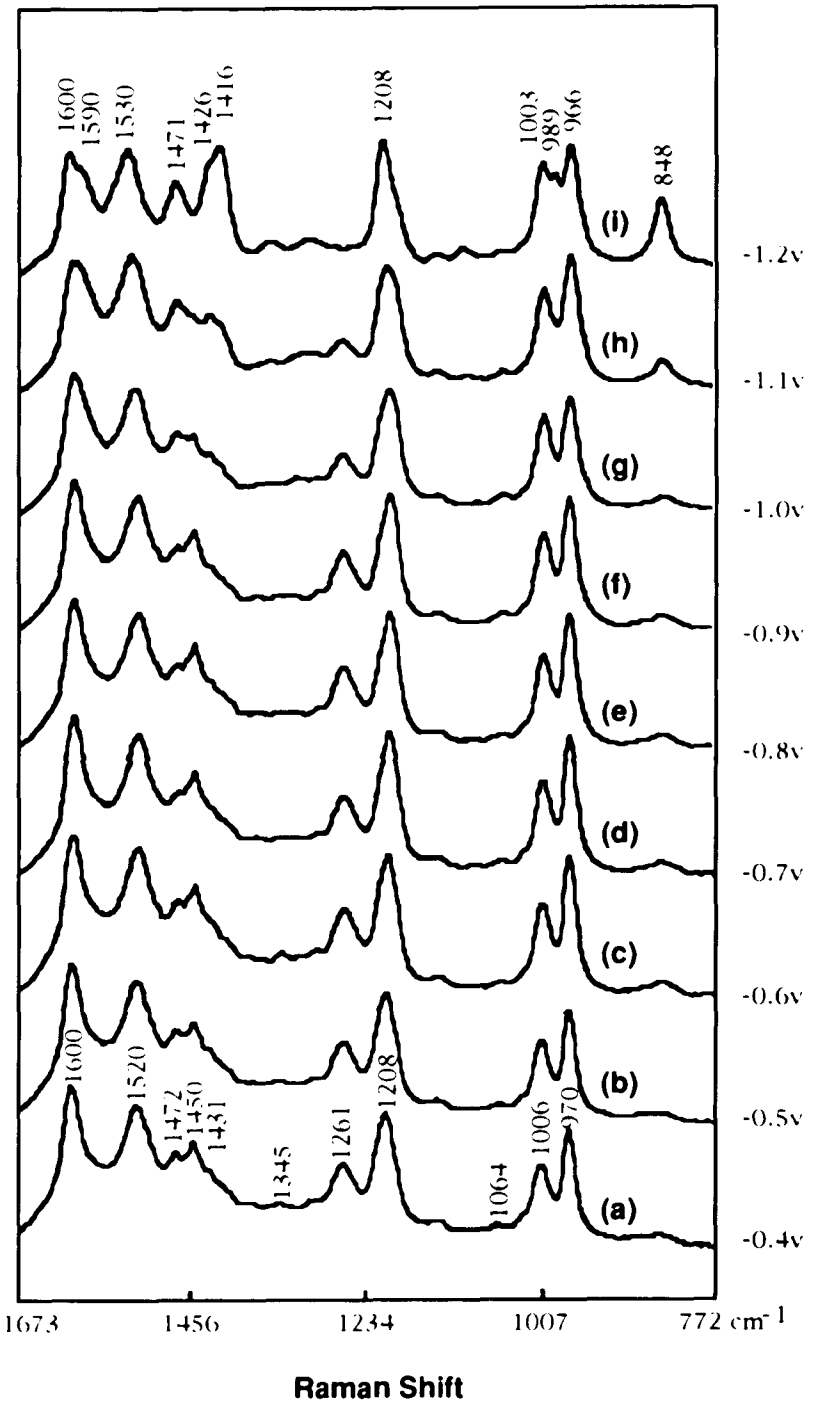

Fig. 3.9 Potential dependence of 4-CNPY SERS spectra in 20.0 mM 4-CNPY 0.1M KCl solution.

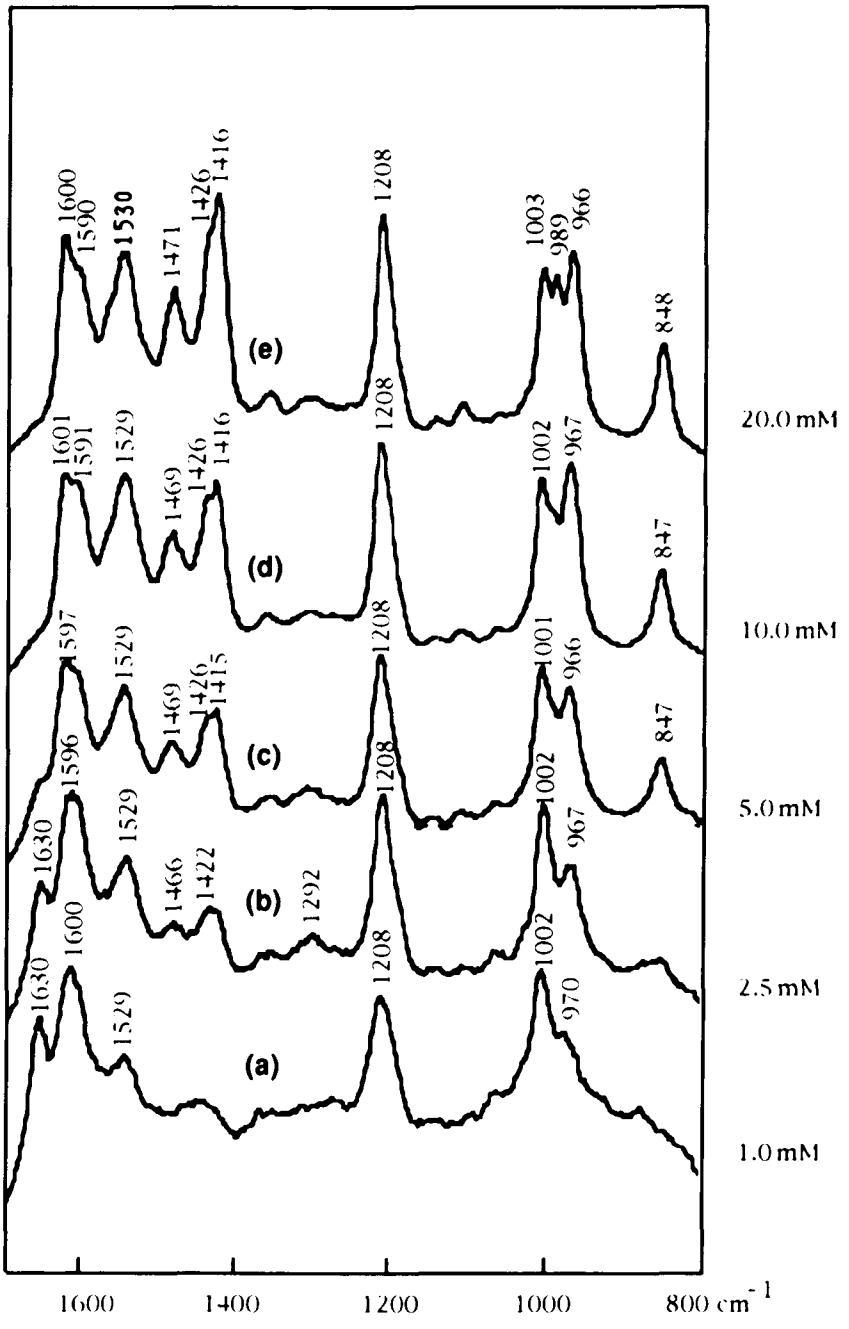

Fig. 3.10 Concentration dependence of SERS spectra of the products of 4-CNPY reduction. The electrode potential is swept slowly (0.33mV/s) form -0.4V to -1.2V.

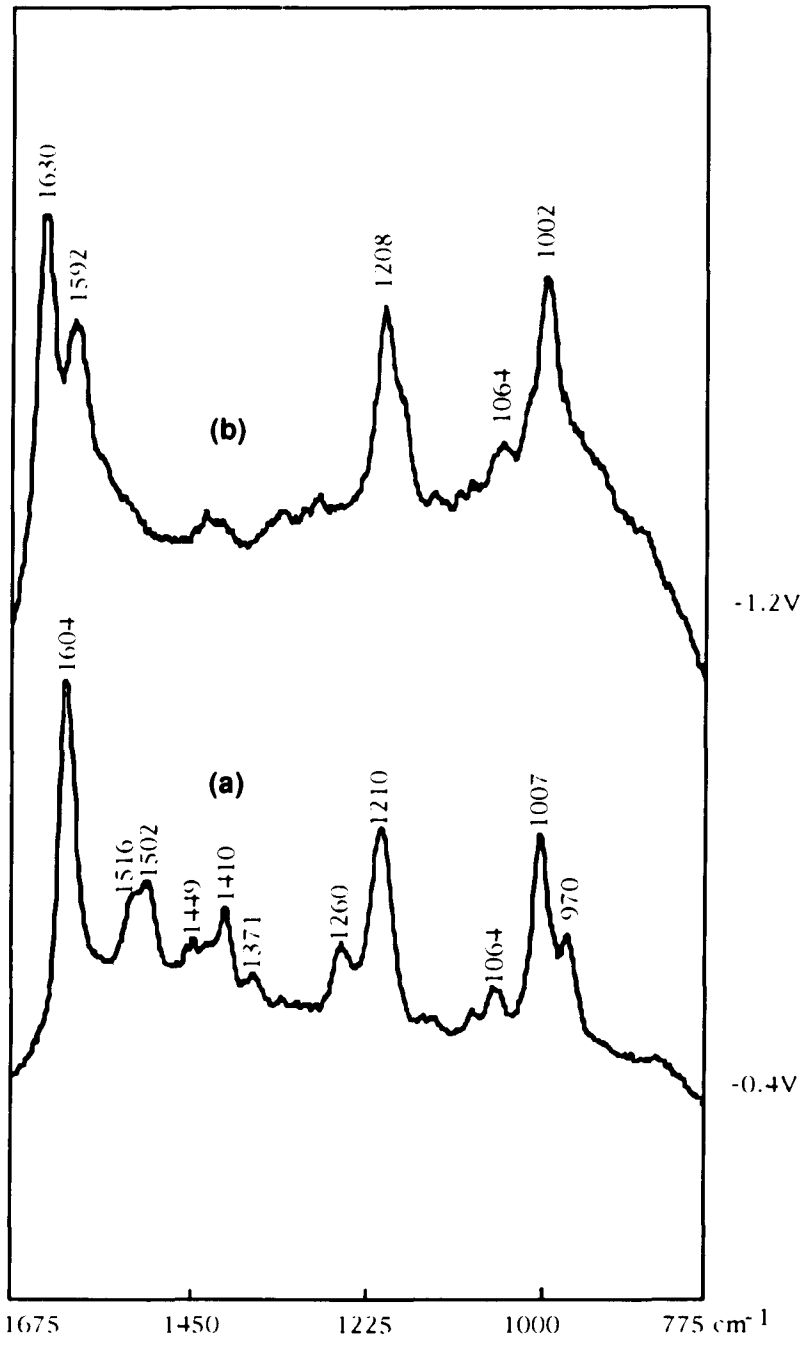

Fig. 3.11 SERS spectra of 4-CNPY at -0.4V (a) and its reduction product at -1.2V (b) in 2.5 mM 4-CNPY-0.1M KCl solution. The electrode potential is steped from -0.4V to -1.2V directly.

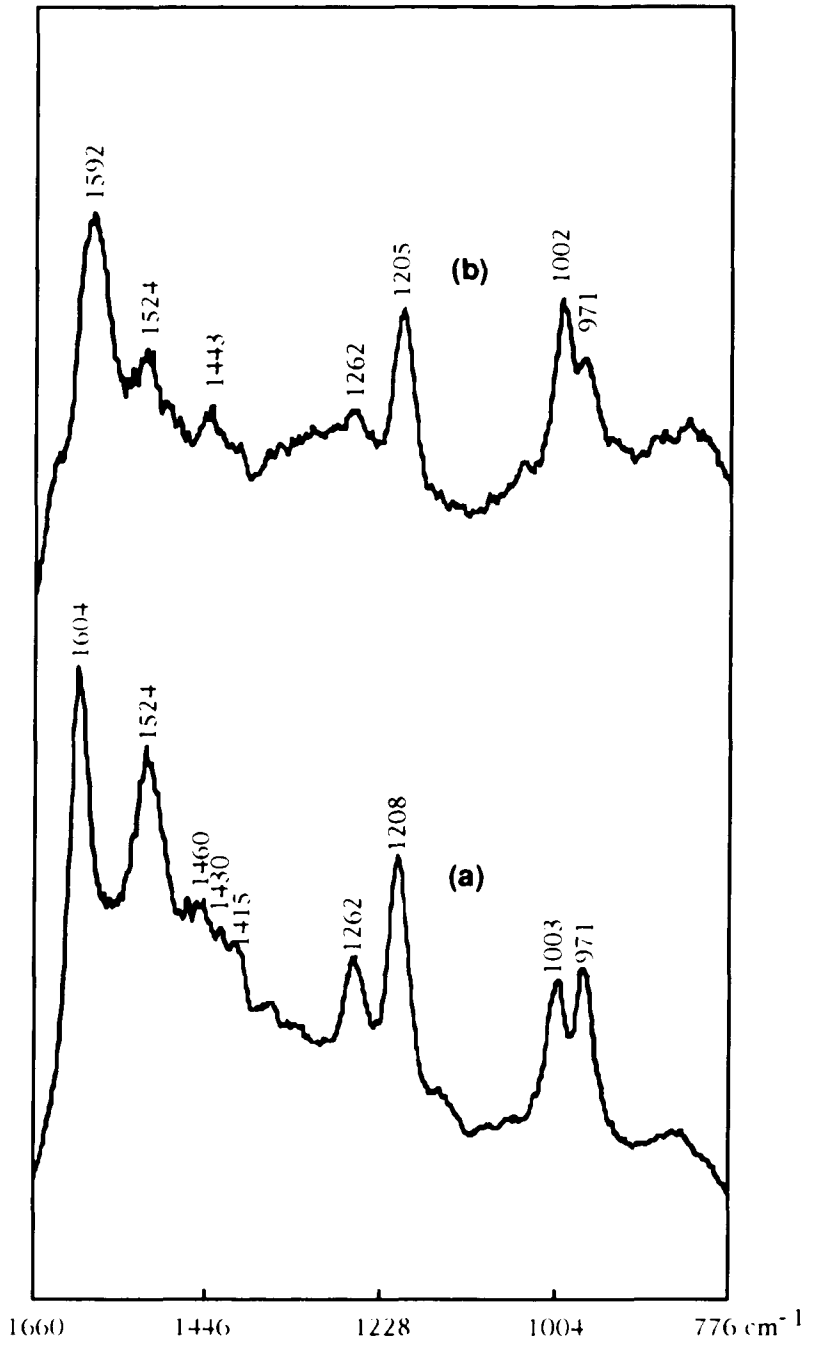

Fig. 3.12 SERS spectra in 0.1 M KCl solution on an electrochemically modified electrode: (a) 4-CNPY at -0.4V; (b) its reduction product at -1.2V.

Chapter IV

Study of Adsorption and Electrochemical Reduction of 4-Pyridinecarboxaldehyde by Time-Resolved Surface-Enhanced Raman Spectroscopy

Section 4.1 Introduction

The reductions of aldehydes and ketones always undergo different pathways in acidic and basic media.[1,2] Both the products and the intermediates from the reduction processes vary with reaction conditions. The two main factors that affect the products are the nature of the electrode material[3-7] and the pH of solution.[8-11] For example, the electroreduction of acetone on a lead electrode produces isopropanol[3] and pinalcol,[4] while on a mercury electrode the major product is isopropanol with some amount of propane.[5] The reduction of p-amino-acetophenone in aqueous acid on a Hg electrode produces the corresponding alcohol, but on a tin electrode the main product is pinacol.[6] The effect of pH on the reduction of aldehydes and ketones is also significant. Acidic conditions favor the formation of pinacols[8,9] while in basic conditions the major products are the corresponding alcohols.[10,11] In some situations, electrode potential and current density also have an effect on the products of the reduction.[1] As a special case, the electrochemical reduction of aromatic aldehydes deviates from the general rules above.[12-15] For example, the reduction of formylbenzene on a Hg electrode in basic aqueous solution produces pinacol isomers as the major product.

The course of the electroreduction of aromatic aldehydes and ketones has been studied intensively by polarography.[12-22] The general reaction scheme of the reduction was proposed as follows,[15,19]

$$Py\text{-}CHO + H_2O = Py\text{-}CH(OH)_2 \qquad K_1 = 1.525$$

$$Py\text{-}CHO + e^- + H_2O = Py\text{-}CHOH\cdot + OH^-$$

$$2Py\text{-}CHOH\cdot = dimer$$

$$Py\text{-}CHOH\cdot + e^- = Py\text{-}CHOH^-$$

$$Py\text{-}CHOH^- + H_2O = Py\text{-}CH_2OH + OH^-$$

The protonated forms of the species are related to these unprotonated species by the following equations,[16,23-25]

$$H^+Py\text{-}CH(OH)_2 = Py\text{-}CH(OH)_2 + H^+ \qquad K_{a1} = 1.8 \times 10^{-5}$$

$$H^+Py\text{-}CHO = Py\text{-}CHO + H^+ \qquad K_{a2} = 6.3 \times 10^{-4}$$

$$H^+Py\text{-}CHO + H_2O = H^+Py\text{-}CH(OH)_2 \qquad K_2 = 52$$

Both H^+Py-CHO and Py-CHO are electroactive. The products of the electroreduction were analyzed ex-situ by UV-Vis, IR spectroscopy or chromatography after long time electrolysis. Thus, no information about the identity of the intermediate was obtained.

Time-resolved Surface-enhanced Raman spectroscopy (SERS) is a powerful real-time in-situ method for investigating the heterogeneous electrochemical reduction processes which occur on or near the electrode surface.[26] This method can produce information on the stable products at different potentials and the unstable intermediates as well. In this chapter, the electrochemical reduction process of 4-pyridinecarboxaldehyde (ALPY) in both acidic and basic media is investigated by time-resolved SERS and a possible reaction mechanism is proposed.

Section 4.2 Experimental

The experiment setup is described in Section 1.4. The Ag electrode is pretreated before the spectrum is measured. During the pretreatment, the electrode potential is held at -0.1V and two +0.3V pulses are applied to the electrode each for two-second duration. The same spectrum is observed with either in-situ pretreatment in 10 mM 4-ALPY with 0.1M KCl, or ex-situ pretreatment in pure 0.1M KCl solution, but the in-situ pretreatment gives a stronger signal. Thus in-situ pretreatment is used throughout these experiments. In the time-resolved SERS experiments, both the waveform generator and the diode array photo-detector are controlled by a TTL trigger generator. The reduction is initialized by -0.8V potential step which is generated by the waveform generator when it receives a TTL trigger, and which lasts as long as the sum of a delay and an exposure time. Here the exposure time is the time window during which the detector is active and the delay is the time elapsed after the TTL signal is received and before the detector is turned on. The exposure time is 10 μS and five thousand measurements are co-added to improve the signal-to-noise ratio. In order to avoid the accumulation of the product(s) from each previous potential pulse, a +0.3V cleaning pulse with 5 ms duration is applied after each reduction-initiating pulse. When the experiment was moved from one time scale to another, e.g., from 100 μS to 200 μS, the electrode was pretreated again to make sure the starting conditions are the same. 4-Pyridinecarboxaldehyde (ALPY) (99%), 4-(hydroxymethyl)pyridine (HMPY) (99%) and 1,2-bis(4-pyridyl)ethane (BPE) (99%), were purchased from Aldrich Chemical Co. and used without further purification. Reagent grade KCl, HCl, KOH and deionized distilled water were used. All electrode potentials are quoted versus the Saturated Calomel Electrode, SCE, reference.

Section 4.3 Results and Discussions

(a) Effect of pH and Potential Scan Rate on the Electrochemical Measurements

Cyclic voltammetric studies of ALPY in acidic and basic aqueous solutions show different voltammograms (Fig. 4.1). In acidic media when the pH is less than 3.7, the voltammogram is totally different from that in neutral or basic solutions. At pH 2.0 it shows three reduction waves at -0.38, -0.50 and -0.62V and three oxidation waves but only one of them at -0.32V is pronounced (Fig. 4.1a). When the pH is increased from 2.0 to 3.0, the peak potentials for all the waves shift negatively by about 60 mV which indicates that all the electron transfers involve one proton. It was verified by adjusting the switching potential that the anodic wave at -0.32V is paired with the first cathodic wave at -0.38V. Apparently, wave 1 is the first one-electron reduction of the starting compound and can be assigned to reduction of the protonated ALPY, since at pH 2, the protonated ALPY is the major species. Both wave 2 and wave 3 are considered to be the further reduction of the product of wave 1. Because the peak current ratio of wave 3 to wave 2 increases with both pH and potential scan rate, wave 2 can be assigned to the reduction of protonated radical cation, $Py\text{-}CH_2OH^{\cdot +}$, and wave 3 the direct reduction of unprotonated radical, Py-CHOH·,

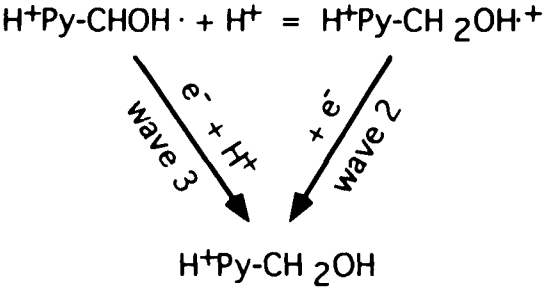

The pH value of the solution effects the distribution of the equilibrium concentrations between unprotonated and protonated species. According to Camacho et. al.,[15,16] both the protonated and the unprotonated ALPY molecules are electroactive and they will be reduced at the same potential at the same pH. Although no data about the dissociation constant of the ALPY radical have been found in literature, It is no doubt that higher pH value favors the unprotonated form of the radical. The effect of potential scan rate comes from the kinetics of the protonation of the neutral radical, Py-CHOH·. The faster the scan rate, the less protonated species is formed during the potential scan and so its reduction current (wave 2) is lowered.

The dimerization of the radical in acidic solutions should also be possible.[1,2,15,16] In both acidic and basic media, the dimerization competes with the further reductions. Which one predominants depends on their reaction rates under the given conditions. In basic or neutral media, dimerization is predominant,[1,2,15] but this is not true in acidic media since further reductions are made easier by high proton concentration. One other thing we have not mentioned is that the protonation of the pyridine nitrogen will occur in low pH solution and it may have some effect on the reduction potentials and the lifetime of the intermediates. For example, the protonation of pyridine ring will make the ring electron-poor through the inductive effect or some kind of resonance effect. This in turn will cause a positive shift in half-wave potential and may also shorten the life time of the radicals which would produce the dimer.

When the pH is greater than 4.5 (Fig. 4.1b), only one reduction wave is detected with a peak potential -0.5V. No oxidation wave is found on the returning sweep. It seems that the reduction in neutral and basic media terminates at reaction (4.3), and this step is much faster than the further

reductions so that no HMPY, Py-CH_2OH, is formed when potential goes further negative and no oxidation wave appears when potential is swept back.

Both dimerization and further reductions are going on in weakly acidic solutions. For example, at pH 3.7, the CV results show a very high wave for the first electron reduction but quite low waves for the second electron reduction. The anodic wave paired to the first cathodic wave is also lowered. These facts indicate that some of the one-electron reduced product is consumed by another reaction, namely the dimerization.

CV experiments do give much valuable information about the reduction process of ALPY; however, in order to elucidate the reaction mechanism with confidence, other evidence is needed to verify the products and the intermediates. CV results alone can only suggest what the species might be but it can not be definitive. SERS and especially time-resolved SERS is a powerful tool for real-time in-situ detection of the electrochemical processes, because it provides structural information about both the intermediates and the products of an electrode reduction.

(b) SERS Spectral Measurements and Assignments

SERS spectra of ALPY in acidic and basic media look quite different, as shown in Fig. 4.2. However, if a careful comparison is made, it can be seen that these two spectra do share some bands with small frequency shifts. Some of the bands have the same relative intensities in both media. For example, the two A_1 symmetry modes 1 and 9a, which are the ring stretching and C-H in-plane bending modes, show two strong bands at 1204 and 1008 cm^{-1} in acidic

medium, and at 1216 and 1012 cm^{-1} in neutral or basic solutions. Two B_1 modes, the ring C-C stretching mode 14 and the C-H bending mode 15, and an A_1 mode, the X-sensitive mode 13, appear as weak bands at 1335, 1150 and 1272 cm^{-1} in basic media and at 1334, 1150 and 1250 cm^{-1} in acidic media respectively. The assignment made here is aided by the assignments of pyridine, 4-substituted pyridines[27-35] and phenylcarboxaldehyde,[36] and the mode numbers used here are after Wilson's notation.[37] Some other shared bands possess just the opposite relative intensities in acidic and basic media. For instance, the 1572, 1512, 1062 and 876 cm^{-1} bands, which corresponds to the ring C-C stretching modes 8b (B_2) and 19a (A_1), the C-H bond in-plane bending mode 18b (B_2), and the C-H bond out-of-plane bending mode 10a (A_2) respectively, are weak in basic solutions but quite strong in acidic media. On the other hand, the two strong 1096 and 849 cm^{-1} bands in basic media, which belong to the C-H in-plane and out-of-plane bending modes 18a (A_1) and 10b (B_1), become very weak in acidic media. Some bands appear in basic solution exclusively, such as the 1375 and 1359 cm^{-1} bands, and some in acidic solution only, such as 1626, 1452, 1427 and 1303 cm^{-1} bands. The 1375 cm^{-1} band is assigned to the deformation of C-H bond of the aldehyde group. The 1427 and 1303 cm^{-1} bands can be assigned to ring C-H in-plane bending modes 19b (B_2) and 3 (B_2). The assignment of the 1626 and 1452 cm^{-1} bands is a little less straight forward. Since these two bands appear exclusively in acidic solutions, they should have some kind of relation with the protonated species. Indeed, the spectrum of pyridinium shows frequency shifts towards higher frequency in many Raman or IR bands, especially of those ring C-C bond stretching modes.[27,28,34] Thus the 1626 and 1452 cm^{-1} bands are assigned to the C-C stretching modes 8a and 19b of the protonated pyridine ring respectively. According to Cabani and Rusling et. al.,[17,23] ALPY is protonated

at pH lower than 3 and unprotonated at pH higher than 5. Although most ALPY molecules are protonated at pH 3, the competition between the surface adsorption and the protonation makes some ALPY molecules adsorbed with an unprotonated form. All these band assignments are listed in Table 4.1. With reference to literature citations 27, 28 and 34, three conclusions can be made from the assignments:

(1) The protonation of the pyridine nitrogen influences the high frequency bands more significantly than the low frequency bands.

(2) The protonation of the pyridine nitrogen always makes the ring carbon-carbon stretching frequency increase.

(3) The protonation of the pyridine ring nitrogen favors the adsorption with a face-on orientation.

Under all pH conditions no C=O stretch band at about 1700 cm^{-1} [27,28] is detected. One reason for the absence of the C=O stretching band is that in aqueous solution, whether acidic or basic, ALPY exists predominantly in the hydrolyzed form, Py-$CH(OH)_2$, rather than aldehyde form[16,23] Another reason for loss of this band would be a surface quenching effect by strong interaction with the surface. The different ALPY spectra in acidic and in basic media is probably related to both protonation and orientations of ALPY on the Ag surface. In basic media the pyridine ring nitrogen is unprotonated so that it can adsorb on the Ag surface firmly through a Ag-N bond. The orientation of ALPY molecules in this case is vertical or end-on. Therefore, those vibrations with A_1 symmetry give strong signals. In acidic media, the protonation of the pyridine ring nitrogen weakens the adsorption with an end-on orientation and this makes other orientations, such as face-on, more likely. Therefore, the bands with A_2,

B_1 and B_2 symmetry including those asymmetric and out-of-plane (γ) vibrational bands show stronger intensities in acidic media (See Table 4.1).

One other thing which can be seen from Table 4.1 is that, even in our most acidic medium, pH 3, the SERS bands corresponding to the base form ALPY still show up with some intensity. This effect is probably related to both the basicity of the aldehyde group and the affinity of the nitrogen lone-pair electron for the roughened Ag surface. ALPY has two base groups, the ring nitrogen and the aldehyde oxygen. Both groups can associate with proton and produce protonated species Py-CHOH$^+$ and H$^+$PY-CHO through the following equilibria,

$$\text{Py-CHOH}^+ = \text{Py-CHO} + \text{H}^+$$

and

$$\text{H}^+\text{Py-CHO} = \text{Py-CHO} + \text{H}^+$$

In neutral or basic medium the equilibrium favors ALPY, therefore only the spectrum of this neutral species is observed. At lower pH, the equilibrium favors the protonated species, but there will still be some amount of neutral molecules left if the proton concentration is not too high. Even in the single protonated species, where the proton can go to either the pyridine nitrogen or the aldehyde oxygen, the later species, Py-CHOH$^+$, still has an unprotonated pyridine ring. Since the aldehyde oxygen is two atoms farther away from the ring, the influence of its protonation on the ring C-C stretching frequencies is much weaker than that due to the protonation of the ring nitrogen. Thus Py-CHOH$^+$ will give rise to similar SERS frequency for the ring system as the neutral ALPY molecules.

Another competition is the adsorption of different species on the Ag

surface. The neutral ALPY and Py-CHOH$^+$ can adsorb more strongly on the Ag surface through the nitrogen lone-pair electron than the species with a protonated ring, H$^+$Py-CHO, which adsorbs through the ring π-system. This situation also favors the existence of the neutral ALPY and Py-CHOH$^+$.

(c) Time-resolved SERS Spectra

Fig. 4.3 shows the time-resolved SERS spectra obtained during ALPY reduction. The reduction is initiated by negative potential steps to -0.8V in neutral 10mM ALPY-0.1M KCl solution in the time window from 100 μs to 30 ms. Up to 1.0 ms, no new bands are found but several original bands decay, located at 1571, 1270, 1150, 1092 and 1059 cm^{-1}. A transient spectrum appears at 3.0 ms and disappears at 10.0 ms. Several new bands are found in the transient spectrum, which are at 1384, 1356, 1330 and 1276 cm^{-1}. This transient spectrum probably belongs to an intermediate 1,2-bishydroxy-1,2-bis(4-pyridyl)ethane (BHBPE). The product spectrum appears after 10 ms and its intensity is much stronger than both that of the reactant and possible intermediates. This product spectrum has two very strong bands at 1592 and 1208 cm^{-1}, six strong bands at 1554, 1532, 1494, 1476, 1322 and 1004 cm^{-1}, four medium strong bands at 1424, 1248, 878 and 842 cm^{-1} and three weak bands at 1636, 1090 and 1056 cm^{-1}.

According to the CV results (Fig. 4.1b), the reduction of ALPY in neutral or basic medium is irreversible, and a following chemical coupling reaction (4.3) is predicted to explain the irreversibility. In order to assign the detected spectra to those species which appear in the reduction process and to get a clear picture about the reduction mechanism, more information is needed to identify

the products and intermediates. For example, does the spectrum after 10 ms correspond to the final stable product? What is the product and is there a potential at which the transient spectrum is stable? What species may the transient spectrum be related to?

The potential dependence of SERS spectrum of ALPY in basic media is shown in Fig. 4.4. The ALPY spectra are stable until -0.3V and many new bands appear when the potential is more negative. The product spectrum is fully developed at -0.8V and remains the same until -1.5V. At more negative potentials, the spectrum is destroyed by the evolution of hydrogen. This product spectrum is exactly the same as that obtained after 10 ms in time-resolved SERS measurement (see Fig. 4.3) and no band corresponding to the transient spectrum is found in this steady state measurement. This result indicates that the product obtained after 10 ms is the final stable product and the intermediates are not stable under the experimental conditions.

It was found that the pH value of the solution has a significant effect on the appearance of the spectra of the product produced in neutral or basic medium. In order to make certain that the reduction products in acidic and in basic media are not the same compound, the pH value of the electrolyte solution was adjusted by adding 0.1M HCl and 0.1M KOH to the neutral solution when the potential was held at -0.8V at which the final product is formed. When the pH is adjusted to a more basic value, pH 11, there is no change in the product spectrum. However, if pH is adjusted to a more acidic value, for example, about pH 3, a large change in the spectrum was found as shown in Fig. 4.5b. Curve b in Fig. 4.5 contains only four strong bands at 1632, 1602, 1201 and 1013 cm^{-1}. Furthermore, when the pH is readjusted to a basic value again, the original spectrum is recovered. Experiments using a modified

electrode which is coated with product give the same result, which excludes the possibility of newly formed product after pH adjustment. This result means that two species are converted reversibly depending on the proton concentration, such as

$$A = B + H^+$$

where A represents the acid form of the product and B represents the base form of the product. The change in spectra could be caused by protonation, since the protonation may not only affect the electron distribution but also the surface orientations.

In acidic media (Fig. 4.6), no significant change in spectrum is found when the electrode potential is swept from the equilibrium value, -0.05V, to -0.9V, although three reduction waves are found in the CV. The possible reason for this is that in acidic medium the adsorptivities of the electroreduction products on the Ag electrode surface are not as strong as that of the reactant, ALPY. Therefore, due to the competitive adsorption with the reactant, the products are repelled from the electrode surface and diffuse into the adjacent solution. When the potential is more negative than -1.0V, the 1602 cm^{-1} band increases and finally becomes very strong. Along with this change small frequency shifts of some bands are observed. According to CV results, the reduction product could be 4-(hydroxymethyl)pyridine (HMPY), Py-CH_2OH or picoline, Py-CH_3 if the former can be further reduced under the experimental conditions. However, as we will see later, the SERS spectrum of both HMPY and picoline are different from the spectra we obtain here.

The change of ALPY in acidic solution at potentials more negative than -1.0V can be explained by one of the following possibilities: (1) the adsorption

of the unprotonated ALPY molecules with an orientation change; and (2) the adsorption of the reduction product at very negative potentials. As we have discussed before, in acidic conditions, most of ALPY molecules are protonated and adsorb on the Ag electrode surface with face-on or slanted orientation. This species gives rise to many strong SERS bands with both A_1 and B_2 symmetry (see Fig. 4.1 and Table 4.1). On the other hand, the SERS spectrum of ALPY shows only three intense bands with A_1 symmetry in basic solutions. This indicates that ALPY molecules adsorb vertically with the pyridine ring nitrogen attaching on the surface in the basic medium. The two strong SERS bands at 1012 and 1216 cm^{-1} are covered by strong corresponding bands in acidic media, but the strong 1601 cm^{-1} bands is still present. Thus the 1601 cm^{-1} band can be used to identify the existence of the vertically adsorbed unprotonated ALPY molecules. In acidic conditions, the protonated ALPY is the major species adsorbed on the electrode surface at potentials more positive than -1.0V. The unprotonated species appears on the electrode surface due to a pH change near the surface caused by H^+ reduction at potentials more negative than -1.0V.

The second possibility is related to the product in neutral or basic media. As we have seen from the pH dependence of its SERS spectrum, the spectrum of the acid form of the product has only four major bands in 800-1650 cm^{-1} region. Three of them overlap with the strong SERS bands of the protonated reactant. Only the strong 1602 cm^{-1} band in the spectrum is distinguished from the reactant spectrum. Thus, if these two spectra are combined, the resulting spectrum will be the same as that obtained in the acidic solution at potentials more negative than -1.0V. From this point of view, the reduction of ALPY in acidic media may, at least in some degree, produce the same product as in

neutral or basic media.

Three conclusions could be drawn from the facts discussed above: (1) the major reduction products produced in acidic and in basic media are different; (2) at very negative potential, the product produced in neutral or basic medium may also be produced in acidic medium as a minor product; (3) the post pH adjustment does not change the product which has been formed before, except for the transformation between the acid and base forms of the product. The change in spectrum due to pH adjustment is reversible and probably caused by protonation and orientation effects.

(d) Product SERS Spectra

According to the literature,[1,2,15,19] the two most likely products of ALPY reduction are HMPY and the dimer 1,2-bishydroxy-1,2-bis(4-pyridyl)ethane (BHBPE), Py-CH(OH)CH(OH)-Py. The former is a direct two-electron reduction product and the latter is a product of a chemical coupling reaction after one electron transfer. However, picoline, Py-CH_3, and 1,2-bis(4-pyridyl)ethane (BPE), Py-CH_2-CH_2-Py, the further reduction products, are also possible.

$$Py\text{-}CH_2OH + 2e^- + 2H^+ = Py\text{-}CH_3 + H_2O$$

and

$$Py\text{-}CH(OH)CH(OH)\text{-}Py + 4e^- + 4H^+ = Py\text{-}CH_2\text{-}CH_2\text{-}Py + 2H_2O$$

In order to identify the product, the SERS spectra of authentic HMPY were measured first under similar experimental conditions and shown in Fig. 4.7. The spectrum of HMPY at pH 3 (Fig. 4.7a) shows three very strong bands at

1633, 1204 and 1008 cm^{-1}, two strong bands at 1063 and 884 cm^{-1} and a shoulder band at 867 cm^{-1}. Apparently, this spectrum is different from both the spectrum of the acid form product of ALPY reduction as shown in Fig. 4.5b and the spectrum of the product produced directly in acidic medium as shown in Fig. 4.6. The spectrum of HMPY in neutral solution at -0.8V (Fig. 4.7b) looks similar to the product spectrum in the same conditions. However, several differences must be noticed. First, the relative intensities are quite different. The 1636 cm^{-1} band in the HMPY spectrum is very strong while the bands in the frequency region 1400-1550 cm^{-1} are quite weak. This is just the opposite to the product spectrum. Second, besides small frequency differences of some of the corresponding bands, the HMPY spectrum shows a medium strong band at 1332 and a shoulder band at 964 cm^{-1}, but there are no corresponding bands in the product spectrum. Thus, the possibility of HMPY as the product, at least as the major product, is excluded.

The possibility of picoline as product is evaluated by comparing with authentic 4-picoline SERS spectrum under similar experimental conditions. Fig. 4.8 shows the SERS spectra of 4-picoline in 0.1M KCl at pH 7. The spectrum of 4-picoline is almost identical to its normal Raman spectrum found from literature[29,34]. Unlike ALPY or HMPY, the spectrum of 4-picoline is not affected by pH very much. The spectrum at pH 3 is similar to that at pH 7. Apparently, 4-picoline is not the product.

The third possible product examined is 1,2-bis(4-pyridyl)ethane (BPE), Py-CH_2-CH_2-Py, which comes from the chemical coupling reaction as mentioned above. SERS spectra of BPE, which is commercially available, were measured at pH 7 and are shown in Fig. 4.9. Since no oxidation or reduction occurs in the potential range employed, the changes in the spectra, which occur

at -0.6V, are due to an orientational or conformational change caused by potential. The BPE spectra at -0.8V at pH 7 are almost identical to the product spectra for reduction of ALPY, except for the absence of the 1636 cm^{-1} band. However, if one compares the HMPY spectrum (Fig. 4.7b) with that of BPE (Fig. 4.9) carefully, it can be seen that 1636 cm^{-1} band exclusively belongs to HMPY, since except for the 1636 cm^{-1} band, all the other SERS bands in HMPY spectra overlap with the corresponding bands in the BPE spectra. Thus the 1636 cm^{-1} band could be used to identify the existence of HMPY during the reaction. Therefore, the product spectrum of ALPY reduction is the sum of the spectra of HMPY and BPE, i.e., both of them are the products of ALPY reduction, but the latter is the major one.

Possible assignments of the 1,2-bis(4-pyridyl)ethane spectra are given in Table 4.2. The base form spectrum of BPE, as shown in Fig. 4.9, can be assigned with reference to the assignment of the 4-substituted pyridine spectra.[27,35] The 1592 and 1554 cm^{-1} bands are assigned to the carbon-carbon stretching modes 8a (A_1) and 8b (B_1), and the 1494 and 1424 cm^{-1} bands belong to the carbon-carbon and carbon-nitrogen stretching modes 19a (A_1) and 19b (B_1), respectively. The other two bands related to the ring carbon stretching modes 1 (A_1) and 14 (B_1) are located at 1004 and 1322 cm^{-1}. The four pyridine ring C-H bending modes 3 (B_1), 9a (A_1), 18b (B_1) and 18a (A_1) appear at 1248, 1208, 1090 and 1056 cm^{-1} respectively. Two C-H out-of-plane vibrations show up at 878 and 842 cm^{-1} and they are modes 10a (A_2) and 10b (B_2).

There are still two bands at 1532 and 1476 cm^{-1} left unassigned. They can not be assigned either to the ethane CH_2 deformation or to the CH_2 wag or rock vibrations. The former has a frequency about 1440 cm^{-1} if it is next to a

double or triple bond or an aromatic group and the later two have even lower frequencies in the ranges of 1347-1182 cm^{-1} and 730-720 cm^{-1} respectively.[27-29] The C-C single band stretching frequency is found at about 970 cm^{-1},[28,29] thus, it can not be the choice for the assignment. A reasonable consideration is to assign the 1532 and 1476 cm^{-1} bands to the ring carbon stretching modes 8b and 19a, respectively. The most stable conformation of BPE is the trans conformation, where the two pyridine rings are away from each other and their normals lie on the same plane which equally divides the angle between the two hydrogens on each ethane carbon. Thus the two pyridine rings are parallel. The two 19a modes of the two pyridine rings, which appears at about 1486 cm^{-1} for a 4-substituted pyridine, couple with both the Py-C-C bending and the ethane C-C stretching modes and split into two slightly different frequencies, 1494 and 1476 cm^{-1}. The two 8b modes also split into two slightly different frequencies, 1554 and 1532 cm^{-1}, due to the coupling with the ethane CH_2 rocking mode.

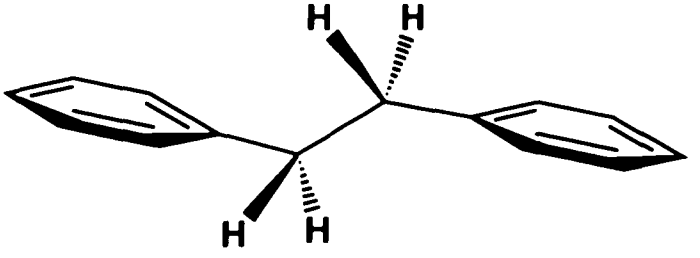

The possible assignments of the spectrum of the acid form product of ALPY reduction is also listed in Table 4.2.

(e) Mechanistic Elucidation from Time-resolved SERS

Now, the time-resolved SERS experimental result shown in Fig. 4.3 can be discussed with more insight. The change in spectrum in the first one millisecond in Fig. 4.3 is most likely due to the one electron addition to the neutral ALPY molecule,

$$Py\text{-}CHO + e^- = Py\text{-}CHO^- \qquad (4.1)$$

The transient spectrum detected during the time window 1.0 ms to 10.0 ms could be related to a radical, Py-CHOH·, which is produced through hydration,

$$Py\text{-}CHO^- + H_2O = Py\text{-}CHOH\cdot + OH^- \qquad (4.2)$$

or the intermediate product from further reactions.

The possibility of HMPY as an intermediate is rejected by the fact that HMPY is still stable at the potential where ALPY has already been reduced to the final product BPE (see Chapter V). If HMPY were the intermediate, the potential for BPE formation in ALPY would be the same as that in HMPY supposing HMPY is readily formed from ALPY. If the formation of HMPY from ALPY is more difficult than BPE from HMPY, then the potential of BPE formation from ALPY would be more negative than from HMPY.

The second possible reaction path is through BHBPE, Py-CH(OH)-CH(OH)-Py, which is formed from the dimerization of the aldehyde radical, Py-CH(OH)·,

$$2Py\text{-}CH(OH)\cdot = Py\text{-}CH(OH)\text{-}CH(OH)\text{-}Py \qquad (4.3)$$

which can be further reduced to BPE by a four electron reduction,

$$Py\text{-}CH(OH)\text{-}CH(OH)\text{-}Py + 4e^- + 2H_2O = Py\text{-}CH_2\text{-}CH_2\text{-}Py + 4OH^- \qquad (4.4)$$

This path seems reasonable, but more efforts have to be made to confirm it. For example, the reduction potential of BHBPE should be measured and its SERS spectrum should be checked too, because we can not exclude the possibility that both BHBPE and BPE have similar SERS spectrum. Unfortunately, since BHBPE is not commercially available, we have to await its synthesis for further conclusions. The transient spectrum is considered to represent the formation of BHBPE through a chemical coupling reaction (4.3) from the radicals formed in reactions (4.1) and (4.2).

Another alternative for reaction (4.3) is

$$Py\text{-}CHOH\cdot + Py\text{-}CHO + e^- + H_2O = Py\text{-}CH(OH)CH(OH)\text{-}Py + OH^- \qquad (4.3')$$

Although reaction (4.3') produces the same product as reaction (4.3) does, it will depend on the ALPY concentration in solution as in case of the reduction of 4-cyanopyridine (see Chapter III). According to eq. (4.3'), if there were no ALPY in solution, the ALPY radical would be further reduced to alcohol rather than dimerize. However, the experiment results by using a modified electrode, which is first pretreated in ALPY solution then put into pure 0.1M KCl solution, show the same product spectrum as the in-situ experiments. Thus, the reaction must go through eq. (4.3) rather than eq. (4.3').

As we have mentioned above, both HMPY and BPE are the reduction products of ALPY, but the latter one is the major product. Experiments show that the irradiation of 488 nm laser light also affects the ratio of these two products. Since the 1636 cm^{-1} band exclusively belongs to HMPY, the ratio of intensity of the 1554 or 1532 cm^{-1} band over that of the 1636 cm^{-1} band is roughly proportional to the ratio of BPE over HMPY. Experimental results indicate that the longer the irradiation, the higher the ratio. The photo-effect could also be

related to the one-electron reduction product of ALPY, Py-CHOH·, according to the following reactions,

$$Py\text{-}CHOH\cdot + Py\text{-}CH_2OH + h\nu + e^- = Py\text{-}CH(OH)CH_2\text{-}Py + OH^- \qquad (4.5)$$

$$Py\text{-}CH(OH)CH_2\text{-}Py + H_2O + 2e^- = Py\text{-}CH_2CH_2\text{-}Py + 2OH^- \qquad (4.6)$$

since no such photo-effect is found in HMPY solution under similar conditions.

Section 4.4 Conclusion

Both the neutral 4-pyridinecarboxaldehyde (ALPY) and its protonated species which is protonated on the aldehyde group (Py-CHOH$^+$) adsorb on the roughened Ag electrode surface with an end-on orientation through the pyridine nitrogen, but the species with a protonated ring (H$^+$Py-CHO) prefers adsorption with a face-on orientation through its π-ring. The electrochemical reduction of ALPY produces, at least to some extent, a common product, 1,2-bis(4-pyridyl)ethane (BPE), in both acidic and basic media. In neutral or basic solutions, the major reaction process involves an ECCE mechanism and produces 1,2-bis(4-pyridyl)ethane,

E $\quad Py\text{-}CHO + e^- = Py\text{-}CHO^-$

C $\quad Py\text{-}CHO^- + H_2O = Py\text{-}CHOH\cdot + OH^-$

C $\quad 2Py\text{-}CHOH\cdot = Py\text{-}CH(OH)CH(OH)\text{-}Py$

E $\quad Py\text{-}CH(OH)\text{-}CH(OH)\text{-}Py + 4e^- + 2H_2O = Py\text{-}CH_2\text{-}CH_2\text{-}Py + 4OH^-$

which is detected by time-resolved SERS and the product is identified by comparing the product spectrum to those of the pure compounds which are the possible products.

Table 4.1 Assignment of ALPY SERS Spectra

Assignment	Mode No.	Symmetry	pH 3	pH 7
ν(CC)	8a*	A1	1626 s	
ν(CC)	8a	A1	1602 w	1601 vs
ν(CC)	8b,8b*	B2	1575 vs	1572 w
ν(CC,CN)	19a,19a*	A1	1510 s	1512 w
ν(CC,CN)	19b*	B2	1452 vs	
ν(CC,CN)	19b	B2	1427 s	
δ(CH)				1375 m
ν(CC,CN)	14	B2	1333 m	1335 w
β(CH)	3	B2	1303 s	
X-sens.,ν(CC)	13	A1	1250 w	1272 w
β(CH)	9a	A1	1204 vs	1216 vs
X-sens.,β(CH)	15	B2	1150 m	1150 m
β(CH)	18a	A1	1096 w	1096 s
β(CH)	18b	B2	1058 s	1062 w
ν(CC,CN)	1	A1	1008 s	1012 vs
γ(CH)	10a or 5	A2 or B1	880 s	880 sh
γ(CH)	10b	B1	850 sh	849 s

* assigned to the protonated pyridine ring.

Table 4.2 Assignment of the SERS Spectra of ALPY Reduction Product

Assignment	Mode No.	Symmetry	pH 3*	pH 7
ν(CC)	8a	A1	1632 s	1592 vs
ν(CC)	8b	B2	1601 s	1554 s
ν(CC)	8b	A1	1537 w	1532 s
ν(CC,CN)	19a	A1	1492 vw	1494 s
ν(CC,CN)	19a	A1		1476 s
ν(CC,CN)	19b	B2	1424 w	1424 m
ν(CC,CN)	14	B2	1335 m	1322 s
β(CH) or ν(CC)	3 or 13	A1 or B2	1219 sh	1248 m
β(CH)	9a	A1	1201 s	1208 vs
β(CH)	18a	A1	1096 w	1090 w
β(CH)	18b	B2	1064 w	1056 w
ν(CC,CN)	1	A1	1013 s	1004 vs

* The product is produced in a neutral solution and then the pH value is adjusted to 3

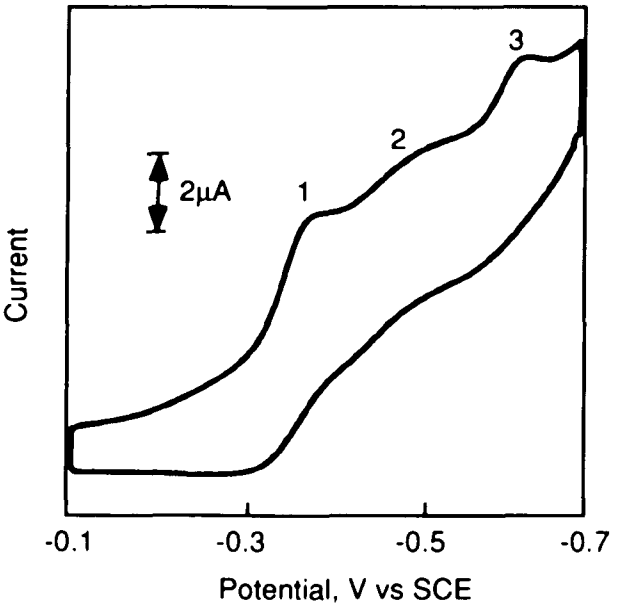

(a)

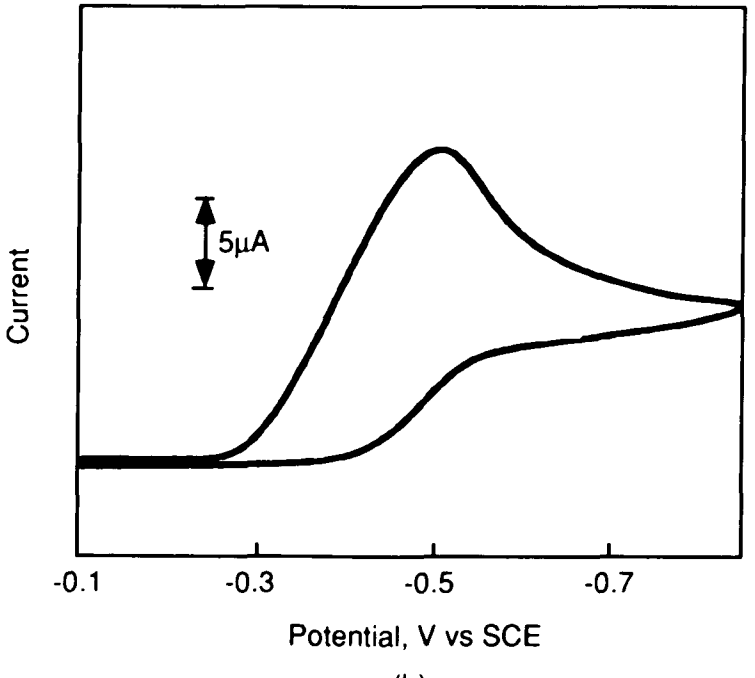

(b)

Figure 4.1 Cyclic Voltammograms of 1.0 mM 4-pyridinecarbox-aldehyde in 0.1 M KCl on a smooth Ag electrode with potential scan rate 100 mV/S. (a) pH 3; (b) pH 7.

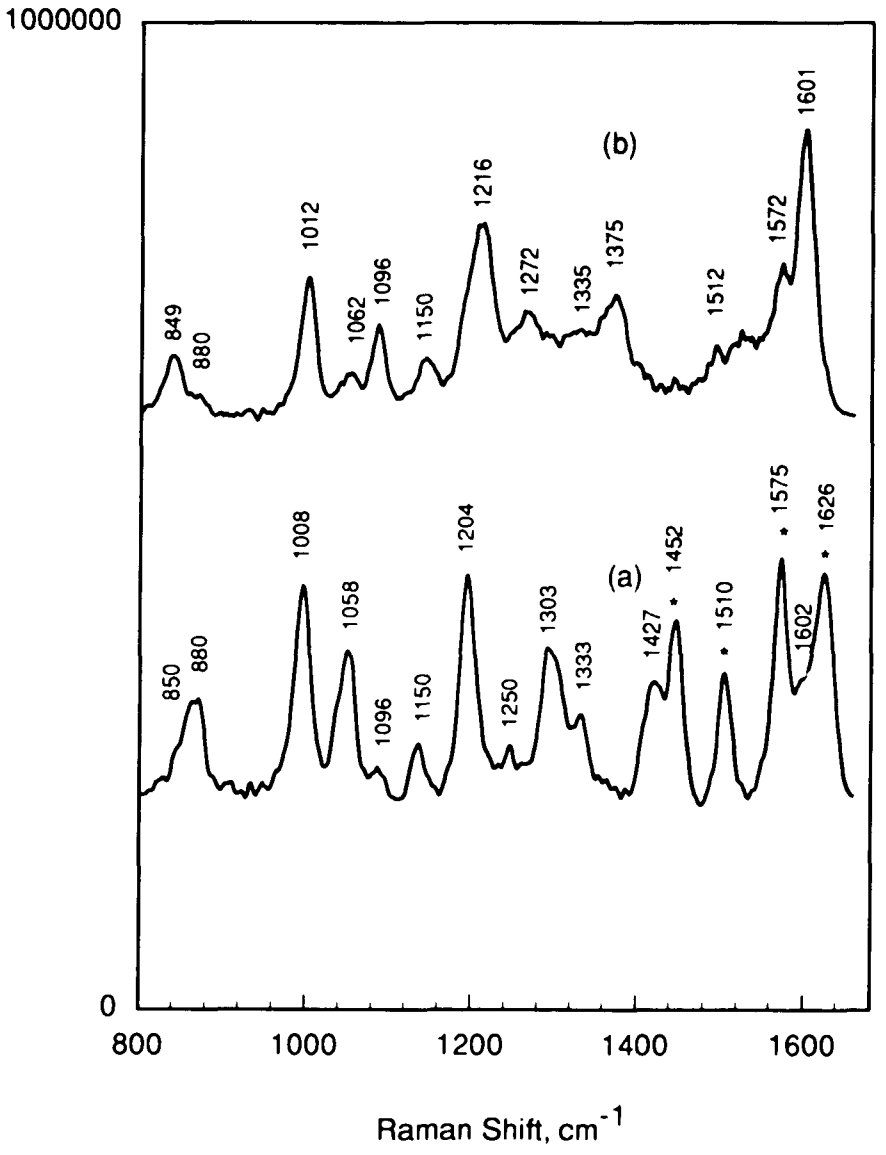

Fig. 4.2 SERS spectra of 4-pyridinecarboxaldehyde in 0.1 M KCl. Curve (a) pH 3; Curve (b) pH 7.

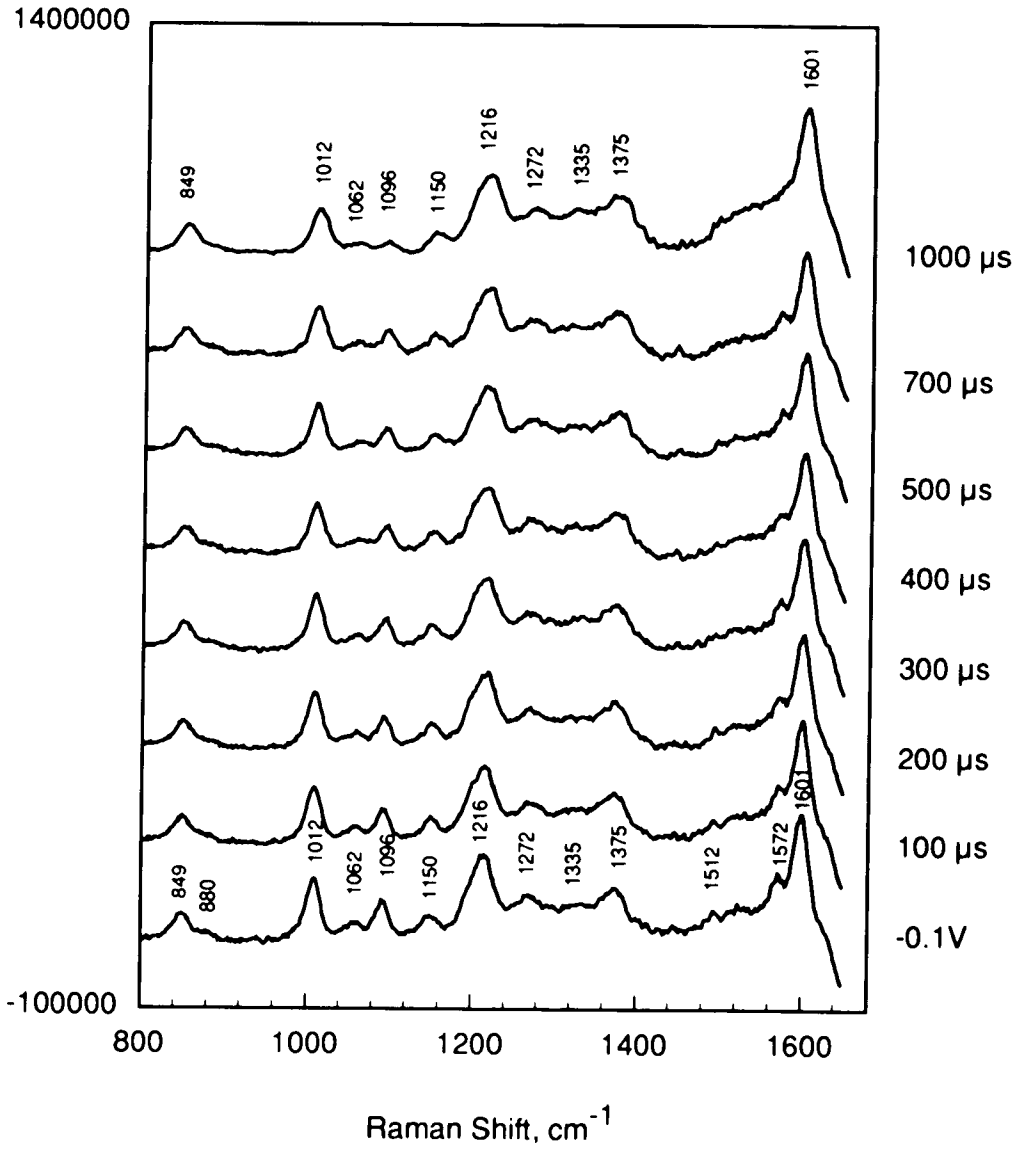
1400000
-100000
800
1000
1200
1400
1600
Raman Shift, cm-1
1000 µs
700 µs
500 µs
400 µs
300 µs
200 µs
100 µs
-0.1V
849
880
1012
1062
1096
1150
1216
1272
1335
1375
1512
1572
1601

Fig. 4.3a

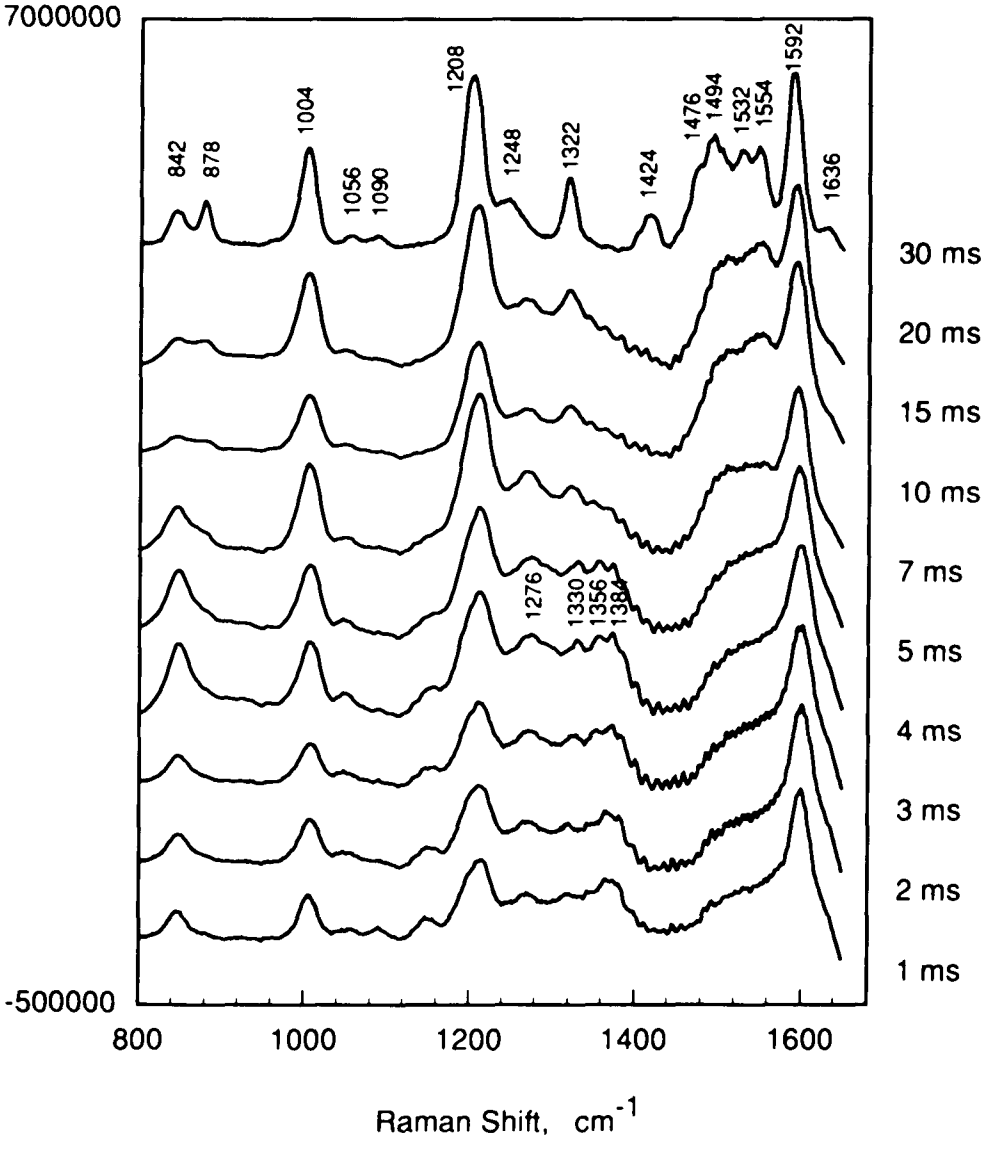

Fig. 4.3b

Figure 4.3 Time-resolved SERS for 4-pyridinecarboxaldehyde reduction initiated by negative potential pulses in neutral 0.1M KCl solution in the time window from 100 μS to 30 mS. Exposure time: 100 μS. Delay time for each spectrum is marked on its right side.

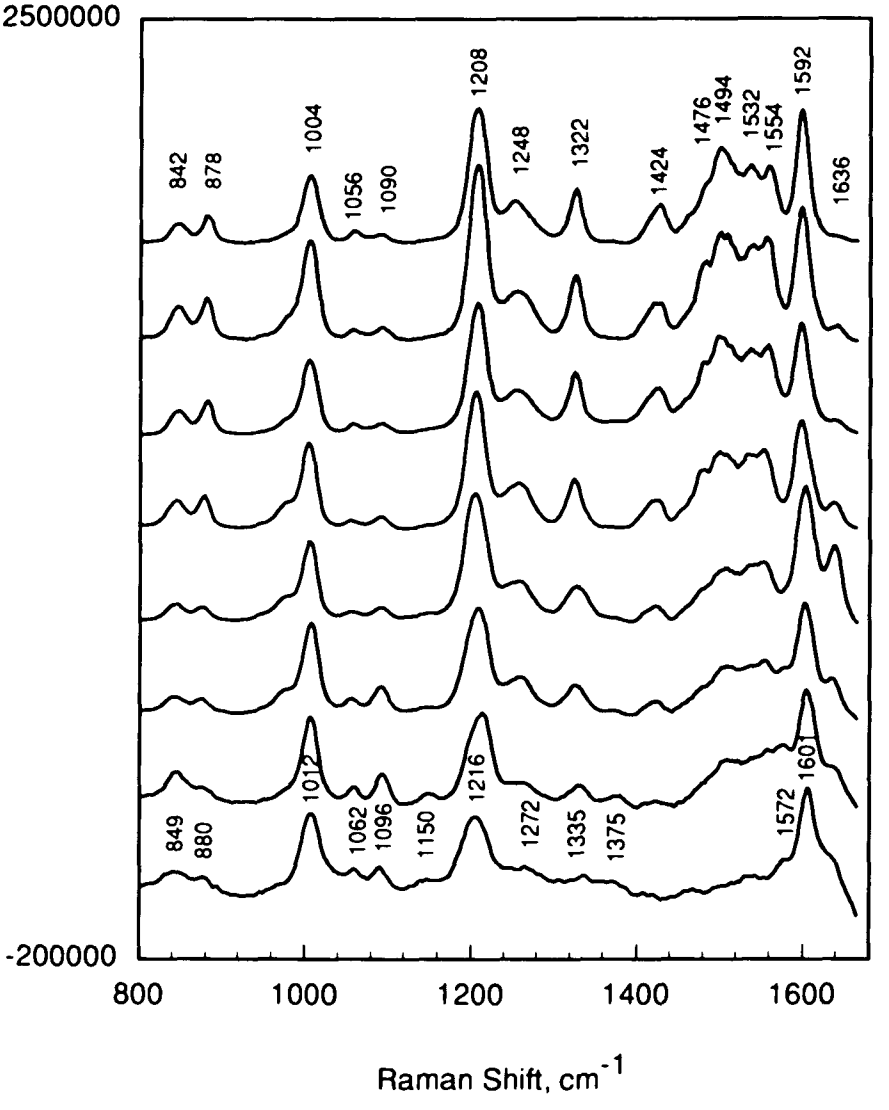

Fig. 4.4 Potential dependence of SERS spectrum of 1.0 mM 4-pyridin-carboxaldehyde in 0.1 M KCl at pH 7. Potential from bottom to top: -0.1V; -0.2V; -0.3V; -0.4V; -0.6V; -0.8V; -1.0V; -1.2V.

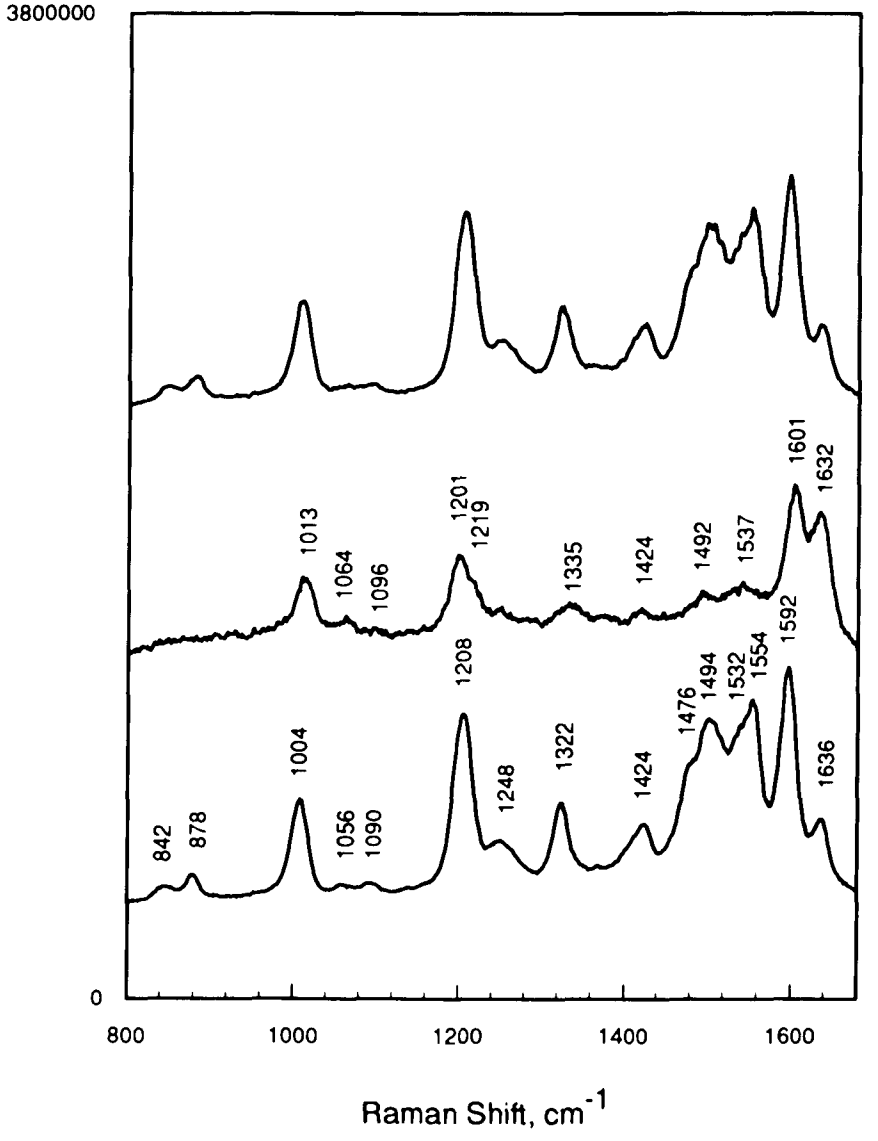

Fig. 4.5 PH dependence of SERS spectrum of 4-pyridinecarboxaldehyde reduction product which was formed in a neutral solution. From bottom to top: pH 7; pH 3; pH 9.

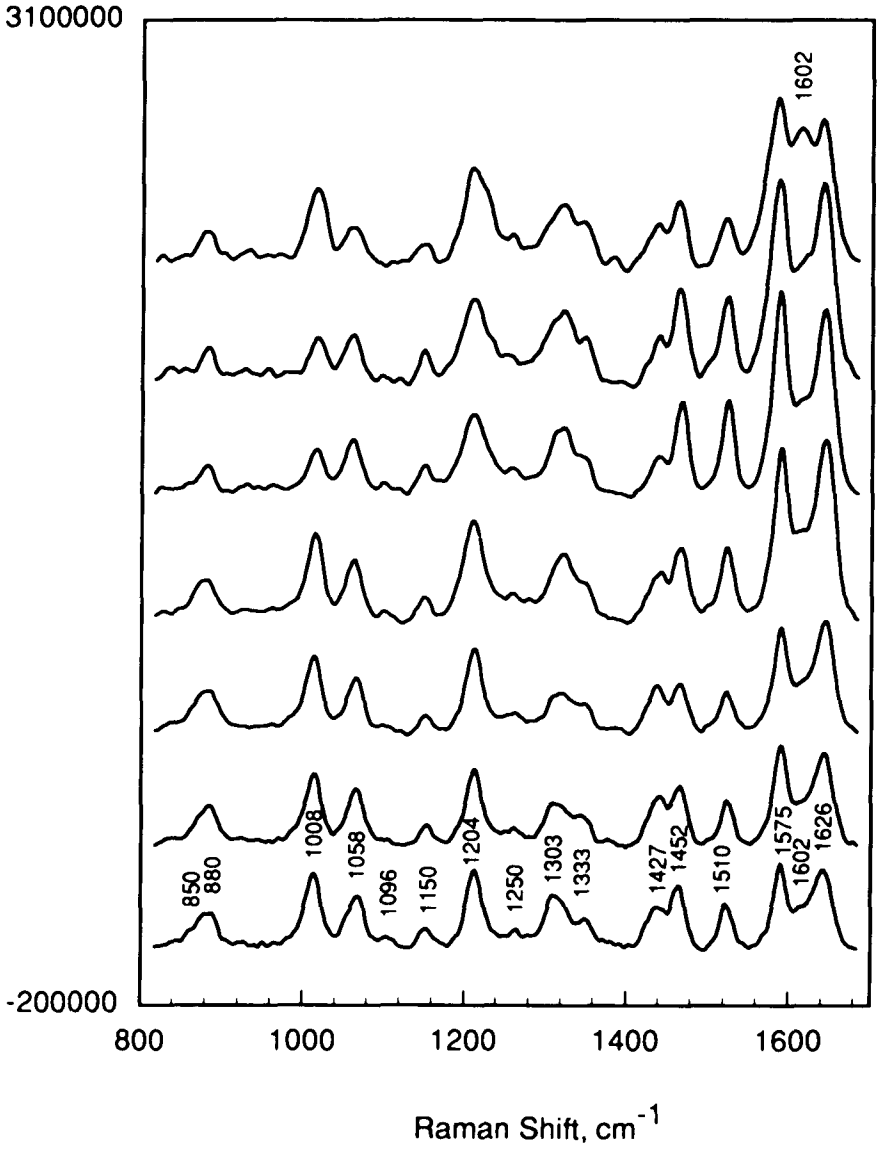

Fig. 4.6 Potential dependence of SERS spectrum of 1.0 mM 4-pyridinecarboxaldehyde in 0.1 M KCl at pH 3. Potential from bottom to top: -0.05V; -0.2V; -0.4V; -0.6V; -0.8V; -1.0V; -1.2V.

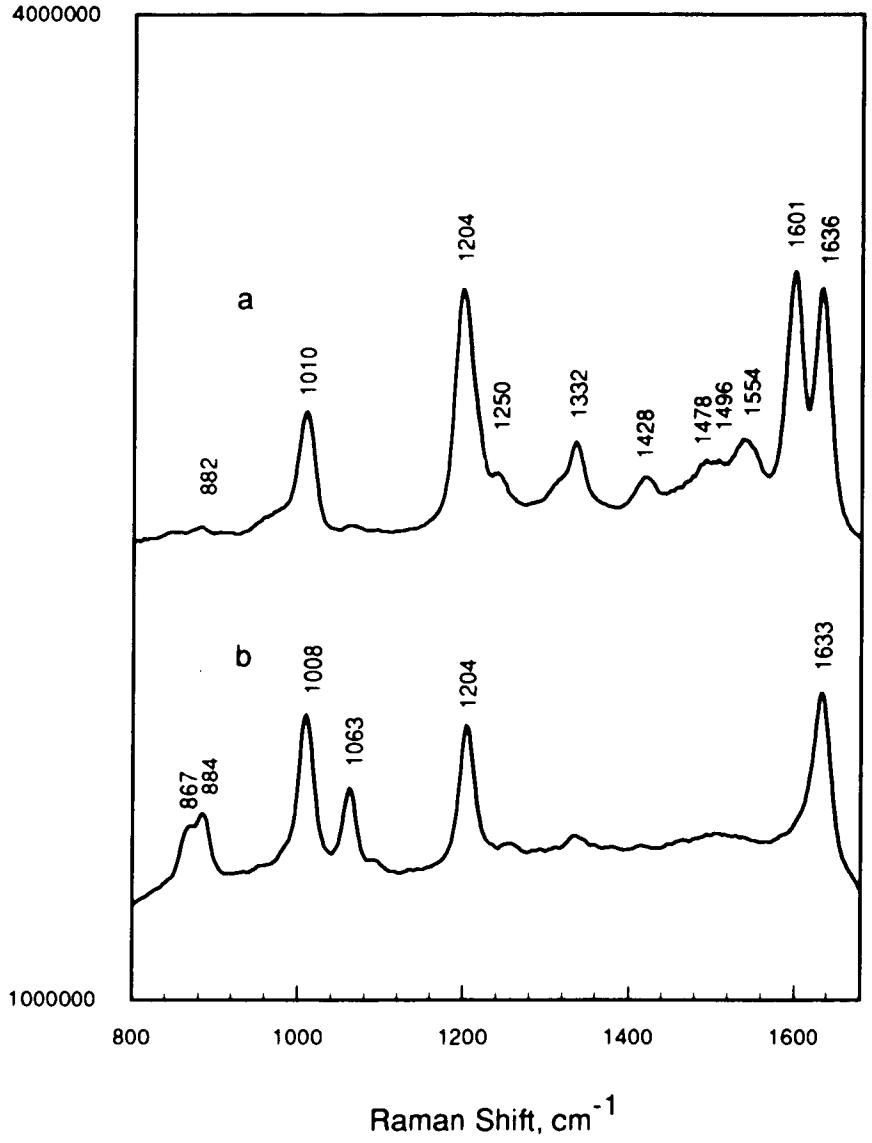

Fig. 4.7 SERS spectra of 4-(hydroxymethyl)pyridine in 0.1 M KCl. a) at -0.8V, pH 7; b) at -0.4V, pH 3.

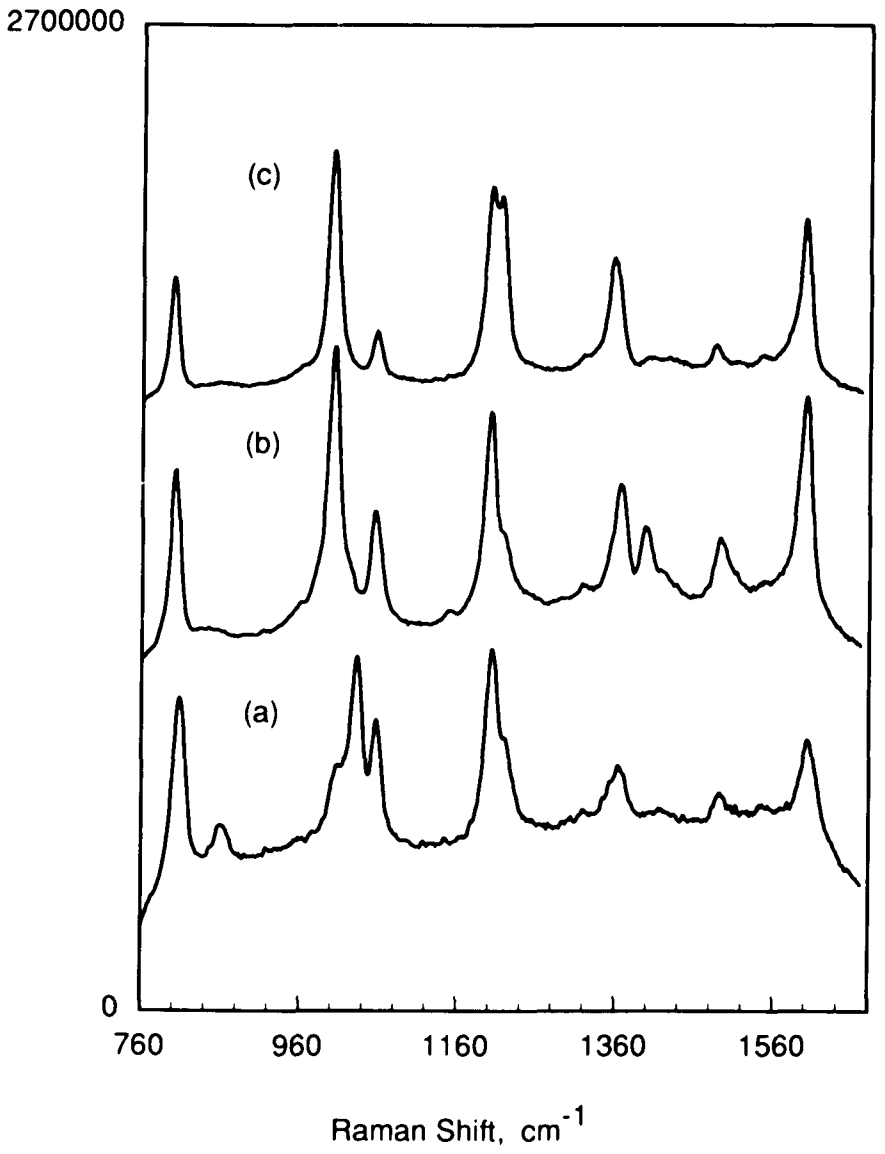

Fig. 4.8 SERS spectra of 4-picoline in 0.1M KCl at pH 7.
Potential from the bottom to the top: -0.1V; -0.4V; -0.8V.

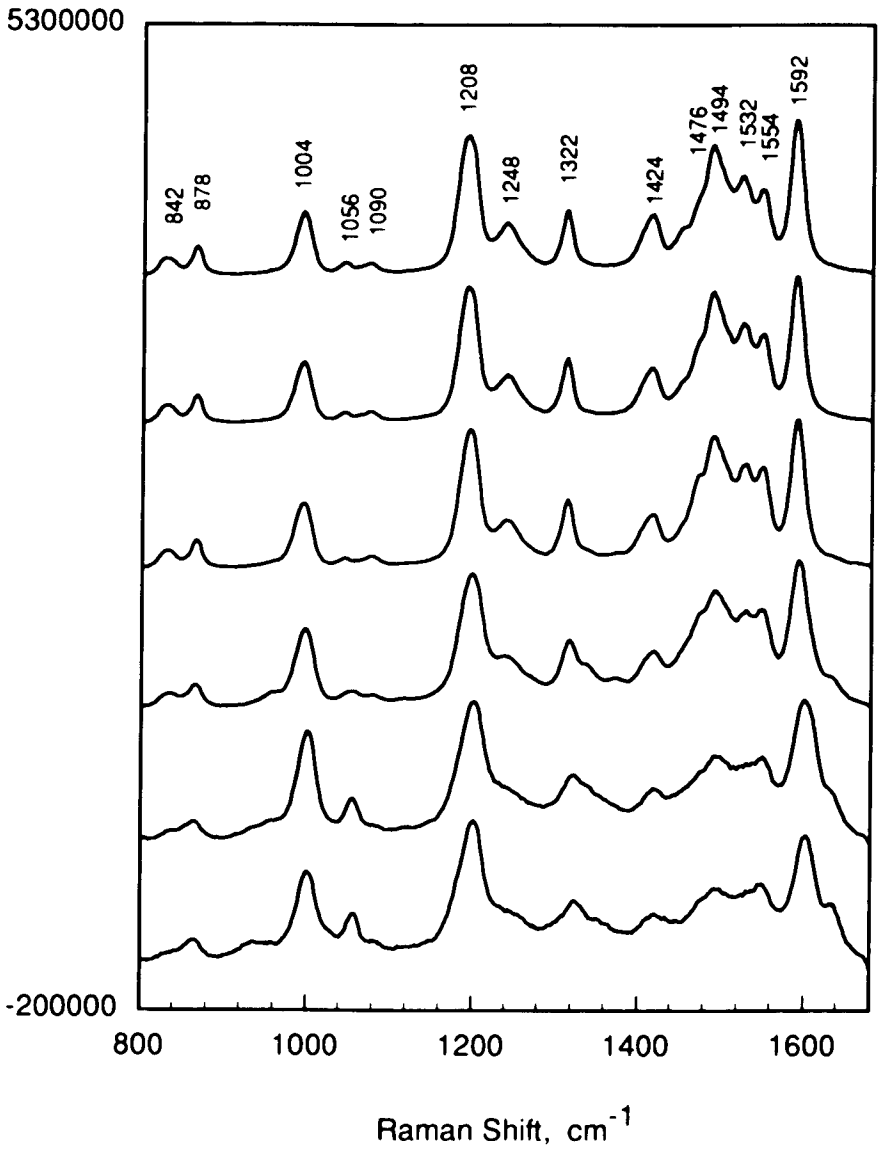

Fig. 4.9 Potential dependence of SERS spectra of 1,2-bis(4-pyridyl)ethane at pH 7. Potential from bottom to top: -0.2V; -0.4V; -0.6V; -0.8V; -1.0V; -1.2V.

Chapter V

Study of the Protonation and Electrochemical Reduction of 4-(Hydroxymethyl)pyridine

Section 5.1 Introduction

As a class of organic compounds, the electrooxidation of alcohols has been extensively studied. However, little attention was paid to the electroreduction of these compounds. According to Baizer and Lund,[1] reductive cleavage occurs during the electroreduction of alcohols, which produces a radical as the intermediate. The final product of the reduction depends on the stability of the radical. Unstable intermediates favor the directly reduced alkanes, while stable radicals will produce, to some extent, rearranged or dimerized products.[1,2] The electroreduction of an aryl-substituted methanol, such as phenylmethanol or pyridylmethanol, could produce only two kinds of products, since there is no possible intramolecular rearrangement. These products are the fully reduced alkanes and the partially reduced dimers. In this chapter, the process and products of the electrochemical reduction of a pyridine substituted alcohol, 4-(hydroxymethyl)pyridine are investigated in both acidic and neutral conditions by means of cyclic voltammetry (CV) and surface-enhanced Raman spectroscopy (SERS). A possible reaction mechanism is suggested.

Section 5.2 Experimental

The experimental setup is similar to that used in previous work (see Experimental Sections in Chapters II and III). A three-electrode SERS cell is used and the electrode potential is controlled by a waveform generator (175 EG&G PARC) through a potentiostat (173 EG&G PARC). A Ag electrode was polished and than pretreated in-situ in 5 mM 4-(hydroxymethyl)pyridine, 0.1M

KCl solution with two +0.3V potential pulses. Each pulse lasted 2 seconds and then the potential was returned to -0.1V. The 488 nm beam from an Ar^+ laser (Spectraphysics) was used to irradiate the Ag working electrode and the scattered Raman light was collected by a lens at a right angle. The Raman signal was dispersed by a triplemate monochromator (Spex) and detected by a diode array detector (EG&G PARC 1455XC). The detector is controlled by a Macintosh computer (Classic) through an OMA detector interface (EG&G PARC 1461). The data were stored in diskettes and plotted using a laser printer. 4-(hydroxymethyl)pyridine (HMPY) (99%) was purchased from Aldrich and used without further purification. Reagent grade KCl, HCl, KOH and deionized distilled water were used. All potentials are versus the saturated calomel electrode, SCE, reference.

Section 5.3 Results and Discussion

(a) Cyclic Voltammetry of HMPY

Generally, the electrochemical reduction of 4-(hydroxymethyl)-pyridine (HMPY) could produce a fully reduced product, 4-picoline,

$$Py\text{-}CH_2OH + 2H^+ + 2e^- = Py\text{-}CH_3 + H_2O \qquad (5.1)$$

and/or a partially reduced product, 1,2-bis(4-pyridyl)ethane,

$$2Py\text{-}CH_2OH + 2H^+ + 2e^- = Py\text{-}CH_2\text{-}CH_2\text{-}Py + 2H_2O \qquad (5.2)$$

Actually, these two reactions involves the same radical, $Py\text{-}CH_2\cdot$ as an intermediate, since the stepwise process can be written as follows,

$$Py\text{-}CH_2OH + e^- + H^+ = Py\text{-}CH_2\cdot + H_2O \qquad (5.1a)$$

$$Py\text{-}CH_2\cdot + e^- + H^+ = Py\text{-}CH_3 \qquad (5.1b)$$

$$2Py\text{-}CH_2\cdot = Py\text{-}CH_2\text{-}CH_2\text{-}Py \qquad (5.2a)$$

or

$$Py\text{-}CH_2\cdot + Py\text{-}CH_2OH + e^- + H^+ = Py\text{-}CH_2\text{-}CH_2\text{-}Py + H_2O \qquad (5.2b)$$

Fig. 5.1 shows the results of a cyclic voltammetric (CV) study of HMPY in both acidic and basic aqueous solutions. CV curves of this compound are obtained at a series of pH values. At pH 3 two separate reduction waves are detected. The peak potential is about -1.07V for the first wave and -1.3V for the second wave. No significant anodic wave is found in the return potential scan with switching potential at -1.2V or -1.5V, even when the scan rate is as high as 50 V/s. This indicates that both electron transfers are irreversible. The ratio of the peak-currents of the first reduction wave over the second wave does not change significantly with the scan rate. A plot of the peak potentials, E_p, versus the logarithm of scan rate shows two straight lines with slopes about 86 mV per decade for the first wave and 72 mV per decade for the second wave, respectively, in the range from 100 mV/s to 50 V/s (Curves (a) and (b) in Fig. 5.2). The irreversibility is probably not due to sluggish electron transfer but rather fast following chemical steps which consume the products of the electron transfer reactions. However, the first reduction wave decreases very rapidly with increasing pH.

The CV result at pH greater than 7 shows only the second reduction wave with a peak potential, E_p, about -1.33V. The relationship between the peak potential and the logarithm of scan rate is also linear with a slope 72 mV per decade (Curve (c) in Fig. 5.2). At pH 5, although both reduction waves appear in the CV, the first wave is much lower than the second. The same

relationship between the E_p of the second wave and the scan rate is found as at pH 7. Therefore, within experimental errors, the second wave detected at all three pH values behaves exactly the same and is probably due to the same electron transfer reaction. The first reduction wave at low pH values could be caused by the electrochemical reduction of the protonated HMPY molecules, $H^+PY\text{-}CH_2OH$ or $H^+PY\text{-}CH_2OH_2^+$, since the pyridine nitrogen is more basic than the hydroxy group and should be protonated first. HMPY is a stronger base ($K_a=3.9x10^{-6}$)[3,4] than 4-pyridinecarboxaldehyde ($K_a=1.8x10^{-5}$).[5,6] Even at pH 7, the pyridine nitrogen is, at least to some degree, protonated. In addition, the protonation of the pyridine N should not influence the reduction potential very significantly since this site is too far away from the reacting group. Thus, the first reduction wave is most likely caused by the reduction of the double protonated species, $H^+Py\text{-}CH_2OH_2^+$. Therefore, in neutral or less acidic solutions, the reduction process can be written as

$$H^+Py\text{-}CH_2OH + e^- + H^+ = H^+Py\text{-}CH_2\cdot + H_2O \qquad (5.1a)$$

$$2H^+Py\text{-}CH_2\cdot = H^+Py\text{-}CH_2\text{-}CH_2\text{-}PyH^+ \qquad (5.2a)$$

or

$$H^+Py\text{-}CH_2\cdot + e^- + H^+ = H^+Py\text{-}CH_3 \qquad (5.1b)$$

All the protonated species in these equations should be substituted by the corresponding non-protonated species in basic solutions. Reaction (5.1b), if it exists, should have a more positive E^0 than the first electron transfer, otherwise, two separate reduction waves would be detected in the CV. While in strong acidic media, besides the reactions listed above, one more reaction can be added

$$H^+Py\text{-}CH_2OH_2^+ + e^- = H^+Py\text{-}CH_2\cdot + H_2O \qquad (5.1a')$$

which occurs at a more positive potential than the species with an unprotonated

hydroxy group, since the protonation of the hydroxy group makes the reduction easier.

Another alternative mechanism for the reaction in acidic media is where the reaction would go through (5.1a') and (5.1b), i.e., the first wave corresponding to reaction (5.1a') and the second wave to reaction (5.1b). However, this mechanism can be eliminated by the fact that no anodic wave is found in the return positive-going sweep. If the second wave involved the reduction of $H^+Py\text{-}CH_2\cdot$, an anodic wave would have been observed when the potential sweep is reversed right after the first reduction wave.

The possibility of (5.1a') followed by the dimerization step (5.2a) and another electron transfer (5.2b') at more negative potential

$$H^+Py\text{-}CH_2\cdot + H^+Py\text{-}CH_2OH + H^+ + e^- = H^+Py\text{-}CH_2\text{-}CH_2\text{-}PyH^+ + H_2O \qquad (5.2b')$$

is also rejected for the same reason as for the (5.1a')-(5.1b) mechanism. Additional evidence for rejecting the (5.1a')-(5.2a)-(5.2b') mechanism is that the ratio of the peak current, i_{p2}/i_{p1}, is independent of the scan rate. According to this mechanism, the ratio would be expected to increase with scan rate.

(b) SERS Spectra of Possible Species Involved in the Electrode Process

From the CV results alone, however, it's still difficult to know which reaction, (5.2a) or (5.1b), occurs after the first electron transfer step (5.1a) and/or (5.1a'), since both reactions (5.2a) and (5.1b) seem to be possible. In order to identify the product produced in the reduction process, SERS spectra of HMPY in both acidic and neutral media are taken and investigated. The SERS spectra of HMPY in acidic and neutral media look quite different, as shown in Fig. 5.3. In

contrast to the situation of 4-pyridinecarboxaldehyde (ALPY) (see Chapter IV), the SERS spectrum of HMPY shows more bands in neutral medium than in acidic medium. The SERS spectrum of Py-CH_2OH at pH 3 (Fig. 5.3a) shows three very strong bands at 1633, 1204 and 1008 cm^{-1}, two strong bands at 1063 and 884 cm^{-1} and a shoulder band at 867 cm^{-1}. If one compares the Py-CH_2OH spectrum in acidic with that in basic or neutral media, it can be seen that although they share most of the SERS bands, the relative intensities are different. For example, In neutral or basic medium, the 1600 cm^{-1} band is very intense and the 1064 and 882 cm^{-1} bands are very weak, while in acidic medium the 1600 cm^{-1} band totally vanishes but the other two bands become quite intense.

The possible assignments (Table 5.1) is made by reference to the literature[7-14] and the assignment of ALPY (see Chapter IV). As in the situation of ALPY in acidic media, several extra bands are found in the HMPY spectrum in neutral solutions. However, if a careful comparison is made, it can be seen that almost all the extra bands which can not be assigned to the neutral HMPY molecules have their corresponding bands in the spectrum in acidic media. If the spectrum obtained at pH 3 is assigned to the acid form or the protonated HMPY,[7,8,13] then those extra bands at pH 7 can be easily assigned to the protonated species. For example, the strong 1636 cm^{-1} band can be assigned to the C-C stretching mode 8a of the protonated pyridine ring, the 1554 and 1496 cm^{-1} bands to the modes 8b and 19a, respectively. Except for the 1633, 1204 and 1010 cm^{-1} bands which are very intense in both acidic and neutral conditions, nearly all the other bands appearing in the spectrum at pH 3 do not belong to A_1 symmetry. Some of them, such as the 1062, 884 and 869 cm^{-1} bands, have more intense relative intensities than their corresponding bands at

pH 7. Since the latter two bands belong the C-H bond out-of-plane vibrations (CH), the enhancement of these two modes is probably related to the orientation change of the adsorbed HMPY molecules due to protonation (see Chapter IV). In neutral or basic solution, the compound is adsorbed on the electrode surface vertically through its pyridine ring nitrogen so that the totally symmetric ring mode vibrations produce very intense Raman signal. Since adsorption with vertical or end-on orientation requires a bare electron lone pair, the loss of the electron lone pair on the pyridine ring nitrogen by protonation will cause a face-on adsorption through the ring π-bonds. The difference between the SERS of ALPY and HMPY is probably due to the difference in their functional groups, which causes the difference in their basicity.[3-6] The aldehyde group in ALPY is not an acid because it can not release a proton and the oxygen in this group is a proton acceptor. Therefore, even in acidic conditions, there are still unprotonated or neutral molecules adsorbing on the surface. HMPY is an alcohol, it can, to some extent, donate a proton even in neutral or weak basic conditions and the donated proton can be captured by the pyridine nitrogen and form a dipolar ion, $H^+Py\text{-}CH_2O^-$. The inductive effect of the hydroxymethyl group also makes the HMPY ring N more basic than ALPY, so that it is partially protonated in the neutral or even weakly basic conditions.

Fig. 5.4 shows the potential dependence of the Py-CH_2OH SERS spectrum at pH 7. The spectrum does not change very much until -1.0V. However, when the electrode potential is more negative than -1.1V, the SERS spectrum of Py-CH_2OH undergoes a significant change. The change in Py-CH_2OH spectrum is consistent with the CV results at pH 7 which show a reduction current rising at about -1.2v. This indicates that the change in the Py-CH_2OH spectrum is mainly caused by the electron transfer rather than an

electric field or orientation effect. A striking fact is that the resulted spectrum is identical to the product spectrum of ALPY electroreduction, that is, the electrochemical reductions of ALPY and HMPY on a Ag electrode in neutral conditions produce the same product, 1,2-bis(4-pyridyl)ethane (BPE). At pH 3 a significant change in spectrum is observed at -0.8V (Fig. 5.5), which is also consistent with the CV results where a reduction wave peaked at -0.9V. A very strong new band appears at about 1600 cm^{-1}. If the potential is held at -0.8V when the reduction of Py-CH_2OH has occurred, and then the pH value of the solution is adjusted to 7 by adding 0.1 M KOH (see Fig. 5.6), the product spectrum undergoes a significant change and is identical to that obtained from the direct reduction at -1.1 V at pH 7. Again the spectrum at pH 3 is recoverable if the pH is adjusted back. The same product is produced in the HMPY reduction no matter whether the medium is acidic, neutral or basic. Furthermore, the spectrum of Py-CH_2OH at -0.8V at pH 3 is also identical to the spectrum of ALPY reduction product (see Chapter IV), where the reduction was carried out at pH 7 and than the pH was adjusted to 3. This is additional evidence for identifying the two reduction products of ALPY and Py-CH_2OH as the same compound. The assignment of the product spectrum has been made in Chapter IV.

The mechanism of HMPY electrochemical reduction is much simpler than that of ALPY. It includes one electron reduction (5.1a) and a following chemical coupling reaction (5.2a) in neutral media, or two parallel electron transfer reactions (5.1a) and (5.1a'), followed by reaction (5.2a) in strong acidic media. Only one product, or one major product, 1,2-bis(4-pyridyl)ethane (EPE), is produced in the electrochemical process.

Section 5.4 Conclusion

4-(Hydroxymethyl)pyridine (HMPY) exists in neutral and less acidic media as a mixture of neutral and single-protonated species. In strong acidic solution, it appears as an equilibrium mixture of both single-protonated and double-protonated species. However, the reduction of HMPY undergoes similar reaction pathways in both acidic and basic media, and the major product is the same. A striking fact is that the reduction of HMPY produces the same product as ALPY, i.e., 1,2-bis(4-pyridyl)ethane. The reduction process can be described best by the following EC mechanism,

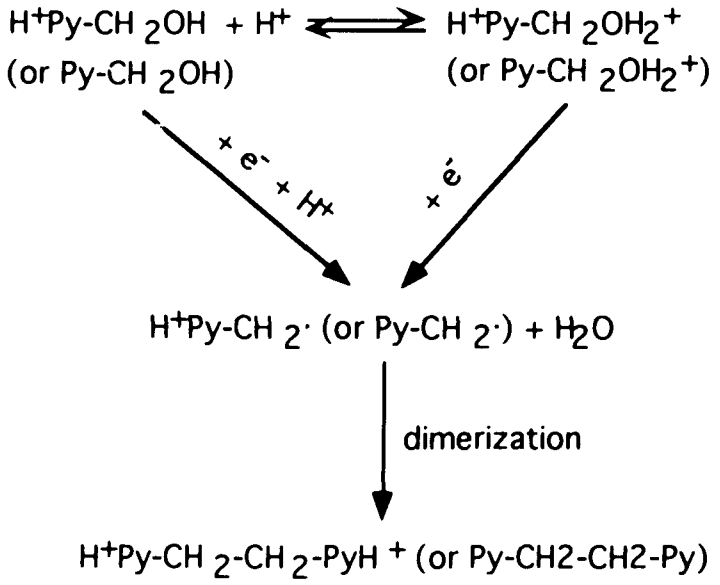

where the reductions of $Py\text{-}CH_2OH$ and $H^+Py\text{-}CH_2OH$ occur at the same potential and $H^+Py\text{-}CH_2OH_2^+$ is reduced more easily than $H^+Py\text{-}CH_2OH$. The surface species of the reactants and the product on the Ag electrode is identified by surface-enhanced Raman spectroscopy (SERS) and the possible assignments has been made.

Table 5.1 Assignment of HMPY SERS Spectra

Assignment	Mode No.	Symmetry	pH 3	pH 7
n(CC)	8a*	A1	1633 vs	1636 s
n(CC)	8a	A1		1601 vs
ν(CC)	8b*	B2		1554 m
ν(CC,CN)	8b	A1		1534 m
ν(CC,CN)	19a*	B2	1501 w	1496 m
ν(CC,CN)	19a			1478 m
ν(CC,CN)	19b,19b*	B2	1422 vw	1428 m
β(CH)				1375 m
ν(CC,CN)	14	B2	1334 w	1335 m
β(CH)	3	B2		1328 m
X-sens.,(CC)	13	A1	1256 w	1250 w
β(CH)	9a	A1	1204 vs	1204 vs
X-sens.,(CH)	15	B2		
β(CH)	18a	A1		1094 vw
β(CH)	18b	B2	1062 s	1064 w
ν(CC,CN)	1	A1	1008 vs	1010 vs
γ(CH)	10a or 5	A2 or B1	884 s	882 m
γ(CH)	10b	B1	869 s	848 m

* assigned to the protonated pyridine ring.

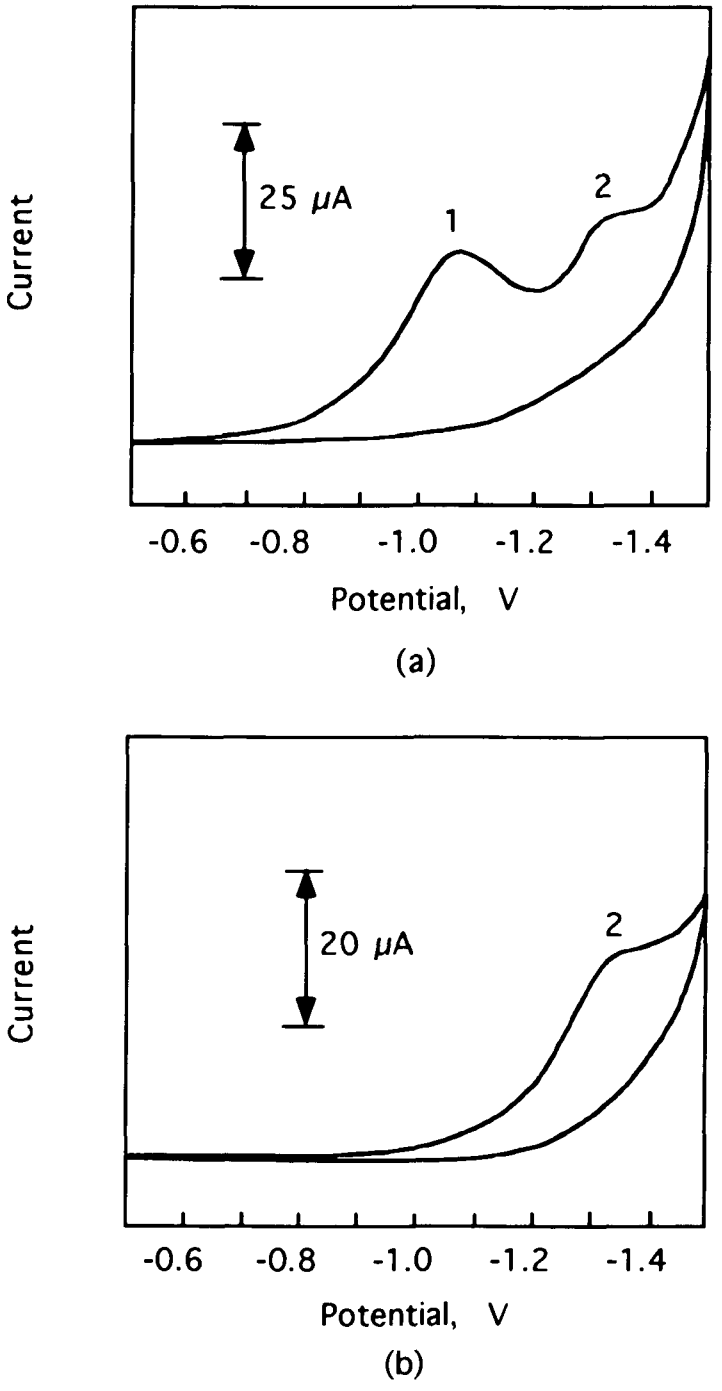

Fig. 5.1 Cyclic Voltammograms of 5.0 mM 4-(hydroxymethyl)pyridin in 0.1 M KCl on a smooth Ag electrode with potential scan rate 100 mV/s. (a) pH 3; (b) pH 7.

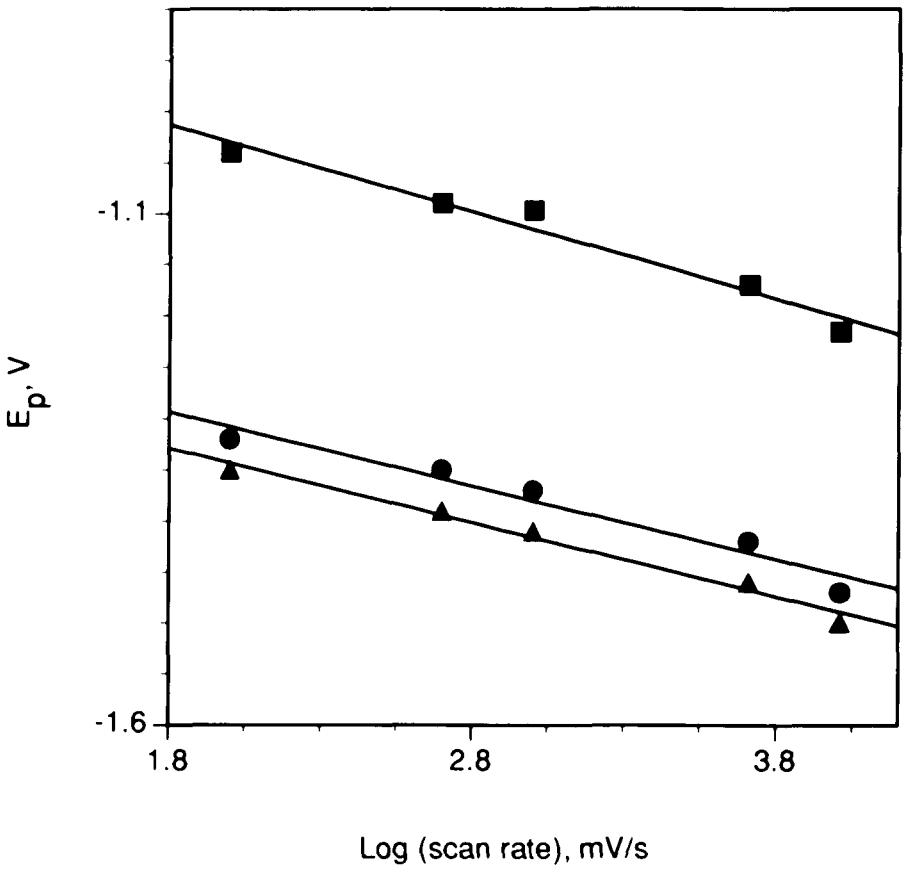

Fig. 5.2 Dependence of peak potential, Ep, on the scan rate: (a) peak 1 at pH 3; (b) peak 2 at pH 3; (c) peak 2 at pH 7.

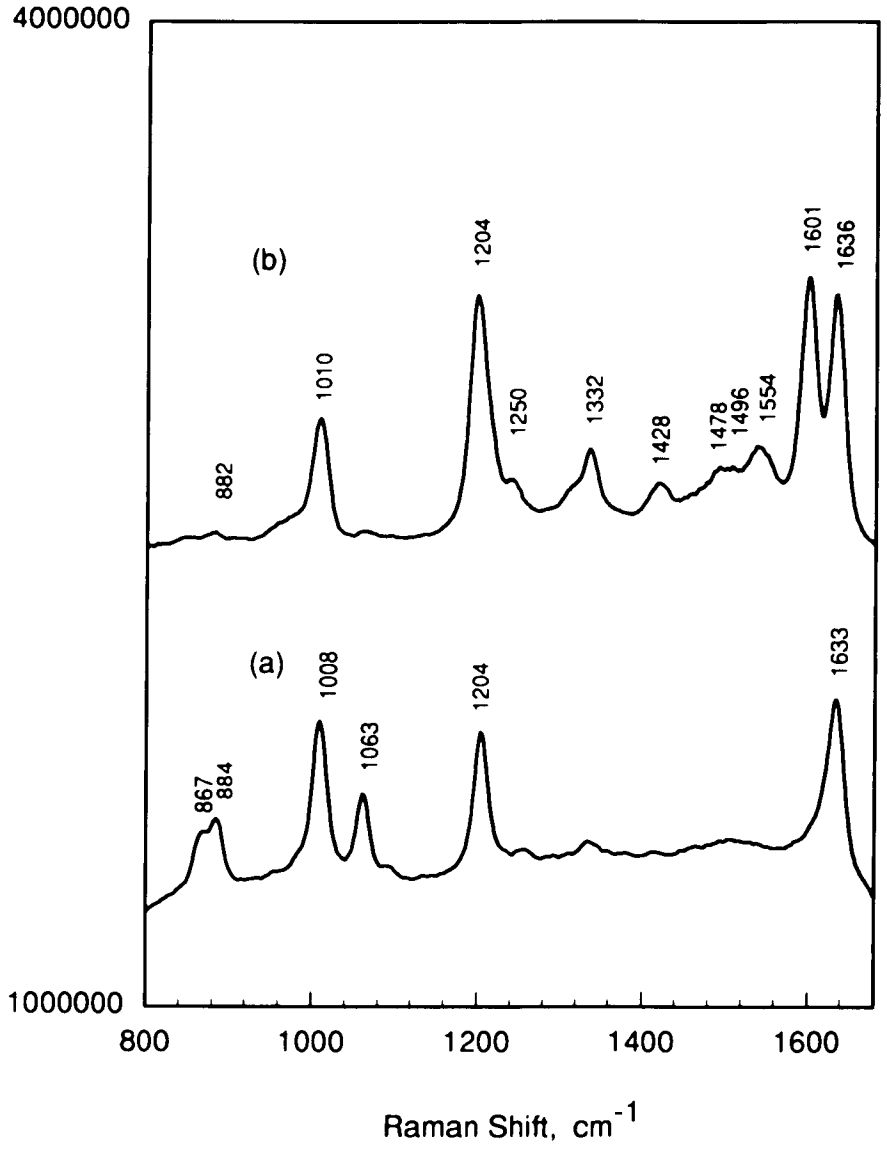

Fig. 5.3 SERS spectra of 4-(hydroxymethyl)pyridin in 0.1 M KCl. Curve (a) pH 3; Curve (b) pH 7.

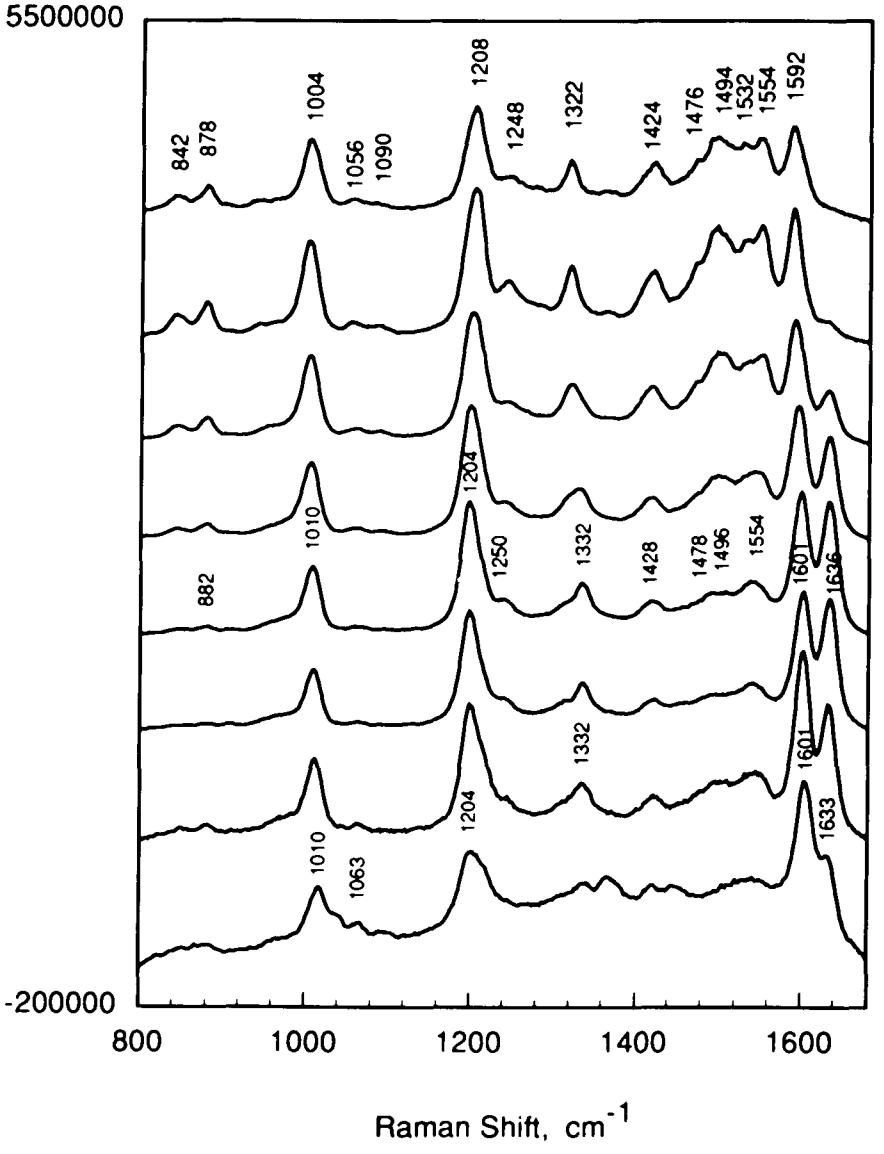

Fig. 5.4 Potential dependence of SERS spectrum of 4-(hydroxymethyl)-pyridine in 0.1 M KCl at pH 7. Potential from bottom to top: -0.1V; -0.3V; -0.5V; -0.7V; -0.9V; -1.1V; -1.2V; -1.3V.

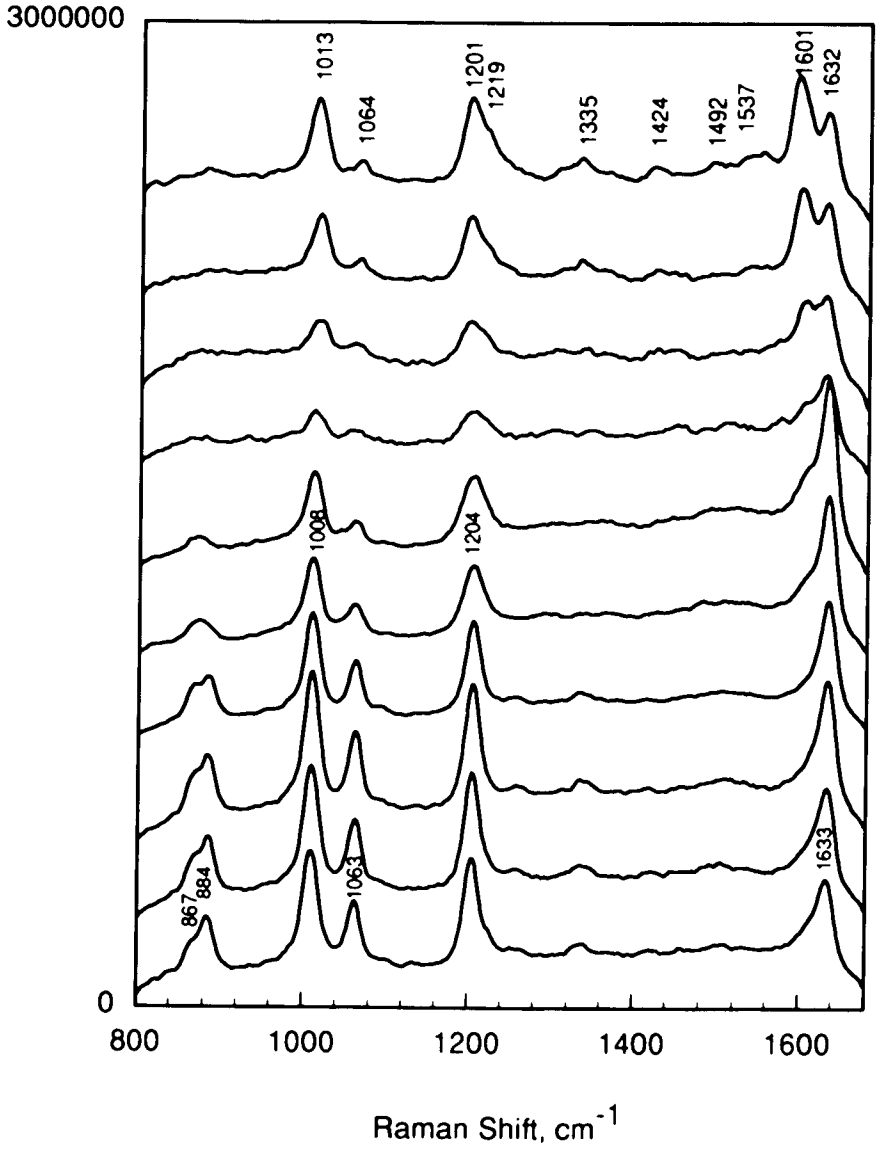

Fig. 5.5 Potential dependence of SERS spectrum of 4-(hydroxymethyl)pyridine in 0.1 M KCl at pH 3. Potential from bottom to top: -0.1V; -0.2V; -0.3V; -0.4V; -0.5V; -0.6V; -0.7V; -0.8V; -0.9V; -1.0V.

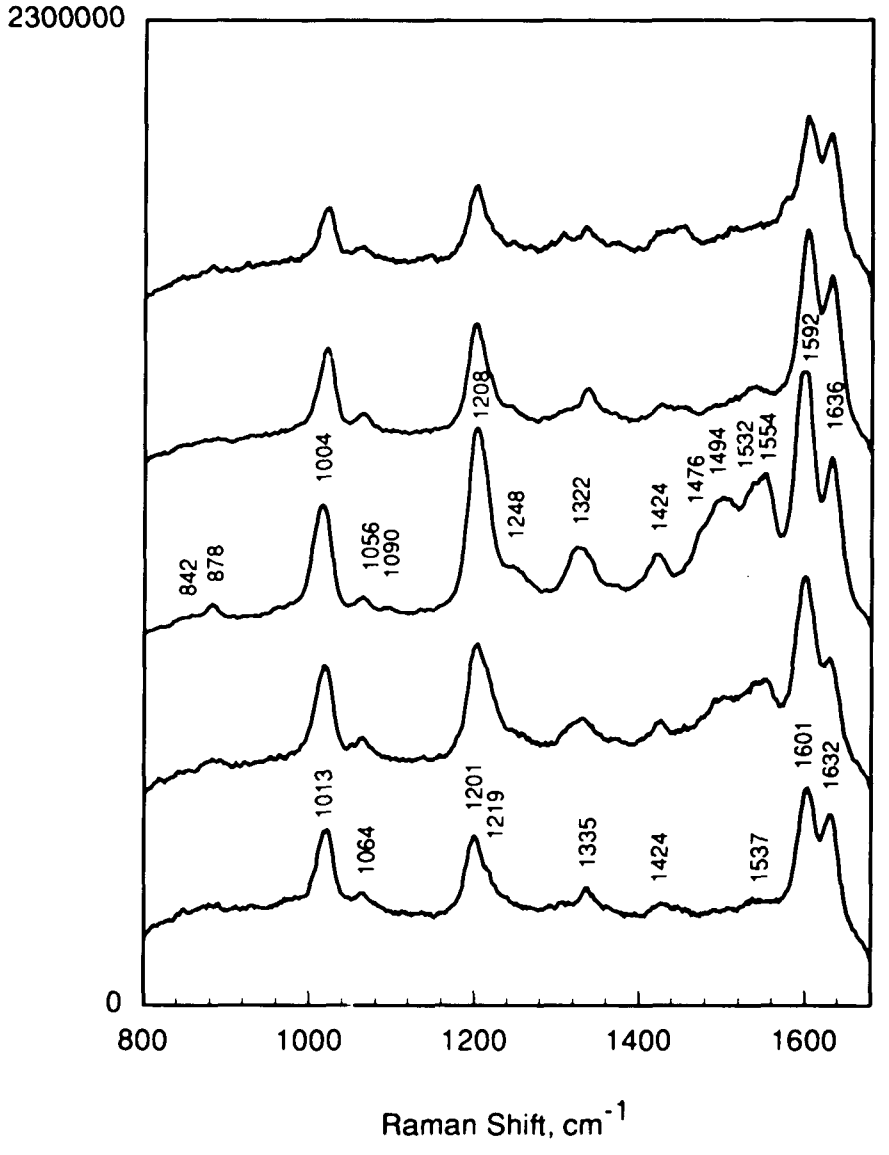

Fig. 5.6 The pH dependence of SERS spectrum of the 4-(hydroxymethyl)-pyridine reduction product which was formed at -0.8V in acidic solution (pH 3). The pH value is changed in following order (from the bottom to the top): a) pH 3; b) pH 6; c) pH 7; d) pH 3; e) pH 2.

BIBLIOGRAPHY

Chapter I

1. H. Baranska in "*Laser Raman Spectrometry - analytical applications*" Ed. H. Baranska, A. Labudzinska and J. Terpinski. Halsted Press, New York (1987).

2. A. Fadini and F. Schnepel in "*Vibrational Spectroscopy: Methods and Applications*", Translation editor: Mary Masson. Halsted Press, New York (1989).

3. D. J. Gardiner and P. R. Graves in "*Practical Raman Spectroscopy*". Springer-Verlag, New York (1989).

4. R. L. Birke and J. R. Lombardi, In " *Spectroelectrochemistry, Theory and Practice*" , Ed. R. J. Gale. Plenum Press, New York (1988).

5. R. K. Chang, B. L. Laube, *CRC Crit. Rev. Solid State Mater. Sci.* 12, 1 (1984).

6. D. L. Jeanmarie, R. P. Van Duyne, *J. Electroanal. Chem.*, 84, 1 (1977).

7. A. M. Stacey, R. P. Van Duyne, in " *Time Resolved Vibrational Spectroscopy, Proc. First Int. Conf. on Time Resolved Spectroscopy*", Vol. 4, 377, Ed. G. H. Atkinson. Academic Press, New York (1983),

8. R. T. Packard, R. L. McCreery, *Anal. Chem.*, 59, 2631 (1987).

9. R. T. Packard, R. L. McCreery, *J. Phys. Chem.*, 92, 6345 (1988).

10. M. A. El-Sayed, *ACS SYMPOSIUM SERIES* , #102, Ch. 10, pp. 215-227. ACS, Washington (1979)

11. G. H. Atkinson, in "*Time-resolved Raman Spectroscopy*", Vol. 9, pp. 1-62, Eds. R. J. H. Clark and R. E. Hester. Hayden, London (1982).

12. R. L. McCreery, R.T. Packard, *Anal. Chem.*, 775A, 61(1989).

13. J. Terpinski in "*Laser Raman Spectrometry - analytical applications*", Ed. H. Baranska, A. Labudzinska and J. Terpinski. Halsted Press, New York (1987).

14. N. B. Colthup, L. H. Daly and S. E. Wiberley in "*Introduction to Infrared and Raman Spectroscopy*", 3rd Edition. Acdemic Press, Boston (1990).

15. Kh. E. Sterin, V.T. Aleksanyan and G. N. Zhizhin in "*Raman Spectra of Hydrocarbons - A Data Bank*". Pergamon Press, New York (1980).

16. F. R. Dollish, W. G. Fateley and F. F. Bentley, in "*Characteristic Raman Frequencies of Organic Compounds*". Wiley, New York (1974).

17. F. A. Cotton in "*Chemical Application of Group Theory*". Wiley, New York, (1963).

18. J. H. S. Green, W. Kynaston and H. M. Paisley, *Spectrochim. Acta*, 19, 549 (1963).

19. D. A. Long and W. O. George, *Spectrochim. Acta*, 19, 1777 (1963).

20. Lester Corrsin, B. J. Fax, and R. C. Lord, *J. Chem. Phys.*, 21, 1170 (1953).

21. E. Spinner, *J. Chem. Soc.*, 1860 (1963).

22. F. A. Andersen, B. Bak, S. Brodersen and J. Rastrup-Andersen, *J. Chem. Phys.*, 23, 1047 (1955).

23. Eric L. Chronister and M. A. El-Sayed in "*Time-resolved Vibrational Spectroscopy*", Edited by George H. Atkinson, 1. Gordon and Breach Science Publishers, New York (1987).

24. G. H. Atkinson, T.L.Brack, I. Grieger, G. Rumbles, D. Blanchard, and L. Siemankowski in "*Time-resolved Vibrational Spectroscopy*", Edited by George H. Atkinson, 55. Gordon and Breach Science Publishers, New York (1987).

25. G. Eyring, B. Curry, A. broek, J. Lugtenberg and R. Matheis, *Biochemistry*, 21, 384 (1982).

26. M. Braiman and R. Matheis, *Proc. Natl. Acad. Sci. U.S.A.*, 79, 403, (1982).

27. C. Hsieh, M. Nagumo, M. Nicol and M. A. El-Sayed, *J. Phys. Chem.* 85, 2714 (1981).

28. C. Hsieh, M. A. El-Sayed, M. Nicol, M Nagumo and J. Lee, *Photochem. and Photobiol.* , 38, 83 (1983).

29. Yasushi Koyama in "*Time-resolved Vibrational Spectroscopy*", Edited by

George H. Atkinson, 15. Gordon and Breach Science Publishers, New York (1987).

30. Teizo Kitagawa and Takashi Ogura in "*Time-resolved Vibrational Spectroscopy*", Edited by George H. Atkinson, 83. Gordon and Breach Science Publishers, New York (1987).

31. M. Wikstrom, *Nature,* 308, 558 (1984).

32. T. Spiro, R. P. Rava, S. P. A. Fodor, S. Dasgupta, and R. A. Copeland in "*Time-resolved Vibrational Spectroscopy*", Edited by George H. Atkinson, 101. Gordon and Breach Science Publishers, New York (1987).

33. J. Terner, T. G. Spiro, M. Nagumo, M. F. Nicol and M. A. El-Sayed, *J. Am. Chem. Soc.*, 102, 3238 (1980).

34. J. Terner, J. D. Stong, T. G. Spiro, M. Nagumo, M. F. Nicol and M. A. El-Sayed, *Proc. Natl. Acad. Sci., USA*, 78, 1313 (1981).

35. S. Dasgupta, T. G. Spiro, C. K. Johnson, G. A. Dalickas and R. M. Hochstrasser, *Biochemistry*, 24, 5295 (1985).

36. T. G. Spiro, "*Iron Porphyrins*" (Vol. II), Addison-Wesley, Reading, MA., (1983).

37. W. L. Peticolas, T. W. Patapoff, and K. Bajdor in "*Time-resolved Vibrational Spectroscopy*", Edited by George H. Atkinson, 160. Gordon and Breach Science Publishers, New York (1987).

38. B. Chance, *J. Biol. Chem.*, 151, 553 (1943).

39. P. George, *Biochem. J.*, 54, 267 (1953)

40. Y. Nishimura, T. Uno, M. Tsuboi, R. Makino, T. Iizuka, and Y. Ishimura in "*Time-resolved Vibrational Spectroscopy*", Edited by George H. Atkinson, 125. Gordon and Breach Science Publishers, New York (1987).

41. R. Makino, T. Uno, Y. Nishimura, T. Iizuka, M. Tsuboi and Y. Ishimura, *J. Biol. Chem.*, 261, 8376 (1986).

42. A. J. Sitter, C. M. Reczek and J. Terner, *J. Biol. Chem.*, 260, 7515 (1985).

43. J. Terner, A. J. Sitter and C. M. Reczek, *Biochim. Biophys. Acta*, 828, 73 (1985).

44. J. Terner, A. J. Sitter and C. M. Reczek, in "*Time-resolved Vibrational Spectroscopy*," edited by A. Laubereau and M. Stockburger, 216. Springer, Berlin (1985).

45. T. Kitagawa, S. Hashimoto and T. Ogura, in "*Time-resolved Vibrational Spectroscopy*," edited by A. Laubereau and M. Stockburger, 211. Springer, Berlin (1985).

46. T. L. Gustafson, D. M. Roberts and D. A. Chernoff, *J. Chem. Phys.*, 79, 1559 (1983).

47. T. L. Gustafson, D. A. Chernoff, J. F. Palmer and D. M. Roberts, in "*Time-resolved Vibrational Spectroscopy*", edited by A. Laubereau and M. Stockburger, 15. Springer, Berlin (1985).

48.T. L. Gustafson, D. A. Chernoff, J. F. Palmer and D. M. Roberts, in "*Time-resolved Vibrational Spectroscopy*", Edited by George H. Atkinson, 265. Gordon and Breach Science Publishers, New York (1987).

49. H. Hamaguchi, C. Kato and M. Tasumi, *Chem. Phys. Lett.*, 100, 3 (1983).

50. H. Hamaguchi, T. Urano and M. Tasumi, *Chem. Phys. Lett.*, 106, 153 (1984).

51.Mitsuo Tasumi, Taeko Urano, and Hiro-o Hamaguchi in "*Time-resolved Vibrational Spectroscopy*", Edited by George H. Atkinson, 252. Gordon and Breach Science Publishers, New York (1987).

52. Hiroaki Takahashi, Shinichi Suzuki, and Hiroaki Isaka in "*Time-resolved Vibrational Spectroscopy*", Edited by George H. Atkinson, 286. Gordon and Breach Science Publishers, New York (1987).

53. V. N. Bagratashvili, Yu. G. Vainer, V. S. Doljikov, S. F. Kol'yakov, A. A. Makarov, L. P. malyavkin, E. A. Ryabov, E. G. Sil'kis, V. D. Titov, *Sov. Phys.*

JETP Lett., 30, 471 (1979).

54. V. N. Bagratashvili, Yu. G. Vainer, V. S. Doljikov, S. F. Kol'yakov, V. S. Letokhov, A. A. Makarov, L. P. malyavkin, E. A. Ryabov, E. G. Sil'kis, V. D. Titov, *Sov. Phys. JETP Lett.*, 53, 512 (1981).

55. V. S. Letokhov and E.A. Ryabov, in "*Time-Resolved Vibrational Spectroscopy*", Edited by A. Laubereau and M. Stockburger, 53. Springer, Berlin (1985).

Chapter II

1. K. Brand, *Die Elektrochemische Reduktion Organischer Nitrokorper*, Stuttgart, 1908.

2. A. T. Tomilov, V. G. Mairanovskii, M. Ya. Fioshin, V. A. Smirnov, "*Electrochemistry of Organic Compounds*"; 248. Halsted Press, New York (1972).

3. W. Kemula, T. M. Krygonski, "*Encyclopedia of Electrochemistry of the Elements*", A. J. Bard, A. Lund, Eds.;Vol. 13, Chap. 2. Dekker, New York (1979).

4. M. R. Rifi, F. H. Covitz, "*Introduction to Organic Electrochemistry*"; p183. Dekker, New York (1974).

5. A. J. Fry,in "*The Chemistry of Amino, Nitroso, Nitro compounds and their Derivitives*", Part I, S. Patai, Ed., p320. Wiley, New York (1982).

6. W. J. Albery, M. L. Hitchman, "*Ring-Disk Electrodes*", p92. Clarendon, Oxford (1971)

7. L. Chuang, I. Fried, P. Elving, *J. Anal. Chem.* , 36, 2426 (1964).

8. I. A. Titova, I. M. Levenson, V. G. Mairanovskii, A. B. Ershler, *Elcktronimiya*, 9, 424 (1973).

9. W. J. Albery, B. A. Coles, A. M. Couper,*J. Electroanal. Chem. Interfacial Electrochem.*, 65, 901 (1975).

10. G. L. McIntire, D. M. Chiappardi, R. L. Casselberry, H. N. Blount, *J. Phys.*

Chem., 86, 2632 (1982).

11. C. Nishihara, M. Kaise, *J. Electroanal. Chem. Interfacial Electrochem.*, 149, 287 (1983).

12. I. Rubinstein, *J. Electroanal. Chem. Interfacial Electrochem.*, 183, 379 (1985).

13. H. Shindo, C. Nishihara, *Surf. Sci.*, 158, 393 (1985).

14. H. Shindo, *J. Chem. Soc., Faraday Trans.* I, 82, 45 (1986).

15. C. Nishihara, H. Shindo, *J. Electroanal. Chem. Interfacial Electrochem.*, 202, 231 (1986).

16. C. Nishihara, H. Shindo, J. Hiraishi, *J. Electranal. Chem.*, 191, 425 (1985).

17. S. Sun, R. L. Birke, J. R. Lombardi, K. P. Leung, and A. Z. Genack, *J. Phys. Chem.*, 92 (21), 5965 (1988).

18. P. Gao, D. Gosztola, M. J. Weaver, *J. Phys. Chem.*, 92, 7122 (1988).

19. P. Gao, D. Gosztola, M. J. Weaver, *Anal. Chim. Acta,* 212, 201 (1988).

20. J. S. Suh, D. P. DiLella, M. Moskovits, *J. Phys. Chem.* 87, 1540 (1983).

21. L. H. Piette, P. Ludwig, R. N. Admas, *J. Am. Chem. Soc.*, 83, 3909 (1961).

22. P. Ludwig, T. Layloff, R. N. Admas, *J. Am. Chem. Soc.*, 86, 4568 (1964).

23. C. Shi, W. Zhang, R. L. Birke and J. R. Lombardi, *J. Phys. Chem.*, 94, 4766 (1990).

24. H. Bauer and S. M. Rosenthal, *J. Am. Chem.* Soc., 66, 611 (1944).

25. R. L. Shriner and R. C. Fuson, "*The Systematic Identification of Organic Compounds*", Second Ed., p.61. J. Wiley & Sons, Inc., New York (1940).

26. D. K. Gosser Jr., and P. Reiger, *Anal. Chem.*, 60, 1159 (1988).

27. D. K. Gosser Jr., and F. Zhang, *Talanta.*, 38(7), 715 (1991).

28. E. Laviron, *J. Electroanal. Chem* ., 146, 14 (1983).

Chapter III

1. R. K. Chang and T. E. Furtak, Eds., "Surface Enhanced Raman Scattering". Plenum Press, New York (1982).

2. R. L. Birke and J. R. Lombardi, In " *Spectroelectrochemistry, Theory and Practice*", Ed. Gale, R. J., Plenum Press, New York (1988).

3. M. J. Weaver, F. Barz, J. G. Gordon II and M. R. Philpott, *Surface Science* 125, 409 (1983). 20ms TR-SERS

4. C. K. Chen, T. F. Heinz, D. Ricard and Y. R. Shen, *Chem. Phys. Lett.*, 83, 455 (1981).

5. C. S. Allen and R. P. Van Duyne, *Chem. Phys. Lett.*, 63, 455 (1979).

6. T. Lu, T. M. Cotton, R. L. Birke and J. R. Lombardi, *Langmuir*, 5(2), 406 (1989).

7. J. Xu, R. L. Birke and J. R. Lombardi, *J. Am. Chem. Soc.*, 109, 5645 (1987).

8. M. Takahashi, M. Fujita and M. Ito, *Surface Science*, 158, 307 (1985).

9. C. J. Scandroff, D. A. Weltz, J. C. Chung and D. R. Herschbach, *J. Phys. Chem.*, 87, 2127 (1983).

10. T. Takenaka, *Advances in Colloid and Interface Science*, 11 291 (1979).

11. H. Shindo and C. Nishihara, *Surface Science*, 158, 393 (1985).

12. M. R. Mahoney, M. W. Howard and R. P. Cooney, *Chem. Phys. Lett.*, 71(1), 59 (1980).

13. J. Volke and A. M. Kardos, *Collection Czechoslov. Chem. Commun.* 33, 2560 (1968).

14. A. M. Kardos, P. Valenta and J. Volke, *J. Electroanal. Chem.*, 12, 84 (1966).

15. M. M. Baizer and H. Lund in "*Organic Electrochemistry*". Second Edition. M. Dekker, New York (1983).

16. H. Furukawa, M. Takahashi and M. Ito, *Chem. Phys. Letters*, 132(6), (1986) 498.

17. M. Takahashi and M. Ito, *Chem. Phys. Letters*, 103, 512 (1984).

18. M. Takahashi, M. Fujita and M. Ito, *Surface Science*, 176, 351 (1986).

19. M. Takahashi, M. Fujita and M. Ito, *Chem. Phys. Letters*, 109, 122 (1984).

20. J. H. S. Green and D. J. Harrison, *Spectrochim. Acta* 33A, 75 (1977).

21. J. H. S. Green, *Spectrochim. Acta* 19, 549 (1963).

22. F. R. Dollish, W. G. Fateley and F. F. Bentley, in "*Characteristic Raman Frequencies of Organic Compounds* ", p264. Wiley, New York (1974).

23. C. S. Allen and R. P. Van Duyne, *Chem. Phys. Lett.*, 63(3), 455 (1979).

24. T. T. Chen, K. U. Von Raben, J. F. Owen, R. K. Chang and B. L. Laube, *Chem. Phys. Letters*, 91, 494 (1982).

25. *Beilsteins Handbuch Der Organischen Chemie*, Band XVI (1933).

26. R. N. Adams, "*Electrochemistry at Solid Electrode*". M. Dekker, New York (1969).

27. N. B. Colthup, L. H. Daly and S. E. Wiberley, in "*Introduction to Infrared and Raman Spectroscopy*", 3rd Edition. Academic Press, Boston (1990).

Chapter IV

1. M. R. Rifi and F. H. Covitz "*Introduction to Organic Electrochemistry*". M. Dekker, New York (1974).

2. M. M. Baizer and H. Lund "*Organic Electrochemistry*", 2nd Edition. M. Dekker, New York (1983).

3. C. K. Mann and K. K. Barnes, "*Electrochemical Reduction in Nonaqueous Systems*", p.70. Dekker, New York (1970).

4. C. L. Perrin, in "*Progress in Physical Organic Chemistry*", Vol. 3, p.195. Wiley, New York, London, Sidney (1965).

5. M. J. Allen, "*Organic Electrode Processes*", p.61. Reinhold, New York (1958).

6. N. J. Leonard, S. Swann, Jr., and G. Fuller, *J. Am. Chem, Soc.*, 75, 5127 (1953).

7. F. Escherich and M. Moest, *Z. Electrochem.*, 8, 849 (1902).

8. J. Stocker and R. M Janevein, Symposium, "*The Synthetic and Mechanistic Aspects of Electroorganic Chemistry*", U. S. Army Office, Durham, N. C., Oct. 14-16, 1968.

9. H. Lund, *Acta Chem. Scand.*, 11, 283 (1957).

10. T. C. Chambers and O. S. Slotterbeck, *U. S. Pat.* 2,485,258 (1949); *C. A.*, 44, 4870 (1950).

11. P. J. Elving and J. T. Leone, *J. Am. Chem. Soc.*, 80, 1021 (1958).

12. E. A. Steck and W. Boehme, *J. Am. Chem.* Soc., 74, 4511 (1952).

13. M. J. Allen, *J. Org. Chem.*, 15, 435 (1950).

14. S. Swan, Jr., R. W. Benoliel, L. B. Lyons and W. H. Paht, *Trans. Electrochem. Soc.*, 79, 83 (1940).

15. E. Munoz, J. L. Avila and L. Camacho, *Anal. Chem.*, 63, 1574 (1991).

16. M. Blazquez, M. Jimenez and L. Camacho, *J. Electroanal. Chem.*, 243, 309 (1988).

17. J. F. Rusling, J. P. Segretario and P. Zuman, *J. Electroanal. Chem.*, 143, 283 (1983)

18. P. Zuman, *J. Electroanal. Chem.*, 75, 523 (1977).

19. P. Zuman, in " *Topics in Organic Polarography*", p.37. Ed. P. Zuman, Plenum Press, London, New York (1970).

20. P. Zuman and B. Turcsanyi, in " *Topics in Organic Polarography*", p.49. Ed. P. Zuman, Plenum Press, London, New York (1970).

21. P. Zuman, B. Turcsanyi and A. K. Mills, in " *Topics in Organic Polarography*", p.57. Ed. P. Zuman, Plenum Press, London, New York (1970).

22. P. Zuman, O. Exner, R. F. Rekker and W. Th. Nauta, in " *Topics in Organic Polarography*", p.66. Ed. P. Zuman, Plenum Press, London, New York (1970).

23. S. Cabani, P. Gianni and E. Matteoli, *J. Phys. Chem.*, 76, 2959 (1972).

24. M. R. Chakrobarty, C. S. Handloser and M. W. Mosher, *J. Chem. Soc. Perkin Trans., II*, 938 (1973).

25. A. Fischer, W. J. Galloway and J. Vaughan, *J. Chem. Soc.*, (1964) 3591.

26. R. L. Birke and J. R. Lombardi, in "*Spectroelectrochemistry: Theory and Practice*", Edited by Robert James Gale, 1988.

27. Norman B. Colthup, Lawrence H. Daly and Stephen E. Wiberley, "*Introduction to Infrared and Raman Spectroscopy*", Third Edition, Academic Press, Boston (1990).

28. Halina Baranska, Anna Labudzinska and Jacek Terpinski, "*Laser Raman Spectrometry-analytical applications*", Translation Editor: J. R. Majer. Halsted Press, New York (1987).

29. F. R. Dollish, W. G. Fateley and F. F. Bentley, "*Characteristic Raman Frequencies of Organic Compounds*". Wiley, New York (1974).

30. J. H. S. Green, W. Kynaston and H. M. Paisley, *Spectrochim. Acta*, 19, 549 (1963).

31. J. H. S. Green and D. J. Harrison, *Spectrochim. Acta*, 33A, 75 (1977).

32. D. A. Long and W. O. George, *Spectrochim. Acta*, 19, 1777 (1963).

33. Lester Corrsin, B. J. Fax, and R. C. Lord, *J. Chem. Phys.*, 21, 1170 (1953).

34. E. Spinner, *J. Chem. Soc.*, 1963, 1860.

35. F. A. Andersen, B. Bak, S. Brodersen and J. Rastrup-Andersen, *J. Chem. Phys.*, 23, 1047 (1955).

36. J. H. S. Green and D. J. Harrison, *Spectrochim. Acta*, 32A, 1265 (1976).

37. E. B. Wilson, Jr., *Physical Review*, 43, 706 (1934).

Chapter V

1. M. R. Rifi and F. H. Covitz "*Introduction to Organic Electrochemistry*". M. Dekker, New York (1974).

2. M. M. Baizer and H. Lund "*Organic Electrochemistry*", 2nd Edition. M. Dekker, New York (1983).

3. P. T. T. Wong and D. G. Brewer, *Can. J. Chem.*, 46, 131 (1968).

4. A. Fischer, M. J. King and F. P. Robinson, *Can. J. Chem.*, 56, 3072 (1978).

5. M. R. Chakrobarty, C. S. Handloser and M. W. Mosher, *J. Chem. Soc. Perkin Trans., II*, 938 (1973).

6. A. Fischer, W. J. Galloway and J. Vaughan, *J. Chem. Soc.*, (1964) 3591.

7. Norman B. Colthup, Lawrence H. Daly and Stephen E. Wiberley, "*Introduction to Infrared and Raman Spectroscopy*", Third Edition, Academic Press, Boston (1990).

8. Halina Baranska, Anna Labudzinska and Jacek Terpinski, "*Laser Raman Spectrometry-analytical applications*", Translation Editor: J. R. Majer. Halsted Press, New York (1987).

9. F. R. Dollish, W. G. Fateley and F. F. Bentley, "*Characteristic Raman Frequencies of Organic Compounds*". Wiley, New York (1974).

10. J. H. S. Green, W. Kynaston and H. M. Paisley, *Spectrochim. Acta*, 19, 549 (1963).

11. D. A. Long and W. O. George, *Spectrochim. Acta*, 19, 1777 (1963).

12. Lester Corrsin, B. J. Fax, and R. C. Lord, *J. Chem. Phys.*, 21, 1170 (1953).

13. E. Spinner, *J. Chem. Soc.*, 1963, 1860.

14. F. A. Andersen, B. Bak, S. Brodersen and J. Rastrup-Andersen, *J. Chem. Phys.*, 23, 1047 (1955).